The dimeric deubiquitinase Usp28 integrates 53bp1 and Myc functions to limit DNA damage

Dissertation

der Mathematisch-Naturwissenschaftlichen Fakultät

der Eberhard Karls Universität Tübingen

zur Erlangung des Grades eines

Doktors der Naturwissenschaften

(Dr. rer. nat.)

vorgelegt von

Chao Jin

aus Nanjing, China

Tübingen

2023

Gedruckt mit Genehmigung der Mathematisch-Naturwissenschaftlichen Fakultät der Eberhard Karls Universität Tübingen.

Tag der mündlichen Qualifikation:	07.11.2023
Dekan:	Prof. Dr. Thilo Stehle
1. Berichterstatter/-in:	Prof. Dr. Jennifer Ewald
2. Berichterstatter/-in:	Prof. Dr. Nikita Popov

Contents

Contents

Summary

Myc is an important transcription factor that regulates a series of cellular functions. It is also well-known as an oncoprotein, as it is frequently dysregulated in more than half of all human cancers. The ubiquitin system regulates the biological functions of Myc. For example, ubiquitination controls the recruitment of the elongation factor Paf1c1, which is critical for Myc activity. Usp28 was identified as a deubiquitinase of Myc that can stabilize it from proteasomal degradation by removing ubiquitin. Usp28 is known to form homodimers *in vitro* and in cells, but the biological role of Usp28 dimerization is unknown.

In this thesis, we showed that Usp28 can regulate Myc stability and Myc-driven transcription in the human liver cancer cell line HLF. Monomeric Usp28 shows enhanced deubiquitination activity towards Myc and facilitates Paf1c recruitment on Myc, but with no transcriptional effect. In contrast, the reinforced Paf1c-Myc binding by Usp28 monomers leads to decreased transcription-replication conflicts and stimulates DNA replication, which further accumulates replication-associated DNA damage.

We further showed that the dimerization of Usp28 is regulated by 53bp1, a known substrate of Usp28 that plays an important role in DNA damage response. 53bp1 can specifically bind to dimeric Usp28, and genotoxic stress disrupts Usp28's association with 53bp1, which promotes the formation of Usp28 monomers and enhances the recruitment of Paf1c by Myc. This triggers ectopic DNA synthesis during the early response to genotoxins, amplifying DNA replication-associated DNA double-strand breaks.

We then tested different cell lines with several different DNA damage inducers to show that this transient effect is universal in the multicellular context. The inhibition of DNA replication concomitantly with genotoxin treatment reduces DNA damage and promotes cell viability, indicating that the stabilization of Myc and acute DNA replication are early pathological effects of genotoxic stress rather than a programmed rescue mechanism.

Overall, our results provide a simple but reasonable explanation of the activation of Usp28 upon DNA damage and we therefore propose a model that dimerization of Usp28 limits aberrant replication at transcriptionally active chromatin to maintain genome stability.

Zusammenfassung

Myc ist ein wichtiger Transkriptionsfaktor, der eine Reihe von Zellfunktionen reguliert. Es ist auch als Onkoprotein bekannt, da es bei mehr als der Hälfte aller menschlichen Krebsarten häufig dysreguliert ist. Das Ubiquitin-System reguliert die biologischen Funktionen von Myc. So steuert die Ubiquitinierung beispielsweise die Rekrutierung des Elongationsfaktors Paf1c1, der für die Aktivität von Myc entscheidend ist. Usp28 wurde als eine Deubiquitinase von Myc identifiziert, die es durch die Entfernung von Ubiquitin vor dem proteasomalen Abbau stabilisieren kann. Es ist bekannt, dass Usp28 in vitro und in Zellen Homodimere bildet, aber die biologische Rolle der Usp28-Dimerisierung ist unbekannt.

In dieser Arbeit haben wir gezeigt, dass Usp28 die Myc-Stabilität und die Myc-gesteuerte Transkription in der menschlichen Leberkrebszelllinie HLF regulieren kann. Monomeres Usp28 zeigt eine verstärkte Deubiquitinierungsaktivität gegenüber Myc und erleichtert die Rekrutierung von Paf1c auf Myc, hat aber keine transkriptionelle Wirkung. Im Gegensatz dazu führt die verstärkte Paf1c-Myc-Bindung durch Usp28-Monomere zu verringerten Transkriptions-Replikationskonflikten und stimuliert die DNA-Replikation, die wiederum replikationsassoziierte DNA-Schäden akkumuliert.

Wir haben außerdem gezeigt, dass die Dimerisierung von Usp28 durch 53bp1 reguliert wird, ein bekanntes Substrat von Usp28, das eine wichtige Rolle bei der Reaktion auf DNA-Schäden spielt. 53bp1 kann spezifisch an dimeres Usp28 binden, und genotoxischer Stress stört die Assoziation von Usp28 mit 53bp1, was die Bildung von Usp28-Monomeren fördert und die Rekrutierung von Paf1c durch Myc verstärkt. Dadurch wird während der frühen Reaktion auf Genotoxine eine ektopische DNA-Synthese ausgelöst, die DNA-Replikations-assoziierte DNA-Doppelstrangbrüche verstärkt.

Anschließend testeten wir verschiedene Zelllinien mit unterschiedlichen Auslösern von DNA-Schäden, um zu zeigen, dass dieser vorübergehende Effekt im multizellulären Kontext universell ist. Die gleichzeitige Hemmung der DNA-Replikation mit einer Genotoxin-Behandlung verringert die DNA-Schäden und fördert die Lebensfähigkeit der Zellen, was darauf hindeutet, dass die Stabilisierung von Myc und die akute DNA-Replikation eher frühe pathologische Auswirkungen von genotoxischem Stress sind als ein programmierter Rettungsmechanismus.

Insgesamt liefern unsere Ergebnisse eine einfache, aber vernünftige Erklärung für die Aktivierung von Usp28 bei DNA-Schäden, und wir schlagen daher ein Modell vor, wonach die Dimerisierung von Usp28 die abnorme Replikation an transkriptionell aktivem Chromatin begrenzt, um die Genomstabilität zu erhalten.

1. Introduction

Part of this chapter is adapted from the manuscript ‘Jin, C., Einig, E., Xu, W., Kollampally, R.B., Schlosser, A., Flentje, M. and Popov, N. (under revision) The dimeric deubiquitinase Usp28 integrates 53bp1 and Myc functions to limit DNA damage.’ (1).

1.1 DNA damage

DNA is the double strand biological macromolecule which contains all the genetic information for the development of the organism. The flawless integrity of DNA is essential for its proper functioning. However, modifications on DNA may lead to the abnormal consequences upon DNA transcription and replication. These aberrant DNA alterations are known as DNA damages (2).

DNA damage is ubiquitous in cells and constitutes a key factor of tumorigenesis. Such DNA damage can result in lesions, making DNA single strand breaks (SSBs) and double strand breaks (DSBs), thereby accelerating the mutation of DNA and incite the genomic instability-a hallmark of cancer (3,4).

1.1.1 DNA damage origins

Up to 1 million lesions may occur on the DNA every day in a single cell due to different DNA damage inducers, such as ionizing radiation or replication errors. In general, the sources of DNA damage inducers can be classified into two catalogs: endogenous and exogenous origins.

1.1.1.1 Endogenous DNA damage

Reactive oxygen species (ROS) account for the majority of the endogenous DNA damage origins. ROS are produced from the metabolism pathways of aerobic organisms and play important roles in cellular when present at a low level. However, when ROS are excess, they may do harm on DNA via directly reacting with DNA bases or impairing DNA chains, leading to DNA single strand breaks. Typical ROS are hydrogen peroxide and hydroxyl/superoxide radicals (5).

DNA replication can also do contributions to the endogenous DNA damage. Although there are a series of strategies (such as mismatch repair pathway or the removal of mistake deoxynucleotides through deoxynucleotide exonuclease) in cells to ensure the accuracy of DNA replication so that all DNA can be replicated with high fidelity, considering that each replication involves up to three billion base pairs, the probability of DNA errors, for example mismatching or insertion/deletion, remains still high, up to 10^{-6} to 10^{-8} each cell per replication (6). These DNA errors can be accumulated in the further DNA replications and cause DNA mutations, as well as DNA damages.

Besides, other approaches such as DNA methylation or base deamination can also induce endogenous DNA damages (5).

1.1.1.2 Exogenous DNA damage

Ionizing radiation (IR) is one of the major ways to induce exogenous DNA damage. IR can either directly lead DNA strand breaks to impair the stability of genome (7,8) or attack DNA indirectly via the ROS such as hydroxyl radicals it generates. Interestingly, this indirect mode of action via ROS accounts for the majority of DNA damages caused by IR (7).

Another exogenous DNA damage inducer is ultraviolet (UV) radiation. UV can link two adjacent pyrimidines covalently. These pyrimidines dimers are detrimental for the DNA helix structure and thus leads to DNA damages (9).

In additional, exogenous chemical substances can also lead to DNA damages, for example alkylating agents can mutate DNA via the alkyl modifications on DNA bases. Crosslinking agents such as cisplatin can damage DNA by linking DNA nucleotides together and blocking the synthesis of DNA. Etoposide induces strand breaks via forming complexes with topoisomerase II and DNA. Hydroxyurea limits the amount of deoxyribonucleotide triphosphate (dNTP) by inhibiting ribonucleotide reductase to stall the DNA replication forks and leads to DNA damage (10).

1.1.2 DNA damage response

Organisms evolve a range of strategies to cope with DNA damage. When the DNA damage is happened, DNA damage response (DDR) pathway is activated by the sensor proteins and transduced by the kinases such as ATM (ataxia-telangiectasia mutated) and ATR (ATM- and Rad3-Related) to initiate downstream pathways subsequently, either to repair the detected DNA damage or to kill the injured cell via programmed death (4,11).

1.1.2.1 ATR-Chk1 pathway in DDR

When DNA single strand breaks are generated at DNA damage sites or at the stalled replication forks, ATR is activated by RPA-coated ssDNA to phosphorylate and activate Chk1. After activation, Chk1 phosphorylates Cdc25A to down regulate the activity of CDK2 and leads to the S-phase arrest. Chk1 also phosphorylates Cdc25B/Cdc25C to diminish the activity of CDK1/cyclin B, leading to the G2/M arrest (12).

Besides the cell cycle regulation, ATR-Chk1 pathway can stabilize the stalled replication fork to avoid further DNA damage in response to replication stress (13). Additionally, it can promote the homologous recombination (HR) upon DSBs (14).

1.1.2.2 ATM-Chk2 pathway in DDR

ATM is primarily activated by the DNA ends from DSBs which induced by radiation and genotoxins. Activated ATM phosphorylates a series of substrates including Chk2. After phosphorylation, Chk2 is activated and acts at several substrates such as p53, Cdc25, BRCA1 and E2F1 to regulate cell cycle, apoptosis and transcription (15). Moreover, ATM is also important for the activation of ATR-Chk1 signaling as ATM is required for the DNA strand resection to generate ssDNA (16).

1.1.3 DNA damage repair

After sensing DNA damage, cells need either to start DNA repair machinery to fix the impaired DNA strands or to promote the cell apoptosis. Various DNA repair pathways can be activated to repair different forms of DNA damage. For example, BER (base excision repair) can fix the single base error due to the alkylation or deamination (17). NER (nucleotide excision repair) is activated in facing the bulky DNA lesions from UV, IR and chemical mutagens (18). Moreover, cells also established several mechanisms in response to DNA SSBs and DSBs.

1.1.3.1 DNA single strand break repair

DNA SSBs usually come from DNA oxidation or the aberrant activity of DNA topoisomerase I. They can lead to the DNA replication collapses and stall the ongoing transcription. In the long patch SSBs repair signaling, the damages are detected and removed by PARP1 followed by

the POL β/δ/ε-driven filling and LIG1-dependent ligation. Besides, SSBs can also be produced during the base excision repair process. In this condition, only POL β participates in the filling step and the ligation is carried out by LIG3 (5).

1.1.3.2 DNA double strand break repair

Non-homologous end joining (NHEJ) and homologous recombination (HR) are the two major mechanisms to repair DNA DSBs. NHEJ pathway is activated by the recruitment of KU70/80 at DNA ends, which further recruits DNA-PKcs and end-processing enzymes. Next, XRCC4–XLF–LIG4 is recruited to ligate DNA and finish repair (19). NHEJ is utilized in the whole cell cycles and it uses microhomologies to guide the DNA repair (3).

In contrast, HR is only activated in S-G2 phase of proliferative cells because it needs the sister chromatids as the template for DNA repair. In short, MRN (MRE11–RAD50–NBS1) complex recognizes and binds to the 3' ends of the DSBs. Enzymes including CtIP, EXO1, BLM and DNA2 are also recruited at 3' ends for resection. Afterwards, the 3' ssDNA is coated by RPA and displaced by RAD51 to form the RAD51–ssDNA nucleofilament with the help of BRCA1, BRCA2 and PALB2. This RAD51–ssDNA nucleofilament further forms a D-loop with a homologous sequence derived from the sister chromatids. This homologous sequence serves as the template for DNA synthesis, facilitating the replacement of the damaged DNA near the breaks (19).

1.1.3.3 53bp1, a key regulator in DSB signaling

53bp1 (p53-binding protein 1) plays an important role in DSBs induced DDR. It is accumulated at the damaged DNA in a histone modification (H2AK15ub and H4K20me2)-dependent manner. 53bp1 can recruit DSB-responsive factors, for example EXPAND1 and RIF1 to the DSB sites (20,21). It is also known to amplify ATM-dependent checkpoint signal under the low DNA damage context (22,23). Additionally, 53bp1 is also a key regulator in NHEJ-driven DNA repair. In G1 phase, it can protect the damaged DNA from end resection, which is essential for HR, in an unknown mechanism (19).

1.1.4 DNA damage in anticancer therapy

Aberrant DNA damage leads genomic instability and apoptosis, therefore, inducing DNA damage could serve as an anticancer strategy. In fact, DNA damage-inducing methods are the most used treatments in cancer cell killing. For example, topotecan, a DNA topoisomerase I inhibitor, induces SSBs via forming the ternary complex with topoisomerase I and DNA (24). Zeocin is known to kill cells by intercalating within the DNA structure, hence inducing DSBs (25).

Another anticancer strategy which involves DNA damage is to interfere the DDR signaling in cancer cells and thus to kill cancer cells with synthetic lethality. One well known example is the use of PARP inhibitors in BRCA1/2-deficient cancers (26). PARP inhibitors, such as olaparib and niraparib, block the function of PARP1, which is essential in SSB repair signal. Unrepaired SSBs further form DSBs during the DNA replication in S phase. However, due to the defect of BRCA1/2, the DSBs cannot be repaired by HR pathway in the BRCA1/2-deficient cancer cells and lead to the death of these cells while the normal cells are not affected (10). In addition, ATM inhibitors and ATR inhibitors, such as KU55933 and AZD6738 (27,28), are also used in clinical trials to kill cancer cells by the synthetic lethality via the inhibition of DNA damage repair pathways.

1.2 The transcription factor Myc

Myc, as a versatile transcription factor (TF), regulates a variety of cellular activities, including cell cycle, signal transduction, metabolism, translation, and DNA repair, among others, by regulating protein-coding or non-coding genes, which are further involved in the regulation of a spectrum of biological functions, such as cell proliferation and differentiation (29,30).

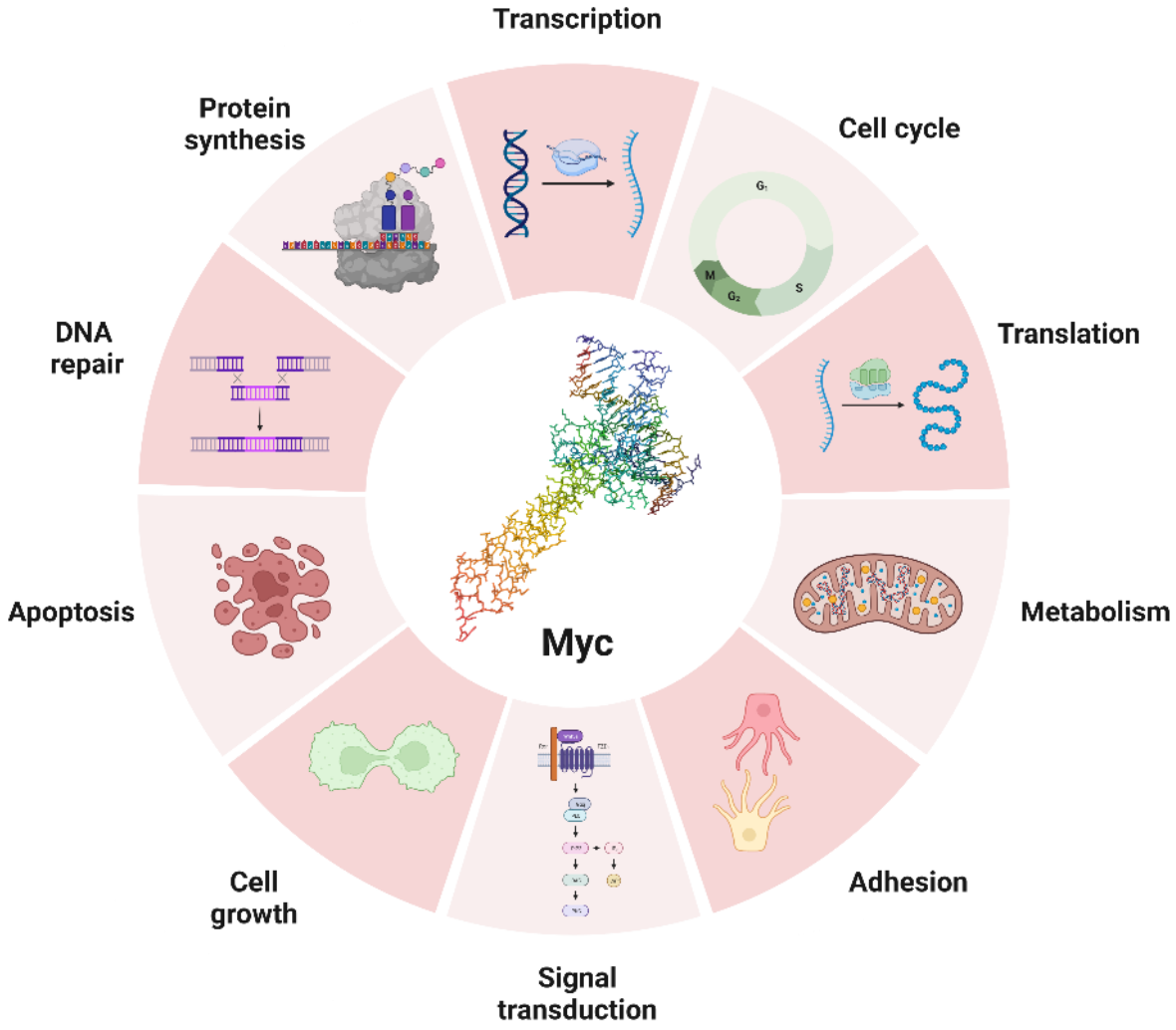

Figure 1. Biological functions of Myc in cellular life (Created with BioRender.com.)

As a widely known oncoprotein, Myc plays an important role in boosting tumorigenesis, development, progression and metastasis in many different types of tumors. In fact, as one of the most important drivers of tumorigenesis, Myc is found to be dysregulated in more than half of all tumors (31). For example, hepatocelluar carcinoma (HCC), the leading type of primary liver cancer and one of the most lethal cancers in the world (32), shows overexpression of the Myc gene in more than 30% of patients (33).

The Myc family contains three isoforms: c-Myc, N-Myc and L-Myc (34-36). These three isoforms are highly homologous between each other, from their conserved DNA

sequence to their similar protein structure (37). The main differences between the three isoforms are their differential expression in different tissue types or developmental stages and their differential deregulation in different tumor types. For example, c-Myc is only present in rapidly proliferating tissues and is generally dysregulated in a large number of tumors, while L-Myc and N-Myc are often expressed specifically in differentiated tissues. In tumors, L-Myc is mainly deregulated in small cell lung carcinoma, while N-Myc is found to be overexpressed in a limited number of neurons or neuroendocrine entities (36,38,39).

1.2.1 Structure and interactors of Myc

As discussed above, the three Myc isoforms are highly homologous and belong to the basic helix-loop-helix leucine zipper(bHLHLZ) transcription factor family. Myc protein has three main domains: The N-terminal transactivation domain (TAD), central region and the C-terminal bHLHLZ domain (40,41).

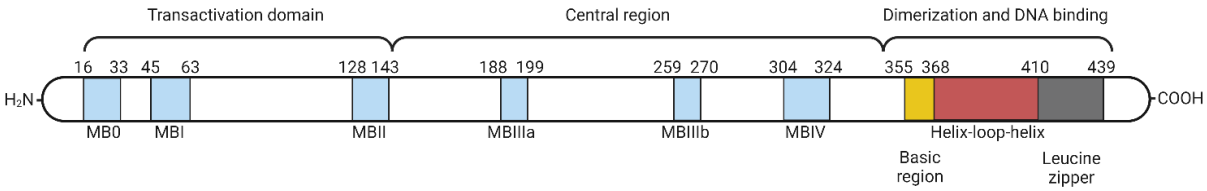

Figure 2. Domain structure of c-Myc (Created with BioRender.com.)

The TAD and central region of Myc contain six highly conserved regions, called Myc boxes (MBs), which are MB0, MBI and MBII in the TAD region and MBIIIa (which is absent in L-Myc), MBIIIb and MBIV in the central region (42,43). These MBs are the main protein-protein interaction (PPI) regions of Myc, which regulate the function of Myc by interacting with different proteins. For example, binding between the general transcription factor IIF (TFIIF) and MB0 has been shown to accelerate Myc-mediated transcription (43). Additionally, MBI plays an important role in regulating the protein stability of Myc and the subsequent degradation through the ubiquitin-proteasome system (UPS) (44,45). MBII activates Myc-mediated transcription by direct interaction with transformation/transcription domain-associated protein (TRRAP) (46). MBIIIa is believed to negatively regulate Myc-induced apoptosis as well as Myc-driven transcription (47). In contrast, MBIIIb is important for Myc chromatin recruitment via the interaction with WD repeat-containing protein 5 (WDR5), which is essential for tumor maintenance (48). Furthermore, MBIV has been proofed to regulate DNA binding, apoptosis, transformation, and G2 arrest (49).

The bHLHLZ domain at the C-terminus, is responsible for the interaction with Myc-associated protein X (Max), one of the most important interaction partners of Myc, to form a stable heterodimer with a specific DNA recognition and binding ability (50). Besides, this C-terminal is also reported to mediate the interaction between Myc and MYC-interacting zinc finger protein 1 (MIZ1) to negatively regulate the Myc-mediated transcriptional activation (51).

1.2.2 Regulation of oncogenic transcription by Myc

As an important transcription factor, many studies have shown that Myc can regulate the expression of many genes in a variety of different cells. For example, Myc occupies more than 15% of all promoters in Burkitt's lymphoma cells, together with its heterodimerization partner Max (52). Meanwhile, in leukemia cell lines U-937 (monoblastic leukemia) and HL60 (myeloid leukemia), around 11% of all cellular loci have detected binding between Myc and the promoters (53). Thus, Myc is sometimes considered a master regulator of genes.

Via binding with the promoters of the target genes at the RNA polymerase II (RNAPII), Myc regulates the expression of them by controlling transcription, either through activation or repression. In fact, the transcriptional regulation of Myc not only through RNAPII but also all three RNA polymerases. Myc can bind to human ribosomal DNA and stimulate the transcription of ribosomal RNA (rRNA) genes by RNA polymerase I (RNAPI) (54,55). It can also directly activate RNA polymerase III (RNAPIII) to promote the generation of transfer RNA (tRNA) and 5S rRNA (56).

In normal tissues, Myc is required to regulate the genes, which are necessary for the cellular biological processes such as cell proliferation, differentiation, senescence, and apoptosis (57), and the protein level of Myc is usually low and tightly regulated with a short half-life between 20-30 minutes (58). However, in tumor tissues, Myc is often dysregulated and activated, mainly due to the amplification or chromosomal translocation rearrangement, as well as the prolonged half-life (59,60).

The carcinogenicity of Myc lies in its ability not only to facilitate the transcription of oncogenes but also to repress the transcription of tumor suppressor genes (61), and this oncogenic transcriptional activation or repression can also be regulated by the interaction between Myc and its binding partners.

1.2.2.1 Myc-dependent transactivation

To activate the gene transcription, Myc first interacts with Max to form the Myc/Max heterodimers. This Myc/Max dimer can recognize the enhancer box (E-box) DNA sequence (5'-CACGTG-3' or related sequences) to regulate their expression (62). In most of the cases, the function of Myc as a transcriptional factor is dependent on the heterodimerization with Max (63). However, new studies have also shown that Myc is able to regulate gene expression independently of Max. For example, N-Myc is reported to regulate the p53 target genes with the direct binding with p53 in N-Myc amplified neuroblastomas (64).

After binding to the E-box, Myc recruits its cofactors to induce transcription. For example, TRRAP, a component of histone-acetylation (HAT) complexes which contains the histone acetyltransferases Tat-interactive protein 60 (Tip60) and General control nonderepressible 5 (Gcn5) (65). Unlike Tip60 or Gcn5, which have histone acetylase activity, TRRAP itself has no catalytic activity (66,67). Instead, it plays a role in linking HAT complex and Myc. Via the direct interaction with the MBII domain, the HAT complex can be recruited to Myc binding DNA and promote the hyperacetylation of lysine on H3 and H4 to open the chromatin, thereby activating transcription (43,68). Studies have also shown that the recruitment of TRRAP contributes to the oncogenic transformation mediated by Myc (69).

Another oncogenic transcription activation cofactor of Myc is WDR5, which can bind to the MBIIIb domain of Myc to promote Myc chromatin recruitment (48) and regulate the transcription of Myc target genes via the demethylation and acetylation of H3K27 (70). The interaction between WDR5 and Myc can stabilize the Myc/Max heterodimers on the promoters of the key cancer-promoting target genes so as to accelerate the transcription of these genes (71). On the other hand, this interaction can also promote the Myc-mediated Hypoxia-inducible factor 1-alpha (HIF1-α) transcription to accelerate the Epithelial-mesenchymal transition (EMT) as well as invasion and metastasis in cholangiocarcinoma (72). Besides, it is also published that the WDR5 and Myc interaction can also contribute to the maintenance of DNA replication in pancreatic ductal adenocarcinoma (73).

Another important cofactor of Myc in oncogenic transcriptional activation is the Positive Transcription Elongation Factor b (P-TEFb). It is a general transcription factor, which contains the cyclin-dependent kinase 9 (CDK9) and its regulatory subunit cyclin T. The former can phosphorylate the C-terminal domain (CTD) of RNAPII (74), while the latter can bind to Myc and promote the transcription activation of the cad promoter (75). The direct interaction between P-TEFb and Myc is also required for Myc to release RNAPII from the paused state, which is believed to play an important role in Myc-driven oncogenic transcriptional activation (76-78).

Furthermore, the interaction between Myc and certain proteins may also activate Myc-driven oncogenic transcription in an indirect manner, such as through the stabilization or accumulation of Myc. Studies have shown that the bindings between Myc and its target DNA binding sites are different from the binding affinities. Overexpression of Myc is associated with the increasing occupancy between Myc and its low affinity binding sites and, in the worst cases, also with non-specific DNA sequences other than the E-box. These effects may turn Myc-driven transcription from normal proliferating to oncogenic direction (53,79).

For example, Aurora-A can interact with the MBI domain of Myc and rescue it from FBXW7-induced proteasomal degradation, thus to stabilize and accumulate Myc (80,81). Moreover, Aurora-A can also promote the expression of Myc, and in turn, Myc can regulate the transcription level of Aurora-A. Thereby, the net effect is that the protein level of Myc is up-regulated, and its oncogenic transcription is activated (82,83).

1.2.2.2 Oncogenic transcriptional repression of Myc

Myc can also act as an oncogenic transcription factor by repressing the transcription of tumor suppressor genes, thereby initiating tumorigenesis or promoting metastasis.

The first candidate as a cofactor of Myc to induce the oncogenic transcriptional repression is MIZ1. In fact, MIZ1 itself is also a transcription factor and can both activate or repress transcription based on its interactors (84). In the case of Myc, it can compete with Max in forming the heterodimers, it can meanwhile interact with zinc-finger (ZF) transcriptional repressor growth factor independence 1 (GFI-1) to form a ternary complex at the promoter of cyclin-dependent kinase inhibitor (CDKN) to repress CDKN1A/2B (85-87). The recruitment of Myc to the promoters of the cell cycle inhibitors p15INK4B and p21CIP1 by MIZ1 can also lead to the inhibition of the famous tumor suppressor p53, resulting in a negative effect on anti-tumor activities. (88,89). Moreover, MIZ1 can also suppress Mad4, which is the endogenous transcription suppressor of Myc (90).

Histone Deacetylase 3 (HDAC3) can also interact with Myc at promoters of tumor suppressor genes miR-15a/16-1 to down regulate their protein levels in mantle cell lymphoma (91). It is also proofed that the interaction between HDAC3 and Myc can repress the transcription of FOXA2 and result in the development of gastric cancer (92).

Another cofactor is G9a, which can promote the methylation of histone 3 lysine 9 (H3K9) and histone 3 lysine 27 (H3K27) (93,94). The methylation level of H3K9 is low at Myc-repressed gene promoters in the absence of G9a, thus reducing Myc ability to bind to chromatin, therefore the deficiency of G9a can inhibit the proliferation of glioblastoma cell as

well as the tumorigenesis ability (95,96). On the contrary, the interaction between G9a and Myc can lead to the transcriptional repression and facilitate breast tumor development.

1.2.3 Non-transcriptional functions of Myc

Although known as a transcription factor, more and more evidence has suggested that Myc also has transcription-independent functions. For example, Myc is reported to promote the formation of the mRNA cap structure by driving the methylation of the mRNA cap. Besides, Myc can control DNA replication via the regulation of replication origins and chromatin modification. Moreover, it can regulate genomic stability via Myc-driven replication stress and DNA repair (97).

1.2.3.1 Myc drives mRNA cap methylation

The capping of the nascent mRNA by capping enzymes is an important procedure at the early stage of the transcription because uncapped mRNA will degrade rapidly (98). However, after capping, mRNA still needs to be methylated so that it can bind with the translation factors, which are required for the translation (99-101).

Myc has been identified to promote the chromatin recruitment of transcription factor TFIIH complex via the direct interaction; In addition, Myc can also relax the DNA structure to boost this recruitment (46,102,103). The recruitment of TFIIH can further phosphorylate RNAPII at its Ser5 on the N-terminus, which subsequently promotes the recruitment of the cap RNA methyltransferase (RNMT) and stimulates the mRNA cap methylation.

1.2.3.2 Myc controls DNA replication

DNA replication is an essential for all forms of life. In human cells, three billion base pairs have to be faithfully replicated during the S phase. Any errors that occur during the replication, for example the DNA damage or the stalled replication fork, may lead to the cell cycle arrest, which further contribute to the DNA mutations and genomic instability, the hallmarkers of the tumorigenesis (97).

Myc was initially thought to induce genomic instability via transcriptional regulation. For example, Myc can directly regulate the expression of relevant genes which are involved in the DNA replication (104). Besides, via the regulation of the expression of proteins like

cyclins and cyclin-dependent kinases (CDKs), Myc can then regulate the cell cycle such as G1/S transition (105,106). In addition, Myc can also regulate the biosynthesis of purine and pyrimidine, which are essential metabolites required for DNA replication, via the regulation of the relevant genes, and therefore control the DNA replication (107,108). However, subsequent research has demonstrated that Myc also has transcription-independent functions in regulating DNA replication.

Myc can establish physical interactions with MCM 2-7, ORC, Cdc6, and Cdt1, which are subunits of the pre-replicative complex (pre-RC) (109). The pre-RC is a critical complex involved in DNA replication origins, the loci where chromosomal replication starts. ORC, Cdc6 and Cdt1 collaborate to recruit MCM 2-7, which functions as the catalytic components of the replicative DNA helicase, to the origins of replication, to unwind DNA for replication. Additionally, Cdc45 and GINS complex are also required to form the CMG (Cdc45/MCM/GINS) to active pre-RC and continue DNA synthesis. The presence of these novel Myc-associated interactions within the pre-RC implies a direct role of Myc in DNA replication. For example, Myc can regulate the chromatin accessibility at its target sites via MBII to stimulate the recruitment of Cdc45 and GINS to MCM and thus to activate CMG and to accelerate DNA replication (110).

Furthermore, Myc can also regulate DNA replication via the modification of chromatin to regulate the assembly and activity of DNA replication origins. For example, Myc interacts with an E box located in the Lamin B origin to recruit MLL1 methyltransferase to modify the nucleosomes in the vicinity of H3K4. This process further leads to the establishment of a chromatin region that is free of nucleosomes, allowing for the subsequent recruitment of MCM at the origin (111).

Moreover, a study performed in the Xenopus extracts have shown that the depletion of c-Myc arrests cells in early G1 phase and blocks DNA replication, and this defect can be rescued by the addition of recombinant full-length Myc protein. as Xenopus extracts allow DNA replication without transcription and new protein synthesis, this experiment shows that Myc can regulate DNA replication in a non-transcriptional manner (109).

1.2.3.3 Myc regulates genomic stability

Deregulated origin firings can contribute to the DNA replication stress, which can further induce DNA damage. In fact, the overexpression of Myc increases the density of replication origins and elevates the level of pH2AX, the biomarker of DNA damage, in S phase. This is probably due to the conflict between the Myc-driven transcription machinery and Myc-

regulated DNA replication, which further leads to the genome instability and accelerates tumorigenesis (112-114).

Studies have shown that Myc can recruit Brca1 and the exosome complex to facilitate R-loops (DNA-RNA hybrids formed by RNAPII) resolution. This recruitment can limit collisions between RNAPII and replisome (transcription-replication conflicts, TRCs), thereby maintain genomic stability (115,116). Another mechanism involves the recruitment of the elongation factor Paf1c by Myc, which not only has transcriptional effects but also contributes to the resolution of TRCs and promotes DNA repair (117-119). Mechanistically, Paf1c stimulates histone H2B ubiquitination (120), leading to the stabilization of replication forks and promoting homologous recombination. However, Paf1c is also known to contribute to the accumulation of R-loops and activate ATM and RAD3-related protein (ATR) signaling pathway, thereby increasing replicative stress (121,122). This indicates that the non-transcriptional function of Myc via the recruitment of Paf1c in genome stability is genetic- or signaling context-dependent.

1.2.4 Targeting Myc for cancer strategy

Since Myc plays such an important role in tumorigenesis, targeting Myc seems to be a promising anti-tumor strategy. Indeed, studies have shown that the inhibition of Myc via the expression of the dominant-negative Myc mutant can lead to the rapid regression of the Ras-induced lung adenocarcinoma in mouse models (123).

However, the structure of Myc limits the development the small molecule inhibitors that can target Myc directly, as it lacks hydrophobic pockets for binding of small molecules. Besides, as a transcription factor, unlike other oncogenic enzymes, Myc has no catalytic activity for small molecule inhibitors to block. As Myc is a nuclear protein, it is unrealistic to develop specific monoclonal antibodies against it due to the difficulty of these antibodies penetrating cellular membranes (37,41).

Due to the problems mentioned above, researchers have begun to investigate methods to indirectly target Myc, for example, inhibition of Myc at the transcriptional or translational level or blocking interactions between Myc and its key binding partners. In addition, targeting the stability of Myc can be a potential strategy.

1.2.4.1 Targeting Myc at the transcriptional level

Transcription of Myc is regulated by the BRD4 protein (Bromodomain-containing 4), which is a transcriptional regulator of the bromodomain and extra terminal domain (BET) family (124). BRD4 functions via recruitment of P-TEFb, which phosphorylates RNAPII at the C-terminal domain and leads to the transcriptional elongation (125). JQ1, a small molecule inhibitor, can inhibit the function of BRD4 via competing for binding to acetylated lysines.

Other molecules that can target transcription of Myc are CDK7 and CDK9 inhibitors, for example THZ1 (CDK7 inhibitor) and PC585 (CDK9 inhibitor), as CDK7/9 are frequently located in the SEs, which dysregulate Myc. Studies have shown that inhibition of CDK7/9 can down regulate the transcription of Myc gene, as well as Myc target genes (126,127).

Rather than directly targeting the Myc transcription process, targeting the Myc mRNA, the product of Myc transcription, can present another strategy. Over the past 40 years, many efforts have been made to silence Myc mRNA, from the use of antisense oligonucleotides to attempts at short hairpin RNAs (shRNAs) carried by oncolytic adenoviruses (128,129). Although some of these strategies have shown the ability to inhibit tumor growth, the follow-up clinical trials failed due to the drug instability as well as the difficulties in drug delivery.

1.2.4.2 Targeting Myc at the translational level

Targeting the translation of Myc protein is also a potential method to down regulate Myc. The translation of Myc mRNA is encouraged by the eukaryotic initiation factor 4E (eIF4E), which can be negatively regulated by the eIF4E binding protein 1 (4EBP1) with the mTORC1 mediated phosphorylation. Thus, the inhibition of mTORC1 by small molecule inhibitor, for example Rapamycin, may contribute to the down regulation of Myc (130,131). Indeed, inhibition of mTORC1 by Rapamycin or its analogues has demonstrated a therapeutic potential for Myc-driven tumors (132-134).

1.2.4.3 Targeting interactions between Myc and its cofactors

As discussed previously, the oncogenic transcriptional function of Myc also requires the interaction of Myc and its cofactors, which also provides scientists with a potential way to regulate Myc.

One candidate cofactor is Max, as the Myc/Max heterodimer is required for DNA recognition and binding to initiate the Myc-driven transcription (135). Several small molecule

inhibitors have been found to block the heterodimerization of Myc and Max via high-throughput screening (HTS) and have been verified both *in vitro* and *in vivo*. For example, the compound 10058-F4 showed the ability to disrupt the Myc/Max heterodimer and to inhibit proliferation in HL60 cells (136). The compound MYCi361 and its analog MYCi975 suppressed tumorigenesis in mouse models (137).

Efforts have also been made to inhibit the interaction between Myc and Max using peptides. Omomyc is one such peptide that was designed to mimic the bHLHLZ domain of Myc with four point-mutations in the leucine zipper domain (138). It can form a homodimer with another Omomyc peptide or to form a heterodimer with Max. In either case, Omomyc-containing dimer can compete with endogenous Myc/Max heterodimers for DNA and thereby interfere with Myc-dependent transcription (123,139).

Another frequently studied Myc cofactor is WDR5. As discussed above, the interaction between WDR5 and Myc can promote Myc chromatin recruitment, thereby activating Myc-driven oncogenic transcription. Additionally, the high protein level of WDR5 in neuroblastoma is also an independent biomarker of poor prognosis (140). Recently, two small molecule inhibitors have been shown to block the WDR5 and Myc interaction. One is a methyl sulfone-containing compound that can strongly disrupt WDR5-Myc binding at 5 μM in HEK293 cells by binding with the WDR5 binding motif (141). The other is a dihydroisoquinolinone bicyclic core-containing compound that can block the recruitment of Myc to chromatin at Myc/WDR5 co-bound genes. It can inhibit the proliferation of Myc-driven cancer cells at around 50 nM with high selectivity by binding with the WDR5 interaction site (142).

1.2.4.4 Targeting Myc stability

Myc is an unstable protein with a half-life of approximately 30 minutes and is continuously regulated by the ubiquitin-proteasome system. Degradation of Myc is initiated by the phosphorylation of the Ser62 and Thr58 threonine, mediated by Cdk and glycogen synthase kinase 3 (Gsk3), respectively. Ser62 is subsequently dephosphorylated by protein phosphatase PP2A, allowing the E3 ligase FBXW7 to recognize and ubiquitinate Myc for degradation by the proteasome. (45,143). Mutations in FBXW7 can enhance leukemia-initiating cell activity, while loss of FBXW7 has been found to induce Myc-dependent cholangiocarcinogenesis in mice (144,145).

Many deubiquitinases have been identified to antagonize Myc ubiquitination and stabilize Myc. For example, the USP36 and USP7 can stabilize Myc via interaction with different FBXW7 isoforms (146,147). Moreover, USP28 has also been verified as a

deubiquitinase of Myc (detains see the coming section), which is overexpressed in many Myc-driven tumor cells. The inhibition of USP28, either with USP28-targeting shRNA or with its inhibitor AZ1, can downregulate the protein level of Myc both *in vitro* and *in vivo* (148-153).

A new strategy technology for targeting Myc stability is based on Proteolysis Targeting Chimeras (PROTACs) - heterobifunctional molecules with one ligand that binds a protein of interest, and another ligand to bind the E3 ligase on the other side, and these two ligands are connected by a linker in between (154). Many researchers attempted to downregulate Myc via the PROTAC-mediated Myc degradation, however, due to the disordered structure of Myc, it is hard to find a ligand which can capture Myc with high affinity, so more efforts are put to target Myc interactors with PROTAC, for example the PROTAC compound ARV-771 and ARV-825 were shown to inhibit Myc in castration-resistant prostate cancer and neuroblastoma, respectively, by inducing the degradation of BRD4 and other BET family members (155,156).

Table 1. Reported compounds or peptides targeting Myc

Type	Target	Compound	Progress
Myc transcription	BRD4 and other BET family members	JQ1	Pre-clinical
		GSK525762	Phase II
		ARV-771; ARV-825	Pre-clinical
	CDK7	THZ1	Pre-clinical
	CDK9	PC585	Pre-clinical
Myc translation	mTOR	Rapamycin; RAD001; CCI-779	Phase I-IV
Myc-cofactor interaction	Max	10058-F4	Pre-clinical
		10074-G5	Pre-clinical
		MYCi361; MYCi975	Pre-clinical
		Omomyc; OMO-103	Phase I-II
Myc stability	Survivin	PC002	Phase II
	Usp7	P22077	Pre-clinical
	Usp28	AZ1; FT206	Pre-clinical

1.3 The ubiquitin proteasome system and the deubiquitinase Usp28

1.3.1 The ubiquitin proteasome system

1.3.1.1 Ubiquitination cascade

Ubiquitin is a 76-amino-acid protein that is highly conserved and ubiquitously expressed in all eukaryotic tissues, first identified in 1975 (157). Ubiquitin can modify other proteins via the formation of an isopeptide bond between its C-terminal glycine and a lysine residue on the substrate protein (158). This modification, known as ubiquitination, is one of the most important posttranslational modifications (PTM), playing a key role in protein degradation, signaling pathways, DNA repair, and other biological processes.

The ubiquitination cascade involves three types of enzymes and three steps: activation, conjugation, and ligation. First, the E1 ubiquitin-activating enzymes activate ubiquitin in an ATP-dependent manner, forming a ubiquitin/E1 complex through a thioester linkage between the C-terminal glycine of ubiquitin and a cysteine residue in E1. Next, the activated ubiquitin is transferred to an E2 ubiquitin-conjugating enzyme through a transthioesterification reaction. Finally, the E3 ubiquitin ligases catalyze the transfer of the ubiquitin molecule from the E2 enzyme to the substrate protein, forming an isopeptide bond between the C-terminal glycine of ubiquitin and a lysine residue on the substrate. (159,160).

As the last step of the ubiquitination cascade, the target protein is modified by the addition of a single ubiquitin molecule, a process known as monoubiquitination. The site of monoubiquitination on the substrate may differ among different substrates; it may be a specific amino acid site, such as the Lys164 in proliferating cell nuclear antigen (PCNA), or a large domain of the target protein, such as the six C-terminal lysines in p53. In some cases, multiple lysine residues on the same protein can be modified by monoubiquitination, a process called multimonoubiquitylation, as in the case of the epidermal growth factor receptor (EGFR). (161-163).

Ubiquitin itself has seven lysine residues, in addition to its N-terminal methionine, all of which can serve as binding sites to be targeted by E3 ligases and E4 ubiquitin-chain elongation factors to elongate the ubiquitin chain, known as a polyubiquitin chain, ranging from two ubiquitin units to more than ten moieties (164). Polyubiquitin chain has eight different homotypic types, as well as numerous heterotypic types with different topology

structures and biological functions. While all possible types of linkages have been detected in cells through proteomics research, not all of them are well understood (165,166).

The Lys48 (K48)-linked chain was the first identified and most studied polyubiquitin chain. K48-linked chains account for more than half of all polyubiquitin chains, and their best understood biological function is to target their substrates for degradation by the proteasome (167).

Another well-characterized type is the Lys63 (K63)-linked chain, which is the second most common type in the cell. Unlike K48-linked chains, K63-linked chains are thought to play primarily non-degradative roles, such as regulating DNA repair and protein activity (168). Recent studies have started to unveil the functions of other types of polyubiquitin chains. For example, the Lys6 (K6)-linked polyubiquitin chain has been shown to regulate the stability of some E3 enzymes (169). The Lys11 (K11)-linked polyubiquitin chain is assembled by the anaphase-promoting complex or cyclosome Apc/c, and recent data show that homotypic K11-linked polyubiquitin chain-modified substrates are poor substrates for the proteasome (170,171). The Lys29 (K29)-linked polyubiquitin chain is reported to be linked with lysosomal degradation, mediated by the Notch signaling modulator DTX (172). Finally, the Lys33 (K33)-linked polyubiquitin modification is believed to regulate the activity of some AMPK-related kinases (173).

Interestingly, in addition to their well-known canonical functions, an increasing number of studies have identified non-canonical functions of different types of polyubiquitin chains. For instance, Met4 has been found to contain a ubiquitin binding domain that can interact with its own K48-linked polyubiquitin chain, limiting the amount of ubiquitin moieties on the chain. This prevents the chain from being recognized and degraded by the proteasome, resulting in a more stable Met4 that regulates Met4-mediated transcription (174).

Another example of a non-canonical function is the proteolytic function mediated by K63-linked polyubiquitin chains. Scientists have shown that K63-linked polyubiquitination of TXNIP, a proapoptotic regulator, can trigger proteasome-mediated degradation by boosting the assembly of K48/K63 branched ubiquitin chains through the recruitment of ubiquitin ligases (175).

1.3.1.2 The 26S Proteasome

After polyubiquitination, the modified target proteins can be shuttled to the 26S proteasome for proteolytic degradation. The 26S proteasome consists of two subcomplexes: the catalytic core particle, also known as the 20S proteasome, and one or two 19S regulatory particles that are attached to one or both sides of the 20S proteasome (176).

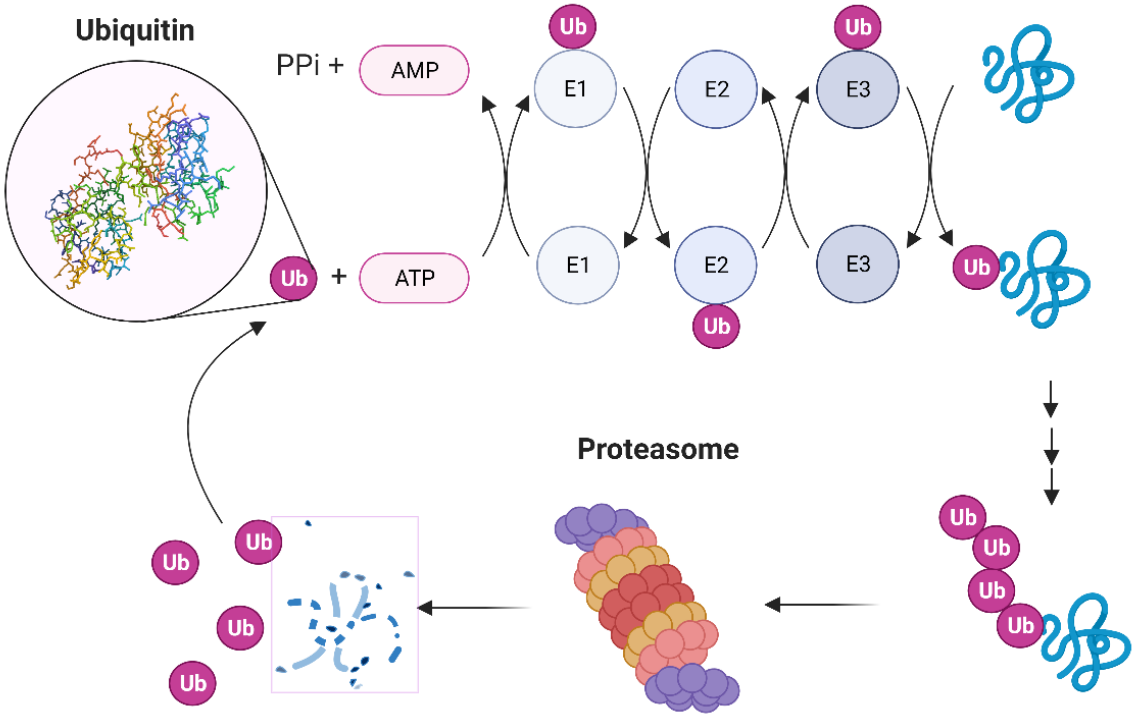

Figure 3. Schematic of ubiquitination (Created with BioRender.com.)

1.3.1.3 E3 ligases

As mentioned above, ubiquitination is carried out by E1, E2, and E3 enzymes. There are two E1 enzymes, approximately 40 E2 enzymes, and over 600 E3 ligases encoded by the human genome (177-179). Among all the participating enzymes, E3 ligases may play the most critical role in the ubiquitination cascade. They can regulate the reaction efficiency and are mainly responsible for the specificity of ubiquitination through direct interaction with substrates (180). E3 ligases can be classified into four major groups based on their structure and function: Really Interesting New Gene (RING) finger, Homologous to the E6-AP Carboxyl Terminus (HECT), U-box, and the newly identified RING-IBR-RING (RBR) (181).

RING finger E3 ligases can directly bind to the E2 enzymes and transfer the ubiquitin to the substrates during the ubiquitination cascade. This group is the largest among all the E3 ligases with over 600 family members (179). RING finger E3 ligases can be divided into two subgroups: monomeric RING finger and multi-subunit E3 ligases. The former type has both substrate binding domain and ubiquitination catalytic domain on the same single polypeptide, while the latter separates different functional modules into different subunits to form a complex. For example, the Skp1-cullin 1-F-box (SCF) E3 ligase complex, the largest family of E3 ligases, consists of Skp1, cullin1, and F-box, which are responsible for the

interaction between the catalytic core of the ligase and F-box, modulation of the interaction with other subunits, and recognition of the ligase's substrates, respectively (182-184).

The HECT E3 ligases family is also one of the biggest and well-studied E3 ligase subgroup. The catalytic HECT (Homologous to the E6-AP Carboxyl Terminus) domain at the C-terminal of the ligase and it can accept the ubiquitin at its active cysteine site transferred from E2 enzymes and subsequently directly delivers the ubiquitin to its target substrate which binds at the N-terminal of the ligase (185). The HECT E3 ligases can be further classified into Nedd4 family, HERC family and another HECTs based on the difference of their N-terminal (186).

The U-box E3 ligases are quite similar to the RING finger E3 ligases in terms of the structure (187). However, unlike the RING finger ligases with the zinc finger domain at the N-terminal, U-box ligases have a conserved U-box domain at their C- terminal which can interact with the E2 enzymes and directly transfer the ubiquitin to the lysine site of their substrates (188). The newly classified RBR E3 ligases exhibit characteristics that resemble a combination of the RING finger E3 ligases and HECT E3 ligases. On one hand, like RING finger E3 ligases, they also have a RING domain at their N-terminal to bind with the E2 enzymes, however, on the other hand, the transfer of ubiquitin from E2 enzymes to target substrates is a two-step reaction, which is similar to the HECT E3 ligases. The ubiquitin is firstly accepted by the second RING domain which connects to the first RING domain by the central in-between-RINGs (IBR), and then further delivered to the target substrates (189).

1.3.2 The deubiquitinases (DUBs)

As a reversible process, the ubiquitin modification on substrates can be removed by the DUBs, as they can cleavage the ubiquitin chain via the hydrolysis of the isopeptide between ubiquitin and another ubiquitin or the target substrates.

Human cells express approximately 100 different DUBs. These can be classified into six cysteine protease families and one metalloprotease family: ubiquitin-specific proteases (USPs, which is also the largest family among all DUBs), ubiquitin C-terminal hydrolases (UCHs), ovarian tumour proteases (OTUs), Machado-Josephin domain proteases (MJDs), motif interacting with ubiquitin (MIU)- containing novel DUB family (MINDY), Zn-finger and UFSP domain protein (ZUFSP) and Zn-dependent JAB1/MPN/MOV34 metalloprotease (JAMMs) (190,191).

More and more studies have shown that DUBs are involved in the regulation of many other physiological processes, such as DNA damage response, cell cycle regulation,

chromatin remodeling, in addition to the deubiquitination stabilization of substrate proteins (192,193).

1.3.2.1 Deubiquitinase Usp28

Usp28 was first described in 2001 as a homologous of Usp25, and it shares more than 50% of the sequence identity with Usp25. The human Usp28 protein contains 1077 amino acids while the canonical Usp28 is a shorter isoform which lacks the exon 19a (62 amino acids) and is expressed across different tissues, while the full length Usp28 is only found in muscle, heart and brain (194).

1.3.2.1.1 The structure of Usp28

As a member of the USP family, Usp28 has a conserved ubiquitin specific peptidase domain (USP). Similar to the homologous Usp25, Usp28 has a ubiquitin binding region (UBR) which contains the ubiquitin associated domain (UBA), the sumo interacting motif (SIM) and two ubiquitin interacting motifs (UIMs) (193,195). Interestingly, Usp28 has a dimerization domain that allows it to form an active dimer *in vivo*. In contrast, Usp25 forms a catalytically inactive tetramer (196,197).

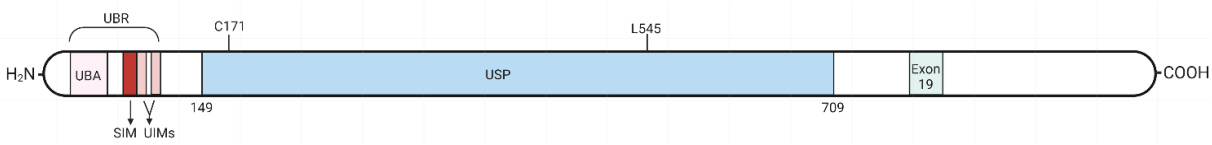

Figure 4. Domain structure of Usp28 (Created with BioRender.com.)

1.3.2.1.2 Usp28 in tumorigenesis

Usp28 is the first DUB found to antagonize FBXW7 and stabilize the oncoprotein Myc (148). FBXW7 is considered to be a tumor suppressor because it can ubiquitinate oncoprotein substrates such as Myc and cyclin E1, leading to their proteasomal degradation and lower protein levels. However, this process can be reversed by Usp28, as it can remove the ubiquitin from the substrates before their proteolysis. Indeed, Usp28 is found overexpressed in many different tumors such as liver cancer, colorectal cancer, bladder cancer, breast cancer, non-small cell lung cancer and glioma. Meanwhile Myc, as well as other non-FBWX7

mediated Usp28 oncoprotein substrates (e.g., LSD1), are also found overexpressed in these tumors. Additionally, the Usp28 protein level was negatively correlated with prognosis (150,198-202).

Intriguingly, Usp28 can not only stabilize the substrates of FBXW7 but also deubiquitinate and stabilize FBXW7 when FBXW7 autocatalytically ubiquitinate itself (149). In this case, Usp28 exhibits a tumor-suppressive function via the destabilization of the oncoproteins through the stabilization of FBXW7. Besides, Usp28 has also been reported to stabilize tumor-suppressive proteins, such as p53, CHK2 and others (203-207). This dual roles of Usp28 elicit an interesting question: is Usp28 a tumor promoter or a tumor suppressor? One reasonable explanation is that the role of Usp28 varies depending on the genetic conditions of the cells, particularly the states of FBXW7 and p53.

The recognition of Usp28 substrates can be mediated by FBXW7 in what is known as the "piggyback" model (208). However, it has also been reported that Usp28 is able to deubiquitinate and stabilize its substrates in the absence of functional FBXW7 (151,209). This suggests that Usp28 can recognize its substrates via other E3 ligases in addition to FBXW7, such as PIRH2, which can modulate the deubiquitination of CHK2 by Usp28 (207). Alternatively, Usp28 may interact with its substrates directly, without the need for any E3 ligases, which is a common feature of many other DUBs (193).

Another important factor in the role of Usp28 is p53, a well-known tumor suppressor that has been reported as a substrate of Usp28, which can deubiquitinate and stabilize it (205). However, p53 is frequently found to be mutated in more than half of all cancers, and the stabilization of mutated p53 by Usp28 is considered a tumor-promoting event, as mutant p53 is known to be an oncoprotein. Mutated p53 not only loses its tumor-suppressive function but also contributes to metastasis and anti-tumor therapy resistance (210).

In short, we cannot simply draw the conclusion that Usp28 is a tumor promoter or a tumor suppressor without considering the genetic environment of the tumor.

1.3.2.1.3 Usp28 and the DNA damage response

Eukaryotic cells have several mechanisms to detect and repair DNA damage upon genotoxic stress. Phosphatidylinositol 3-kinase-like kinases (PIKKs) such as ATM, ATR and DNA-PKcs play a crucial role in initiating a series of intracellular cascades to modulate cellular activities. These activities include gene transcription regulation, cell cycle arrest, DNA repair, and apoptosis (211,212).

Usp28 has shown to play an important role in the DNA damage response as it can regulate the Chk2-p53-PUMA signaling pathway, the key pathway that modulates the

apoptosis induced by DNA damage in response to the most harmful types of DNA damage, such as DNA DSBs (213). The regulation of Usp28 on the Chk2-p53-PUMA signaling pathway depends on the physical interactions between Usp28 and the signaling factors, such as 53bp1 and Chk2. When Chk2-p53-PUMA signaling pathway is activated during DNA damage response, Usp28 is recruited by 53bp1 and can deubiquitinate and stabilize both 53bp1 and Chk2. Furthermore, Usp28 can regulate the pathway via the regulation of p53-mediated pro-apoptotic genes such as PUMA.

However, it is also reported that the significance of Usp28 in the DNA DSB-induced DNA damage response may be less significant than originally expected. It has been shown that Usp28 has minimal effects on DNA damage response in Usp28-deficient cells or mice. Furthermore, the lifespan, immunity, and response to external damage in Usp28-deficient mice are comparable to those of Usp28-wildtype mice (214).

The complex role of Usp28 in DNA damage response may be due to the different pathways in which Usp28 is involved, which can have opposing effects. For example, Usp28 can promote the Chk2-p53-PUMA pathway-induced apoptosis, but it can also contribute to ion radiotherapy resistance through stabilizing Claspin (215). Taken together, the role of Usp28 in DNA damage response must be considered in the context of specific physiological conditions, as it may depend on the cell or tumor type (216).

1.3.2.1.4 Usp28 and cell cycle

Cyclin E, similar to many other cyclin family members, is responsible for the phosphorylation of many downstream proteins by forming a complex with cyclin-dependent kinase 2 (CDK2), thus regulating many cellular processes. For example, it can phosphorylate the retinoblastoma-associated protein (Rb), a key cell cycle regulator and tumor suppressor that can arrest the cell cycle in G1 phase. However, phosphorylation by the Cyclin E-CDK2 complex causes Rb to dissociate from the transcription factor E2F. As a result, E2F can enter the nucleus to transcribe related genes, driving the transition from G1 to S phase and promoting cell proliferation (217).

In normal cells, Cyclin E can be ubiquitinated by FBXW7 and degraded by the proteasome. In several types of cancer, including breast cancer, colon cancer, and bladder cancer, Cyclin E is found to be overexpressed and further promotes tumorigenesis and progression of the cancer. The overexpression of Cyclin E is likely indirectly regulated by Usp28 via the regulation on FBXW7, as the loss of Usp28 can downregulate Cyclin E *in vivo* (149,218).

Usp28 can also regulate cell cycle via stabilization of Claspin. Claspin can activate CHK1 in response to genotoxic stress, but it is ubiquitinated by the E3 ligase SCFβ-TrCP and degraded at the G2 phase when cells are repaired from DNA damage. Therefore, Claspin protein level acts as a threshold for checkpoint activation and the degradation of Claspin allows mitotic entry. The stabilization of Claspin by Usp28 can thereby lead to G2 phase arrest (216). Furthermore, Usp28 can stabilize 53bp1 and lead to activation of p53 in response to ionizing radiation, prolonged mitosis and disruption of centrosomes (204-206).

1.3.2.2 Targeting Usp28 as an anti-tumor strategy

The ubiquitin-proteasome system plays an important role in regulating protein homeostasis via ubiquitin-mediated protein degradation. However, in tumor cells, the balance between oncoproteins and tumor suppressors is usually deregulated, such as over-stabilized oncoproteins or destabilized tumor suppressors, promoting tumorigenesis. Therefore, targeting the ubiquitin-proteasome system can be a promising approach to combat tumors.

In fact, there are already some FDA-approved antitumor drugs that target the ubiquitin-proteasome system, including Bortezomib, the first drug used clinically to treat multiple myeloma (MM) and mantle cell lymphoma, which targets the proteasome, as well as Carfilzomib, a second-generation proteasome inhibitor (219,220). However, due to high toxicity (lack of selectivity towards tumor cells) and patient-unfriendly administration methods (cannot be taken orally) of the current proteasome inhibitors (221,222), scientists have now focused on inhibiting DUBs, since they may stabilize specific oncoproteins and contribute to tumorigenesis.

Indeed, several DUB inhibitors have been reported, such as the Usp1 inhibitor ML323, Usp2 inhibitor ML364 and Usp7 inhibitor P5091 (223). Notably, the Usp14 and UCHL5 inhibitor VLX1570 is the first DUB inhibitor to enter clinical trials (224).

Several inhibitors of Usp28 have also been reported, including AZ1, a small molecule identified by Astra Zeneca through HTS that showed specific activity against Usp28 enzymatic activity and downregulation of Myc (152). Another promising Usp28 inhibitor is FT206, which showed an anti-lung squamous cell carcinoma (LSCC) activity both *in vitro* and *in vivo* (225). Some FDA-approved drugs also exhibited the anti-Usp28 activity, such as vismodegib, a compound clinical used for basal cell carcinoma, showed anti-human colorectal cancer cells activity *in vitro* (226). However, due to the homology between Usp28 and Usp25, the small molecule compounds mentioned above usually show little or no selectivity between Usp28 and Usp25, which limits their further clinical application.

1.4 Aims of the study

Deubiquitinase Usp28 was identified to stabilize Myc, the essential tumorigenesis factor which is dysregulated in a huge number of cancers. Usp28 forms homodimers in cells while the biological role of dimerization remains unknown. Therefore, it is important to understand how Usp28 dimerization controls Myc, especially in the field of Myc-dependent transcription or replication in tumorigenesis. In this thesis, we aim to address the following topics:

To investigate the biological role of Usp28 dimerization on Myc and Myc-dependent functions in the human liver cancer cell line HLF.

To explore the mechanism and key regulators/factors that regulate Usp28 dimerization.

To identify potential clinical benefits arising from a comprehensive understanding of Usp28 dimerization to develop novel antineoplastic therapies.

2. Materials

2.1 Chemicals and reagents

Name	Manufacture	Cat. Number
1-Bromo-3-chloropropane	Sigma	B9673
5-Chloro-2'-deoxyuridine (CIdU)	Cayman	18155
5-Ethynyl-2′-deoxyuridine (EdU)	Cayman	61135-33-9
5-Iodo-2'-deoxyuridine (IdU)	TCI	I0258
Acetic acid	Sigma	ARK2183
Acrylamide-, bisacrylamide, 37.5:1	Roth	3029.1
Agarose Standard	Roth	3810.3
Albumin Fraction V	Roth	8076.4
Ammonium persulfate (APS)	Sigma	A4418
Ampicillin	Roth	HP62.1
Beta-mercaptoethanol	Acros Organics	A0247450
Biotin-16-dCTP	Jena Bioscience	NU-809-BIO16-S
Biotin-16-dUTP	Jena Bioscience	NU-803-BIO16-S
Biotin-Ahx-Ub-VME	UbiQ-054	UbiQ
Biotin-Ahx-Ub-VS	UbiQ-188	UbiQ
Bis-Tris	Sigma	B9754
Blasticidin	Invivogen	ant-bl-1
Bromophenol blue	Sigma	B0126
$CaCl_2$	Sigma	21115
Concanavalin A-coated beads	Cytiva	17044003
Crystal violet solution	Sigma	V5265
$CuSO_4$	Sigma	C8027
Cycloheximide (CHX)	Sigma	C7698
DAPI-containing mounting solution	Biozol	VEC-H-1500
Dithiothreitol (DTT)	Roth	6908.3
DMSO	Roth	A994.2
DNA loading dye 6X	Thermo Fisher Scientific	R0611
Dulbecco's Modified Eagle Medium-high glycose (DMEM)	Life Technologies	41966052
EDTA	Sigma	EDS
EGTA	Sigma	E4378

Name	Manufacture	Cat. Number
Ethanol	Sigma	32205
Ethidium bromide	Roth	2218.1
Etoposide	Cayman	12092
Fetal Bovine Serum (FBS)	Pan Biotech	P40-37500
Fugene transfection reagent	Promega	E2311
GeneRuler 1kb DNA Ladder	Thermo Fisher Scientific	SM0311
GFP-Trap Agarose beads	Chromotec	gta-20
Glycerol	Sigma	G5516
Glycine	Sigma	G7126
Glycoblue	Thermo Fisher Scientific	AM9516
HCl	VWR Chemicals	1099110001
HEPES	Sigma	H0887
Highprep PCR magnetic beads	MagBio Genomics Europe	RC-90005
Hydroxyurea (HU)	Sigma	H8627
Hygromycin B Gold	InvivoGen	ant-hg-1
Imidazole	Sigma	I0250
Immobilon Western HRP substrate A & B	Merck Millipore	WBKLS0500
Isoproponal	Sigma	33539
Kanamycin	Sigma	K0129
KCl	Sigma	P9333
LMP agarose	Promega	V2111
Methanol	Roth	8388.6
MG-132	Selleckchem	S2619
$MgCl_2$	Roth	KK36.1
$MnCl_2$	Roth	4320.1
MOPS	Merck	M1254
NaCl	Roth	3957.2
$NaHSO_3$	Sigma	799394
Nail polish	Essence	-
Native gel (4–20% Precast Protein Gel)	Bio-Rad	4561096
Native sample buffer 2X	Bio-Rad	1610738
N-laurylsarcosine	Sigma	61739
Non-Essential Amino Acids 100X	Sigma	M7145
Non-fat dry milk	Hartenstein	CM35
Opti-MEM	Thermo Fisher Scientific	31985062
PageRuler prestained protein ladder	Thermo Fisher Scientific	26617
Paraformaldehyde (PFA)	Sigma	P6148
PBS	Life Technologies	10010-056

Materials

Name	Manufacture	Cat. Number
PBS tablet	Thermo Fisher Scientific	18912014
Penicillin-Streptomycin	Life Technologies	15140122
Phenol/Chloroform/Isoamyl Alcohol	Roth	A156.1
Phosphatase inhibitor	Sigma	P0044
Picolyl-Azide-Biotin	Sigma	900912
Polybrene	Sigma	107689
Polyethylenimine (PEI)	Sigma	P3143
PolyJet transfection reagent	SignaGen Laboratories	SL100688
Ponceau S	Roth	5938.1
Protease inhibitor	Sigma	P8340
Protein A agarose beads	Thermo Fisher Scientific	20333
Protein A magnetic beads	NEB	S1425S
Protein G agarose beads	Thermo Fisher Scientific	20398
Protein G magnetic beads	NEB	S1430S
PureCube Ni-NTA Agarose beads	Cube Biotech	31105
Puromycin	InvivoGen	ant-pr-1
Quant-iT™ PicoGreen™ dsDNA Reagent	Thermo Fisher Scientific	P7581
SOC medium	NEB	B9020S
Sodium ascorbate	Roth	3149.1
Sodium azide	Sigma	S2002
Sodium dodecyl sulfate	Roth	CN30.3
Sodium acetate	Roth	6773.1
Spermidine	Roth	7161.1
Streptavidin magnetic beads	NEB	S1420S
Sulfo-Cy3-azide	Lumiprobe	A1330
Tetramethylethylenediamine (TEMED)	Roth	2367.3
Thymidine	Biomol	Cay20519-5
Topotecan	Sigma	1672257
Tris	Sigma	T1503
Tris Base	Hartenstein	CT62
Tris-HCl	Sigma	T5941
TritonX-100	Amresco	M143
TRI RNA isolation reagent	Sigma	T9424
Trypsin-EDTA	Life Technologies	25300054
Tween20	Sigma	P1379
Ultra pure water	Life Technologies	10977-035
Urea	Roth	7638.1
Zeocin	InvivoGen	ant-zn-1

2.2 Buffers

Name	Composition
Annealing buffer 10X	1 M NaCl, 100 mM Tris-HCl (pH 7.4)
Bis-Tris buffer	1.25 M Bis-Tris (pH 6.8)
C & R antibody buffer	C & R tritonX-wash buffer with 2 mM EDTA
C & R binding buffer	20 mM Hepes (pH 7.5), 10 mM KCl, 1 mM $CaCl_2$, 1 mM $MnCl_2$
C & R incubation buffer	3.5 mM Hepes (pH 7.5), 10 mM $CaCl_2$, 0.1% TritonX-100
C & R low-salt rinse buffer	20 mM Hepes (pH 7.5), 0.5 mM Spermidine, 0.1% TritonX-100
C & R stop buffer	170 mM NaCl, 20 mM EGTA, 0.1% TritonX-100, 50 µg/ml RNase A
C & R tritonX-wash buffer	C & R wash buffer with 0.1% TritonX-100
C & R wash buffer	20 mM Hepes (pH 7.5), 150 mM NaCl, 0.5 mM Spermidine, add Protease/Phosphatase inhibitors before use
Fiber lysis buffer	200 mM Tris (pH 7.5), 50 mM EDTA, 0.5% SDS
Hypotonic buffer	50 mM KCl, 10 mM Hepes (pH 7.5)
Laemmli sample buffer 4X	277.8 mM Tris-HCl (pH 6.8), 44.4% Glycerol, 4.4% SDS, 0.02% Bromophenol blue
Native gel running buffer	192 mM Glycin, 25 mM Tris
Neutral comet lysis buffer	2.5 M NaCl, 100 mM EDTA, 10 mM Tris base (pH 10), 1% N-laurylsarcosine, 0.5%TritonX-100, 10% DMSO
Running buffer 1X	5% Running buffer 20X, 2 mM $NaHSO_3$
Running buffer 20X	1 M MOPS, 1 M Tris, 20 mM EDTA, 2% SDS
Stripping buffer	60 mM Tris (pH 6.8), 2% SDS, 0.7% Beta-mercaptoethanol
TAE buffer 50X	2 M Tris base, 1 M Acetic acid, 50 mM EDTA
TBS buffer 10X	1.5 M NaCl, 500 mM Tris base
TBST buffer	10% TBS 10X, 0.05% Tween20
TE buffer	10 mM Tris-HCl (pH 8.0), 1 mM EDTA
TNT lysis buffer	25 mM Tris-HCl (pH 8.0), 0-300 mM NaCl, 1% TritonX-100
Transferring buffer 10X	1.92 M Glycin, 250 mM Tris
Transferring buffer 1X	10% Transferring buffer 10X, 10% Methanol
Urea lysis buffer	8 M Urea, 10 mM Imidazole in PBS

2.3 Enzymes and Readymixs

Name	Manufacture	Cat. Number
AgeI	Thermo Fisher Scientific	ER1461
DNase I	Thermo Fisher Scientific	EN0521
EcoRI	Thermo Fisher Scientific	ER0271
KAPA HiFi HotStart ReadyMix	Roche	7958927001
Micrococcal Nuclease	NEB	M0247S
MLV reverse transcriptase	Promega	M1705
NEBNext Ultra II Q5 Master Mix	NEB	M0544L
Protein A/G MNase	Dr. Giacomo Cossa	-
Proteinase K	Thermo Fisher Scientific	EO0491
RiboLock RNase inhibitor	Thermo Fisher Scientific	EO0382
RNase A	Thermo Fisher Scientific	EN0531
SpeI	Thermo Fisher Scientific	ER1251
SYBR Green JumpStart Taq ReadyMix	Sigma	S4438-500RXN
T4 DNA Ligase	NEB	M0202S
XhoI	Thermo Fisher Scientific	ER0691

2.4 Kits

Name	Manufacture	Cat. Number
Duolink In Situ Detection Reagents Green	Sigma	DUO92014-100RXN
Duolink In Situ Detection Reagents Red	Sigma	DUO92008-100RXN
Duolink In Situ PLA® Probe Anti-Mouse PLUS	Sigma	DUO92001-100RXN
Duolink In Situ PLA® Probe Anti-Rabbit MINUS	Sigma	DUO92005-100RXN
GenElute HP Plasmid Midiprep Kit	Sigma	NA0200-1KT
GenElute HP Plasmid Miniprep Kit	Sigma	PLN70-1KT
Monarch DNA Gel Extraction Kit	NEB	T1020S
Mycoplasma detection Kit	abm	G238
NEBNext Multiplex Oligos for Illumina (Index Primer Set 1)	NEB	E7600S
NEBNext Multiplex Oligos for Illumina (Index Primer Set 2)	NEB	E7500S
NEBNext Poly(A) mRNA Magnetic Isolation Module	NEB	E7490S
NEBNext Ultra II DNA Library Prep Kit for Illumina	NEB	E7645S
NEBNext Ultra RNA Library Prep Kit for Illumina	NEB	E7770S
NEBuilder HiFi DNA Assembly Cloning Kit	NEB	E5520S
Pierce BCA Protein Assay Kit	Thermo Fisher Scientific	23225

2.5 Bacterias

Name	Manufacture	Cat. Number
NEB® 10-beta competent E. coli (high efficiency)	NEB	C3019I

2.6 Cell lines

Name	Feature	Source
HLF	parental HLF cells	Dr. Ramona Rudalska
HLF Usp28KO	Usp28KO by crispr, puromycin resistence (0.5 µg/ml)	Established in this thesis
HLF sh53bp1	53bp1 depletion by lentiviral, puromycin resistence (0.6 µg/ml)	Established in this thesis
HLF shCtrl	empty pLKO vector, puromycin resistence (0.5 µg/ml)	Established in this thesis
HLF Usp28KO+shCtrl	Usp28KO with empty pLKO vector, puromycin resistence (5 µg/ml)	Established in this thesis
HLF Usp28KO+sh53bp1	Usp28KO with 53bp1 depletion, puromycin resistence (5 µg/ml)	Established in this thesis
HLF Usp28-WT	Usp28KO cells with HA-tagged Usp28-WT expressing, hygromycin resistence (250 µg/ml)	Prof. Nikita Popov
HLF Usp28-M	Usp28KO cells with HA-tagged Usp28-Monomer (L545E) expressing, hygromycin resistence (250 µg/ml)	Prof. Nikita Popov
HLF mCherry	Usp28KO cells with mCherry expressing, hygromycin resistence (250 µg/ml)	Prof. Nikita Popov
HLF Usp28-WT+shCtrl	HLF Usp28-WT cells with empty pLKO vector, puromycin resistence (5.5 µg/ml)	Established in this thesis
HLF Usp28-WT+sh53bp1	HLF Usp28-WT cells with 53bp1 depletion, puromycin resistence (5.5 µg/ml)	Established in this thesis
HLF Usp28-M+shCtrl	HLF Usp28-M cells with empty pLKO vector, puromycin resistence (5.5 µg/ml)	Established in this thesis
HLF Usp28-M+sh53bp1	HLF Usp28-M cells with 53bp1 depletion, puromycin resistence (5.5 µg/ml)	Established in this thesis
HLF Usp28-WT+shCtr9	HLF Usp28-WT cells with Ctr9 depletion, puromycin resistence (5 µg/ml)	Established in this thesis
HLF Usp28-M+shCtr9	HLF Usp28-M cells with Ctr9 depletion, puromycin resistence (5 µg/ml)	Established in this thesis
HLF Usp28-WT+shCdc73	HLF Usp28-WT cells with Cdc73 depletion, puromycin resistence (5 µg/ml)	Established in this thesis

Name	Feature	Source
HLF Usp28-M+shCdc73	HLF Usp28-M cells with Cdc73 depletion, puromycin resistence (5 µg/ml)	Established in this thesis
HCT116 shCtrl	HCT116 parental cells with empty pLKO vector (Dox inducible)	Elias Einig
HCT116 shMyc-1	HCT116 parental cells with Myc depletion (Dox inducible)	Elias Einig
HCT116 shMyc-2	HCT116 parental cells with Myc depletion (Dox inducible)	Elias Einig
HeLa	parental HeLa cells	Ravi B Kollampaly
HeLa Usp28KO	Usp28KO by crispr	Ravi B Kollampaly
HeLa 53bp1KO	53bp1KO by crispr	Ravi B Kollampaly
p19$^{-/-}$Nras HA-Usp28 + mCherry	p19$^{-/-}$Nras cells with HA-tagged Usp28 (blasticidin resistence) and mCherry expressing (hygromycin resistence, 100 µg/ml)	Established in this thesis
p19$^{-/-}$Nras HA/GFP-Usp28	p19$^{-/-}$Nras cells with HA-tagged Usp28 (blasticidin resistence) and GFP-tagged Usp28 expressing (hygromycin resistence, 100 µg/ml)	Established in this thesis
p19$^{-/-}$Nras HA-Usp28 + mCherry + shCtrl	p19$^{-/-}$Nras HA-Usp28 + mCherry cells with empty pLKO vector, puromycin resistence (4.5 µg/ml)	Established in this thesis
p19$^{-/-}$Nras HA-Usp28 + mCherry + sh53bp1	p19$^{-/-}$Nras HA-Usp28 + mCherry cells with 53bp1 depletion, puromycin resistence (4.5 µg/ml)	Established in this thesis
p19$^{-/-}$Nras HA/GFP-Usp28 + shCtrl	p19$^{-/-}$Nras HA/GFP-Usp28 cells with empty pLKO vector, puromycin resistence (4.5 µg/ml)	Established in this thesis
p19$^{-/-}$Nras HA/GFP-Usp28 + sh53bp1	p19$^{-/-}$Nras HA/GFP-Usp28 cells with 53bp1 depletion, puromycin resistence (4.5 µg/ml)	Established in this thesis
p19$^{-/-}$Nras Usp28-WT	p19$^{-/-}$Nras cells with Usp28-WT expressing	Ravi B Kollampaly
p19$^{-/-}$Nras Usp28-M	p19$^{-/-}$Nras cells with Usp28-Monomer (L545E) expressing	Ravi B Kollampaly
p19$^{-/-}$Nras shCtrl	p19$^{-/-}$Nras cells with empty pLKO vector	Ravi B Kollampaly
p19$^{-/-}$Nras sh53bp1	p19$^{-/-}$Nras cells with 53bp1 depletion	Ravi B Kollampaly
LentiX	subclone of the transformed human embryonic kidney cell line, HEK293 (TaKaRa)	Dr. Liudmyla Taranets

2.7 Antibodies

Name	Application	Catalog No.	Manufacture
53bp1 (BP13), Mouse	IP	MAB3802	Millipore
53bp1, Rabbit	IB, IF, PLA	NB100-304	Novus
anti-BrdU (B44), Mouse	Fiber	BD347580	Biosciences
anti-BrdU (BU1/75 (ICR1), Rat	Fiber	ab6326	Abcom
Anti-Mouse IgG-HRP	IB	7076S	CST
Anti-Mouse-Alexa 488	IF	4408S	CST
Anti-Mouse-Alexa 555	Fiber	4409S	CST
Anti-Rabbit IgG-HRP	IB	7074S	CST
Anti-Rabbit-Alexa 488	IF	4412S	CST
Anti-Rabbit-Alexa 555	IF	4413S	CST
Anti-Rat-Alexa 488	Fiber	4416S	CST
Beta-Actin (AC15), Mouse	IB	A5441	Sigma
Cdc73 (2H1), Mouse	PLA	sc-33638	Santa Cruz
Ctr9, Rabbit	PLA	12619S	CST
FLAG (M2), Mouse	IB, IP	F1804-200UG	Sigma
GAPDH, Rabbit	IB	5174S	CST
GFP (B-2), Mouse	IB, PLA	sc-9996	Santa Cruz
GFP-Trap Agarose	IP	gta-20	Chromotek
HA-Tag (6E2), Mouse	PLA	2367S	CST
HA-Tag (C29F4), Rabbit	IB, PLA	3724S	CST
IgG (DA1E), Rabbit	IP	3900S	CST
IgG (G3A1), Mouse	IP	5415S	CST
Leo1, Rabbit	C & R	A300-175A	Bethyl
Myc (C-33), Mouse	PLA	sc-42	Santa Cruz
Myc, Rabbit	IB	9402S	CST
Myc (D3N8F), Rabbit	IB	13987S	CST
Myc (Y69), Rabbit	PLA	ab32072	Abcom
Paf1, Rabbit	PLA	15441-1-AP	Proteintech
PCNA (PC10), Mouse	PLA	sc-56	Santa Cruz
pH2AX (Ser139), Mouse	IB, IF	sc-517348	Santa Cruz
pS5-RNAPII (D9N5I), Rabbit	PLA	13523S	CST
RNAPII (D8L4Y), Rabbit	PLA	14958S	CST
Usp25, Rabbit	IB	12199-1-AP	Proteintech
Usp28, Rabbit	IB, IF, PLA	17707-1-AP	Proteintech
Usp28, Rabbit	IB	HPA006778-100	Sigma
Vinculin (hVIN-1), Mouse	IB	V9131	Sigma

2.8 Oligonucleotides

Name	Sequence (5'-3')	Application
Usp28-monomer forward	GTTAAGACCTGTGAACAGAGATGGAGGAG	Mutagenesis
Usp28-monomer reverse	CTCCTCCATCTCTGTTCACAGGTCTTAAC	Mutagenesis
sfGFP forward	TGAGTCGGCCGGTGGATCCAATGAGCAAG GGCGAGGAG	cloning
sfGFP reverse	CCGCAGTCATCTTGTACAGCTCGTCCATG	cloning
Usp28 forward	GCTGTACAAGATGACTGCGGAGCTGCAG	cloning
Usp28 reverse	GAGGGGCGGATCCGTCGACATTATTTCAC TGTCACAGTTGAAACTCC	cloning
sfGFP-Usp28 forward	CGGCATGGACGAGCTGTACAAGGGAGGCT CTACTGCGGAGCTGCAGCAGGACG	cloning
sfGFP-Usp28 reverse	CGTCCTGCTGCAGCTCCGCAGTAGAGCCT CCCTTGTACAGCTCGTCCATGCCG	cloning
h53bp1-1 forward	CCGGCCCTTGTTCAGGACAGTCTTTCTCGA GAAAGACTGTCCTGAACAAGGGTTTTTG	shRNA
h53bp1-1 reverse	AATTCAAAAACCCTTGTTCAGGACAGTCTT TCTCGAGAAAGACTGTCCTGAACAAGGG	shRNA
h53bp1-2 forward	CCGGGATACTTGGTCTTACTGGTTTCTCGA GAAACCAGTAAGACCAAGTATCTTTTTG	shRNA
h53bp1-2 reverse	AATTCAAAAAGATACTTGGTCTTACTGGTTT CTCGAGAAACCAGTAAGACCAAGTATC	shRNA
m53bp1-1 forward	CCGGCAAGTCCTTCACCCGCATTATCTCGA GATAATGCGGGTGAAGGACTTGTTTTTG	shRNA
m53bp1-1 reverse	AATTCAAAAACAAGTCCTTCACCCGCATTA TCTCGAGATAATGCGGGTGAAGGACTTG	shRNA
m53bp1-2 forward	CCGGTGAATGGACAGTGACTATAAACTCGA GTTTATAGTCACTGTCCATTCATTTTTG	shRNA
m53bp1-2 reverse	AATTCAAAAATGAATGGACAGTGACTATAA ACTCGAGTTTATAGTCACTGTCCATTCA	shRNA
hUsp28 forward	CACCGGAGTTGATGGTTGGCCAGTT	sgRNA
hUsp28 reverse	AAACAACTGGCCAACCATCAACTCC	sgRNA
hCALM2 forward	CGGACTAATTCGCCTCCTCC	qPCR
hCALM2 reverse	GTGAAGAAAGGGGTCCCGAG	qPCR
hNPM1 forward	CTCGCGAGATCTTCAGGGTC	qPCR
hNPM1 reverse	AGAACGCTGCTCCAGAGAAC	qPCR
hRPS13 forward	GAAGTGACCTCACACGTCCC	qPCR
hRPS13 reverse	CTCTTGCGACGCTGAAATGC	qPCR

Name	Sequence (5'-3')	Application
hSRSF7 forward	GCGTCATCTCGTTGTTCTGC	qPCR
hSRSF7 reverse	CATGACCCGCGTGTTAGTCT	qPCR
hMTIF2 forward	CGCTGGAAAAGGTTCTTTCCG	qPCR
hMTIF2 reverse	AGGTTGAACCAGCGCCTC	qPCR
hMyc forward	TCCTACGTTGCGGTCACA	qPCR
hMyc reverse	GCTCGGTCACCATCTCCA	qPCR
hBeta-actin forward	CCAACCGCGAGAAGATGA	qPCR
hBeta-actin reverse	TCCATCACGATGCCAGTG	qPCR
U6 forward	GAGGGCCTATTTCCCATGATTCC	sequencing
SFFV forward	CTTCTGCTTCCCGAGCTCTA	sequencing
CMV forward	CGCAAATGGGCGGTAGGCGTG	sequencing

2.9 Plasmids (vectors, generated plasmids)

Vectors:

Name	Feature	Source
pSpCas9(BB)-2A-Puro (PX459)	cloning backbone for sgRNA with Cas9 from S. pyogenes, puromycin resistance, U6 promoter	Feng Zhang, Addgene plasmid # 62988
pLKO1	lentiviral expression vector, puromycin resistance, U6 promoter	Bob Weinberg, Addgene plasmid # 8453
pRRL	lentiviral expression vector, hygromycin resistance, SFFV promoter	Prof. Martin Eilers
pcDNA3.1	eukaryotic expression vector, CMV promoter	Prof. Nikita Popov
pPAX2	packaging plasmid for lentiviral production vector	Didier Trono, Addgene plasmid # 12260
pMD2G/VSVG	envelope plasmid for lentiviral production vector	Didier Trono, Addgene plasmid # 12259

Cloned constructs:

Name	Feature	Source
PX459-h-sgUsp28	with sgRNA targets gene coding human Usp28	Established in this thesis
pSpCas9(BB)-2A-GFP (PX458)	with gene expresses green fluorescent protein (GFP)	Dr. Liudmyla Taranets, Addgene plasmid # 48138
pLKO1-h-sh53bp1-1	with shRNA (pair 1) against human 53bp1 mRNA	Established in this thesis
pLKO1-h-sh53bp1-2	with shRNA (pair 2) against human 53bp1 mRNA	Established in this thesis
pLKO1-h-sh53bp1-3	with shRNA (pair 1&2) against human 53bp1 mRNA	Established in this thesis
pRRL-HA-Usp28-WT	with cDNA expresses HA-tagged human wild type Usp28	Prof. Nikita Popov
pRRL-HA-Usp28-M	with cDNA expresses HA-tagged human monomeric Usp28 (L545E)	Prof. Nikita Popov
pRRL-mCherry	with cDNA expresses cherry red fluorescent protein (RFP)	Prof. Nikita Popov
pLKO1-h-shCtr9-1	with shRNA against human Ctr9 mRNA	Sigma, TRCN0000008739
pLKO1-h-shCtr9-2	with shRNA against human Ctr9 mRNA	Sigma, TRCN0000008741
pLKO1-h-shCdc73-1	with shRNA against human Cdc73 mRNA	Sigma, TRCN0000008728
pLKO1-h-shCdc73-2	with shRNA against human Cdc73 mRNA	Sigma, TRCN0000011464
pRRL-GFP-Usp28	with cDNA expresses GFP-tagged human wild type Usp28	Established in this thesis
pLKO1-m-sh53bp1	with shRNA (pair 1&2) against mouse 53bp1 mRNA	Ravi B Kollampaly
pcDNA3.1-His-Ub-WT	with cDNA expresses His-tagged wild type ubiquitin	Prof. Nikita Popov
pcDNA3.1-His-Ub-K11o	with cDNA expresses His-tagged K11 only ubiquitin	Prof. Nikita Popov
pcDNA3.1-His-Ub-K48o	with cDNA expresses His-tagged K48 only ubiquitin	Prof. Nikita Popov
pcDNA3.1-HA-Usp28-WT	with cDNA expresses HA-tagged wild type Usp28	Prof. Nikita Popov
pcDNA3.1-Strep-HA-Usp28-M	with cDNA expresses Strep-HA-tagged monomeric Usp28	Prof. Nikita Popov
pcDNA3.1-Myc	with cDNA expresses wild type Myc	Prof. Nikita Popov
pDZ-Flag-Usp28	with cDNA expresses Flag-tagged Usp28	Prof. Martin Eilers, Addgene plasmid # 15665

2.10 Instrumentation

Device	Manufacturer
4 °C/-20 °C fridge	LIEBHERR
-80 °C freezer	SANYO VIP series -86 °C
Agarose gel imaging machine	INTAS
Bacteria incubator	Thermo scientific Heraeus FUNCTION Line
Bacteria shaker	INFORS HAT Multitron Standard
Cell counter	Countess II FL
Cell culture cabinet	Thermo scientific HERASAFE 2030i
Cell culture incubator	BINDER
Centrifuge	VWR MICRO STAR 17R; Thermo scientific Multifuge X Pro Series; Thermo scientific SORVALL LYNX 6000
Chemiluminescence imaging machine	Bio-rad ChemiDoc MP Imaging System
Electrophoresis chamber	Bio-Rad Compact XS/S, M
Heating	SUN lab SU1150
Heating block	Labnet
Illumina NextSeq instrument	Illumina NextSeq 500
Micro centrifuge	Roth; CORNING; VWR PCR PLATE SPINNER
Microscope	OLYMPUS DP28; OLYMPUS DP80
Mixer	STAR LAB Mixer HC
Nanodrop	Thermo scientific NANODROP 1000
PCR thermal cycler	Bio-rad T100 Thermal Cycler
pH meter	Schott Lab850
Power supply	VWR
Quantitative RT-PCR machine	Bio-rad CFX Connect Real-Time System
Reader	TECAN INFINITE M PLEX
Rotator	Thermo scientific; PHOENIX RS-TR05; A.Hartenstein
SDS PAGE chamber	Bio-Rad
Shaker	CAT ST15
Ultrasonificator	hielscher UP200ST Ultrasonic Processor
Vortexer	neoLab D-6012
Water bath	GFL
Wet transfer chamber	biostep GB33-N1010

2.11 Software

Softwares:

Name	Manufacturer
ApE plasmid editor	by M. Wayne Davis
Bio-Rad CFX Manager 3.1	Bio-Rad
Endnote 20	Clarivate
GraphPad 9	GraphPad Software, Inc.
ImageJ (version 1.53f)	FIJI
ImageLab	Bio-Rad
Integrated Genome Browser	by Nicol et al., 2009
Office 365	Microsoft
SnapGene Viewer	GSL Biotech

Websites:

Name	Source
BioGrid	https://thebiogrid.org/
bioRENDER	https://www.biorender.com/
cBioPortal	https://www.cbioportal.org/
Ensembl	https://www.ensembl.org/index.html
GPP Web Portal	https://portals.broadinstitute.org/gpp/public/
Microsynth	https://srvweb.microsynth.ch/
Oligo order	https://www.sigmaaldrich.com/DE/de/configurators/tube?product=standard
Predesigned shRNA	https://www.sigmaaldrich.com/DE/de/semi-configurators/shrna?activeLink=productSearch
Primer designing tool	https://www.ncbi.nlm.nih.gov/tools/primer-blast/index.cgi
Primer3web	https://primer3.ut.ee/
Protein Blast	https://blast.ncbi.nlm.nih.gov/Blast.cgi?PROGRAM=blastp&PAGE_TYPE=BlastSearch&BLAST_SPEC=blast2seq&LINK_LOC=blasttab
UniProt	https://www.uniprot.org/

2.12 Others

All the consumables items such as plastic products (cell culture plates and dished, pipette tips, tubes, falcons and so on) were purchased from Zentrallager, Sarstedt, Thermo Fisher Scientific, Greiner, Merck Millipore, Eppendorf; glass products (slides, coverslips and so on) were purchased from Hartenstein; Immunoblotting PVDF membranes were purchased from VWR and the blotting paper was purchased from Hartenstein.

3. Methods

Part of this chapter is adapted from the manuscript ‘Jin, C., Einig, E., Xu, W., Kollampally, R.B., Schlosser, A., Flentje, M. and Popov, N. (under revision) The dimeric deubiquitinase Usp28 integrates 53bp1 and Myc functions to limit DNA damage.’ (1).

3.1 Cell biology methods

3.1.1 Cultivation of mammalian cells

All cell lines used in this thesis were cultured in DMEM with 10% FBS, 1% Non-Essential Amino Acids, 1% Penicillin-Streptomycin and 56 µM beta-mercaptoethanol in a humidified atmosphere at 37 °C and 5% CO_2.

Cell maintenance and passaging

All cell lines were cultured for a maximum of 3 months and replaced with prior cryopreserved backups to avoid senescence, mutation, or bacterial contamination. Cell morphology and mycoplasma were regularly checked by eye observation and corresponding test kit according to the manufacturer’s protocol.

Cells were passaged or seeded when they reached around 90% confluence. They were washed twice with PBS and then incubated with 0.05% trypsin-EDTA (1 ml for a 10-cm dish) at 37 °C for 5 min until all cells were detached. The same volume of culture medium was added to quench the remaining trypsin. Cells were resuspended and centrifuged at 4 °C for 5 min at a speed of 2500 G. After centrifugation, the supernatant was discarded and the cell pellet was resuspended in fresh culture medium. Cells were then passaged into new dishes at a ratio of 1:10.

For seeding cells in specific experiments that required a certain cell number or confluency, cells were counted using the COUNTESSII cell counter according to the manufacturer’s protocol. The required number of cells were then seeded with the corresponding ratio.

Cell cryopreservation

To store cells long-term, they were collected at around 90% confluence using trypsin-EDTA as described above. After discarding the supernatant, cryopreservation medium (90% FBS and 10% DMSO, freshly prepared) was added to resuspend the cells. The cells were then aliquoted into cryovials, labeled (usually three cryovials for cells from a 90% confluent 10-cm dish), and frozen gradually by storing them in a cryobox containing isopropanol at -80 °C. The cryovials were then transferred into a common box at -80 °C.

For cell lines that were newly established, they should be cryopreserved as soon as the selection was completed in order to preserve the earliest passages.

Cell recovery

The cryovials were thawed in a 37 °C water bath, and the cell suspension was further centrifuged to remove the DMSO from the cryopreservation medium. The cell pellet was then resuspended in culture medium and transferred into a new dish with fresh culture medium. The medium was changed the next day after washing with PBS, and newly thawed cells could be used for further experiments after at least one passage.

3.1.2 Novel mammalian cell lines establishment

Dozens of novel mammalian cell lines with specific features were established in the thesis for study, and different methods were applied to obtain these cell lines.

Stable mammalian cell lines establishment

CRISPR-Cas9 system

SgRNAs against hUsp28 were cloned into the pSpCas9(BB)-2A-Puro (PX459) V2.0 vector and transfected into parental HLF cells using Fugene HD transfection reagent according to the following protocol:

Day 1: 200,000 parental HLF cells were seeded in a 6-well plate with culture medium.

Day 2: 3.3 μg of sgRNA against hUsp28 in PX459 was added to 155 μl of Opti-MEM and mixed well by vortexing. 19.8 μl of Fugene HD transfection reagent was directly added to the DNA solution, and the mixture was incubated at room temperature for 10 min after

vortexing. All the DNA/Fugene HD transfection reagent mixtures were added to the HLF cells without changing the culture medium. The cells were then incubated at 37 °C for 48 h.

Day 4: Transfected HLF cells were splitted into a 10-cm dish and started puromycin selection with a final concentration of 0.5 μg/ml when cells were all attached.

After puromycin selection, the cell pool was verified by Western blotting against Usp28 to confirm a significant reduction of Usp28 protein levels. Subsequently, the cell pool was diluted to a density of 10 cells per ml, and 100 μl of the cell suspension was added into a single well of a 96-well plate to allow for single cell seeding. The cells were cultured until a single colony could be detected, and then transferred into a 6-well plate for expansion. The cells were then subjected to Western blot analysis to confirm the knockout of Usp28.

Lentiviral transduction system

ShRNAs against scramble/h53bp1/hCtr9/hCdc73/hMyc were cloned into pLKO1.puro vector, cDNAs targeting mCherry/Usp28-WT/Usp28-M/GFP-Usp28 were cloned into pRRL-hygro vector. These plasmids were further transduced into target cells via the lentiviral transduction system as follow:

Day 1: 3.5-4.5 million of lentiX cells were seeded into a new 10-cm dish.

Day 2: 30 μl of PEI (1 mg/ml) was mixed with 670 μl of plain DMEM meanwhile 11.1 μg of target plasmids/2.8 μg of packaging plasmid pPAX2/1.4 μg of envelope plasmid pMD2G/VSVG were mixed with 650 μl of plain DMEM (15.3 μg of GFP in PX458 could also be added in a separate group without packaging/envelope plasmids to check the transfection efficiency). All solutions were incubated for 10 min until PEI solution was added into plasmids solution. Afterwards, the mixture was vortexed and incubated for another 10 min, meanwhile lentiX cells were changed with 6 mL fresh culture medium. The PEI-plasmids mixture was added into lentiX cells dropwise and mixed well by gentle swirling. LentiX cells were labeled with “S2” as they were starting lentivirus production and all the rest procedures should be done under S2 requirements.

Day 3: GFP group was checked to confirm the transfection efficiency. The medium of lentiX cells was changed with 7 ml fresh culture medium 24 h after the transfection meanwhile target cells were seeded into a 6-well plate with 10,000 cells per well.

Day 4: The lentivirus-containing medium was harvested from lentiX cells using a syringe 48 hours after transfection. The medium was then filtered through a 0.45 μM filter to remove any floating lentiX cells and debris. The culture medium of the target cells was changed with 1 mL of fresh medium, and 2 ml of filtered virus medium was added dropwise for infection. Polybrene was also added to the target cells with a final concentration of 8 μg/ml. Finally, 7 ml of fresh culture medium was added back to the lentiX cells.

Day 5: Second infection was done 72 h after the transfection the same as described above.

Day 7: Target cells were selected by puromycin or hygromycin with the concentration pre-screened, based on the resistance from corresponding plasmids. Target cells could also be passaged first if they were confluent at this moment, and the selection should be started when target cells were attached again.

Unstable mammalian cell lines establishment

For transient transfection, both PEI and PolyJet reagent were used in this thesis.

For HA/Flag-Usp28 co-immunoprecipitation assay, either HA-Usp28 in pcDNA3 plasmid and Flag-Usp28 in pDZ plasmid were co-transfected with PEI into HeLa WT cells or only the HA-Usp28 in pcDNA3 plasmid was transfected with PEI into HeLa WT cells as a negative control. The transfection was done as follow:

Day 1: 200,000 of HeLa cells were seeded into a 6-well plate per well with culture medium.

Day 2: 1.25 µg of HA-Usp28 pcDNA3 with 1.25 µg of empty pcDNA3 or 1.25 µg of Flag-Usp28 pDZ were mixed well in 100 µl of plain DMEM and 5 µl of PEI (1 mg/ml) was also well mixed with 100 µl of plain DMEM (2.5 µg of GFP in PX458 could also be added in a separate group to check the transfection efficiency). Both solutions were incubated at room temperature for 10 min until PEI solution was added into DNA solution. The mixture was further vortexed and incubated for another 10 min and meanwhile the medium of HeLa WT cells was changed by 2 ml fresh culture medium. The DNA/PEI mixture was added into HeLa WT cells dropwise and incubated at 37 °C overnight.

Day 3: The transfection efficiency could be checked by GFP signal and the medium was changed by fresh culture medium.

The transfected cells should be collected as soon as they were confluent for further verification or other research usage as they were transient transfected and the new feature could not last long.

For ubiquitin pulldown assay, a total amount of 1 µg of Myc-WT/His-Ub/Usp28-WT/Usp28-M in pcDNA3 were co-transfected into HeLa WT/HeLa 53bp1KO cells with 3 µl Polyjet transfection reagent, the procedure was the same as the PEI procedure described above.

3.2 Biochemical methods

3.2.1 Whole cell proteins extraction

To extract proteins from whole cells, the target cells were washed with PBS and then trypsinized using trypsin-EDTA. After centrifuging the cells at 4 °C for 5 min at 2500 G to remove the medium and trypsin, the cell pellets were resuspended in PBS and centrifuged again to discard the supernatant. The pellets were then resuspended in TNT-150 lysis buffer with protease inhibitor and phosphatase inhibitor (both at 1:1000) and sonicated using the following parameters: 4 °C, 100% cycle, 30% amplitude, 30 sec. The lysates were subsequently centrifuged at 4 °C for 10 min at 17000 G, and the supernatant was transferred to a fresh 1.5 ml eppendorf tube. To determine protein concentration, 10 µl of lysate was aliquoted, and the remaining lysates were mixed with 4X Laemmli sample buffer and boiled at 95 °C for 10 min before being stored at -20 °C for long-term storage.

3.2.2 Total protein concentration measurement

The bicinchoninic acid colorimetric assay (BCA) was utilized to determine the total protein concentration of the cell lysates. Initially, 5 µl of the fresh lysates were added to a well of a transparent 96-well plate, followed by the addition of 100 µl of the freshly prepared BCA measurement buffer (Buffer A: Buffer B = 50:1). To avoid pipetting errors, two wells were made for each sample and a blank control was also included, consisting of 5 µl of lysis buffer instead of lysates. The reaction mixture was then incubated for 30 min in a 37 °C incubator, and the absorbance was measured at 560 nm wavelength using the TECAN infinite M200 PRO Reader. The protein concentration of each sample was determined using a standard formula, which was generated using BSA standards of different concentrations included in the BCA kit.

3.2.3 SDS-PAGE and Western Blot

SDS polyacrylamide gel electrophoresis (SDS-PAGE) was used to separate proteins based on their molecular mass. In principle, proteins were denatured and negatively charged by SDS so that they could migrate toward the positively charged electrode during the gel

electrophoresis. Subsequently the western blot was used for specific protein detection. The full procedures are as follow:

Bis-Tris polyacrylamide gel preparation: For 4 Bis-Tris polyacrylamide gels containing 7-15 % resolving and 4% stacking gels with 1.5 mm thickness, the recipe is show in the table below:

Component	Stacking gels (4X)	Resolving gels (4X)
30% acrylamide	1.3 ml	7.5-16.0 (7%-15%) ml
ddH_2O	4.3 ml	15.5-7 (7%-15%) ml
Bis-Tris	2.3 ml	8.8 ml
10% APS	100 µl	320 µl
TEMED	2.5 µl	24 µl

7.5 ml of the resolving gel solution was poured into the 1.5 mm thickness casting chamber and 1 ml 80% ethanol was added on above to make a flat surface. Ethanol was discarded when the resolving gels were solidified and 2 ml of stacking gel solution was added on the top together with a 10/15-well 1.5 mm thickness comb. Gels were ready to use when stacking gels were also solidified and combs were carefully removed.

Gel electrophoresis: Protein samples were boiled again at 95 °C for 10 min and loaded into the gel with equal amounts based on the concentration measurement after cooling. Page Ruler Prestained Protein Ladder was also added as the marker to indicate different molecular weight. The electrophoresis was performed with the prechilled 1X running buffer at 80 V for 20 min and 120 V for 60 min.

Protein transferring: To transfer the proteins from gels to PVDF membranes for further immunoblotting, the gels were assembled with methanol preactivated PVDF membranes in the following order in the prechilled 1X transferring buffer: sponge - two Waterman filter paper - PVDF membrane - gel - two Waterman filter paper - sponge. Make sure the bubbles between the membrane and gel were carefully removed and the membrane towards the positively charged electrode. Wet transfer was performed at 4 °C and 125 V for 125 min.

Immunoblotting: Membranes were carefully taken from the transfer sandwich and washed once with TBST and further incubated in the blocking buffer (5% non-fat dry milk or 5% BSA in TBST) for 60 min at room temperature. Afterwards membranes were washed with TBST

and cut and incubated with specific primary antibodies overnight at 4 °C with rotation. The membranes were washed with TBST three times with 10 min each time before incubated with secondary antibodies at room temperature for 2 h on a shaker and followed by another three times TBST washing with 10 min each time. To visualize the proteins, the membranes were covered by Immobilon Western Substrate (Millipore, 1:1) and the chemiluminescence was performed in the ChemiDocTM MP Imaging Device.

Stripping: The blotted membrane can be directly used to blot for another protein when the antibody comes from another different species. However, for antibodies from the same species, the blotted membrane was first incubated in the stripping buffer at 50 °C for 20 min to remove the previous antibody. Second, the membrane was washed with tap water, ddH_2O and TBST before being blocked again, and then incubated with the new antibodies overnight as described above.

3.2.4 Native PAGE

Native Page was used to verify the expression of dimeric and monomeric Usp28 in HLF Usp28-WT and Usp28-M cell lines. Cells were collected by trypsin-EDTA and washed once with PBS. Subsequently, cell pellets were resuspended in 1 ml TNT-250 buffer with protease/phosphatase inhibitors and 1 mM DTT and lysed on ice for 10 min followed by a fast centrifugation. Supernatant was mixed with 2X Native sample buffer and loaded onto the 4–20% Precast Protein Gels. Page Ruler Prestained Protein Ladder was also added as the marker after mixing with 2X Native sample buffer. The electrophoresis was performed with the prechilled Native gel running buffer at 80 V for 20 min and 120 V for 60 min. The further protein transferring and immunoblotting steps were the same as SDS-PAGE, details see section **3.2.3 SDS-PAGE and Western Blot**.

3.2.5 Immunoprecipitation

Immunoprecipitation (IP) assays were performed in this thesis for the detection of protein-protein interaction (Usp28-53bp1, HA-GFP, LEO1-RNAPII Ser2). In general, cells were collected by trypsin-EDTA or direct scratch and washed once with PBS. Subsequently, cell pellets were resuspended in 1 ml TNT-250 buffer with protease/phosphatase inhibitors and lysed on ice for 10 min followed by the centrifugation at 4 °C for 10 min with a speed of 17000 G. 20 µl of supernatant was taken and boiled with 20 µl 4X Laemmli sample buffer at

95 °C for 10 min as input. The rest of supernatant was aliquoted and incubated with 20 µl agarose beads (50% slurry, prewashed by lysis buffer) together with 1 µg specific antibody or IgG at 4 °C overnight with rotation. The mixture was washed three times with 1 ml lysis buffer and pelleted by centrifugation at 4 °C for 2 min with a speed of 2500 G. All the supernatant was discarded and the remaining beads were resuspended with 40 µl 4X Laemmli sample buffer and boiled at 95 °C for 10 min as pulldown samples for the further western blots.

Optional 1: Cells could also be fixed by 0.2% PFA in PBS for 4 min and quenched by 200 mM Glycine for 1 min. For this alternation, a sonication is used instead of lysis on ice, the parameters for sonication are as follows: 4 °C, 100% cycle, 30% amplitude, 45 sec on/15 sec off for 10 min.

Optional 2: The cell lysates could also be incubated overnight with specific antibodies only and the beads could be added the second day and then incubated together for 2 h to reduce the background.

3.2.6 LC-MS/MS analysis, In-Gel Digestion and NanoLC-MS/MS data analysis

This section was originally written by Prof. Andreas Schlosser and optimized by Elias Einig. The samples were prepared by Ravi B Kollampaly. The assay was performed and the raw data was analyzed by Prof. Andreas Schlosser. The figure was made by Prof. Nikita Popov and Elias Einig.

For LC-MS/MS analysis, Usp28 and 53bp1 immunoprecipitates were denatured by incubation at 95 °C in Laemmli buffer. Proteins were separated on SDS-PAGE gels. Each gel lane was cut into 15 slices. The excised gel bands were destained with 30% acetonitrile in 0.1 M NH_4HCO_3 (pH 8), shrunk with 100% acetonitrile, and dried in a vacuum concentrator (Concentrator 5301, Eppendorf, Germany). Digests were performed with 0.1 µg trypsin per gel band overnight at 37 °C in 0.1 M NH_4HCO_3 (pH 8). After removing the supernatant, peptides were extracted from the gel slices with acetonitrile and 5% formic acid, and supernatants of extracted peptides were pooled for each gel slice.

NanoLC-MS/MS analyses were performed on an Orbitrap Fusion (Thermo Scientific) equipped with a PicoView Ion Source (New Objective) and coupled to an EASY-nLC 1000 (Thermo Scientific). Peptides were loaded on capillary columns (PicoFrit, 30 cm x 150 µm ID, New Objective) self-packed with ReproSil-Pur 120 C18-AQ, 1.9 µm (Dr. Maisch) and separated with a 30-minute linear gradient from 3% to 30% acetonitrile and 0.1% formic acid and a flow rate of 500 nl/min.

Both MS and MS/MS scans were acquired in the Orbitrap analyzer with a resolution of 60000 for MS scans and 15000 for MS/MS scans. HCD fragmentation with 35%

normalized collision energy was applied. A Top Speed data-dependent MS/MS method with a fixed cycle time of 3 sec was used. Dynamic exclusion was applied with a repeat count of 1 and an exclusion duration of 30 sec; singly charged precursors were excluded from selection. Minimum signal threshold for precursor selection was set to 50000. Predictive AGC was used with an AGC target value of 2e5 for MS scans and 5e4 for MS/MS scans. EASY-IC was used for internal calibration.

Raw MS data files were analyzed with MaxQuant version 1.6.2.2 (227). Database search was performed with Andromeda, which is integrated in the utilized version of MaxQuant. The search was performed against the UniProt human database (September 2018, UP000005640, 73099 entries). Additionally, a database containing common contaminants was used. The search was performed with tryptic cleavage specificity with 3 allowed miscleavages. Protein identification was under control of the false-discovery rate (FDR; <1% FDR on protein and PSM level). In addition to MaxQuant default settings, the search was performed against following variable modifications: Protein N-terminal acetylation, Gln to pyro-Glu formation (N-term. Gln), oxidation (Met), phosphorylation (Ser, Thr, Tyr) and GlyGly (Lys). Carbamidomethyl (Cys) was set as fixed modification. Further data analysis was performed using R scripts developed in-house. Missing LFQ intensities in the control samples were imputed with values close to the baseline. Data imputation was performed with values from a standard normal distribution with a mean of the 5% quantile of the combined log10-transformed LFQ intensities and a standard deviation of 0.1. For the identification of significantly enriched proteins, boxplot outliers were identified in intensity bins of at least 300 proteins. Log2 transformed protein ratios of sample versus control with values outside a 1.5x (significance 1) or 3x (significance 2) interquartile range (IQR), respectively, were considered as significantly enriched. The proteomic data are deposited at the PRIDE database (submission #616633).

3.2.7 Cycloheximide chase assay

To check the stability of Myc in different cell lines, the cycloheximide chase assays were performed in the thesis as it can inhibit the synthesis of proteins in eukaryotes. In brief, cycloheximide was added into the tested cells with a final concentration of 100 µg/ml. Cells were incubated with the cycloheximide for different durations and were collected at the same time for the further western blots.

3.2.8 DUB activity assay

To check the catalytic activities of Usp28 in different conformations or different cell lines or under different situations, the DUB activity assays were performed in this thesis. In brief, cells were collected from 6-cm dish with 80% confluent and lysed in 200 µl of lysis buffer (1% TritonX-100 in PBS, 1 mM DTT, protease/phosphatase inhibitor, 1:1000) on ice for 5 min, and centrifuged at 1000 G and 4 °C for 5 min. 70 µl of supernatant was incubated with either 0.25 ug concentrated probe (a mixture of Biotin-Ahx-Ub-VS and Biotin-Ahx-Ub-VME) dissolved in 5 µl PBS or 5 µl PBS at room temperature for 5 min. The reaction was terminated and proteins were denatured by addition of 25 µl 4x Laemmli sample buffers and boiled at 95 °C for 10 min and analyzed by western blots with antibodies against Usp28.

3.2.9 Ubiquitin pulldown assay

The canonical ubiquitin pulldown assays were performed in this thesis to test the deubiquitination activity of Usp28. Expression vectors for Myc-WT, His-Ub and Usp28 variants in pcDNA3 were transfected into HeLa WT/HeLa 53bp1KO cells with PolyJet transfection reagent. 12 hours after transfection, the cell culture medium was replaced. 48 hours after transfection cells were collected and lysed in 1 ml urea buffer at room temperature for 10 min with rotation. Lysates were briefly sonified (100% cycle, 30% amplitude, 30 sec) and cleared by centrifugation at 17000 G for 10 min at room temperature. 20 µl of supernatants was taken and boiled with 20 µl 4X Laemmli sample buffer at 95 °C for 10 min as input. The rest supernatant was incubated with 20 µl Ni-NTA beads (50% slurry, prewashed by urea buffer) at room temperature overnight with rotation. Beads were centrifuged and washed twice with urea buffer, denatured with 40 µl 4X Laemmli sample buffer at 95 °C for 10 min and analyzed by western blots with antibodies against Myc.

3.2.10 Isolation of proteins on nascent DNA

To check the effect of etoposide for different cell lines on DNA replication, and to check the proteins on these nascent DNA, the isolation of proteins on nascent DNA (iPOND) assays were performed in this thesis. For HLF Usp28-WT and Usp28-M cells, in the etoposide treatment group, cells were treated with etoposide (5 µM) for 20 min and then incubated with etoposide and bio-dUTP and biotin-dCTP (0.5 µM each) in hypotonic buffer for 10 min and followed by another 10 min with etoposide and biotin-dUTP/dCTP in culture medium to label

the nascent DNA. And in the control group, cells were only incubated with biotin-dUTP/dCTP in the hypotonic buffer and culture medium for 10 min each. Cells were fixed by 0.2% PFA in PBS for 4 min and quenched by 200 mM Glycine for 1 min and then lysed in TNT-250 buffer (with protease/phosphatase inhibitors 1:1000) and fragmented via sonication with the following parameters: 100% cycle, 30% amplitude, 45 sec on/15 sec off for 10 min. Lysates were cleared by a centrifugation at 17000 G for 10 min at 4 °C. 20 µl of supernatants was taken and boiled with 20 µl 4X Laemmli sample buffer at 95 °C for 10 min as input. The rest supernatant was incubated with 10 µl streptavidin magnetic beads (prewashed three times with lysis buffer on the magnetic rack) at room temperature for 45 min with rotation. Afterwards, beads were washed three times with TNT-300 buffer (with 0.5% SDS and protease/phosphatase inhibitors 1:1000) and boiled with 40 µl 4X Laemmli sample buffer at 95 °C for 10 min and analyzed by western blots.

3.2.11 Crystal violet staining

Cells were washed with PBS and fixed by 1% PFA for 10 min at room temperature, and then PFA was removed and 2 ml of crystal violet solution was added into each well (6-well plate) and incubated at room temperature for 10 min. Afterwards, cells were washed three times with 2 ml PBS each to remove the remaining crystal violet solution.

3.2.12 Immunofluorescence

Immunofluorescence (IF) assays were performed in this thesis to detect the distribution and abundance of proteins. In brief, cells were seeded on 10-mm round glass slides in 6-well plates, fixed with 1% PFA in PBS for 10 min at room temperature and washed three times with PBS and kept in PBS at 4 °C form long-term storage. Cells were permeabilized/blocked in 50 µl 1% BSA (in TBST with 0.2% TritonX-100) at room temperature for 20 min and incubated in 40 µl 1% BSA (in TBST with 0.2% TritonX-100) with primary antibodies 1:100-1:1000 at room temperature for 2 h. Subsequently, cells were incubated at room temperature for 2 h in the dark with 40 µl 1:100 diluted secondary antibodies in the same buffer after three times washing with PBS. Cells were washed three times with PBS again and mounted on slides with 5 µl DAPI-containing mounting solution and sealed with nail polish for long-term storage at 4 °C in the dark.

3.2.13 Proximity Ligation Assay

Proximity Ligation Assays (PLA) were performed in this thesis to detect the interaction of two proteins *in situ*. The Duolink® In Situ PLA® Probes/Duolink® In Situ Detection Reagents Red and Green Kits/Duolink™ In Situ Wash Buffers Fluorescence were used according to the manufacturer's protocol. In brief, cells were seeded on 10-mm round glass slides in 6-well plates, fixed with 1% PFA in PBS for 10 min at room temperature and washed three times with PBS and kept in PBS at 4 °C form long-term storage. Cells were permeabilized with 100 µl TBS with 0.3% TritonX-100 for 5 min at room temperature, and then blocked with 40 µl PLA blocking buffer (2.5% BSA in TBST) for 30 min at room temperature after washing with PBS. Subsequently, cells were incubated in a 40 µl PLA blocking buffer with 1:200 diluted primary antibodies from different species against proteins of interest for 2 h at room temperature.

After primary antibodies incubation, cells were washed three times with PBS and incubated with 25 µl diluted PLA probe solution (two probes against different species were diluted in PLA blocking buffer 1:10 and well mixed and sat for 20 min at room temperature before using) in a humidified chamber at 37 °C for 1 h.

After probe incubation, cells were washed twice with 100 µl 1X Wash Buffer A for 5 min each on a shaker and then incubated with 25 µl 1X ligation solution (in ddH_2O with ligase 1:40 diluted, ligase was added right before using) in a humidified chamber at 37 °C for 1 h.
After ligation, cells were washed twice with 100 µl 1X Wash Buffer A for 2 min each on a shaker and then incubated with 25 µl 1X amplification solution (in ddH_2O with polymerase 1:80 diluted, polymerase was added right before using, prepared in the dark) in a humidified chamber at 37 °C for 2 h in the dark.

Finally, cells were washed twice with 100 µl 1X Wash Buffer B for 10 min each and with 100 µl ddH_2O for 1 min on a shaker in the dark. The slides were then dried in the dark, mounted with 5 µl DAPI-containing mounting solution and sealed with nail polish for long-term storage at 4 °C in the dark.

3.2.14 EdU incorporation assay

To detect the nascent DNA, EdU incorporation assays were performed in this thesis. Cells were seeded on 10-mm round glass slides in 6-well plates and treated with EdU (25 μM) for 20 min before fixing with 1% PFA in PBS for 10 min at room temperature and permeabilized with 0.3% Triton-X100 (in TBS) for 10 min. Click reaction was carried out by incubation with 25 μl click reaction solution (2 mM $CuSO_4$, 0.4 μM Sulfo-Cy3-azide, 100 mM Na Ascorbate, in PBS) at room temperature for 30 min in the dark, then washed three times with PBS and further mounted with 5 μl DAPI-containing mounting solution and sealed with nail polish for long-term storage at 4 °C in the dark.

Optional: IF could also be done after EdU staining on the same cells to stain proteins. However, those secondary antibodies which show a red staining (for example Alexa Fluor 555) should be excluded as EdU already gave a red color.

3.2.15 DNA fiber assay

To detect the speed of DNA replication fork, the fiber assays were performed in this thesis as described previously (228). Briefly, cells were incubated each 20 min with 25 μM IdU in culture medium and subsequently with 250 μM CIdU in culture medium at 37 °C with PBS washing in between. Cells were resuspended in 100 μl PBS after harvesting and 2 μl mixture was transferred on a coverslip and dried for 5 min (The rest cell suspension could be stored at -20 °C for further research). 7 μl of fiber lysis solution was added and incubated for 2 min at room temperature before the slides were air dried in an angle so that DNA was allowed to spread over the slide. DNA was then fixed with pre-chilled methanol: acetic acid (2:1) for 10 min at room temperature and incubated with 2.5 M HCl for 100 min after ddH_2O washing. Subsequently, the slides were washed with PBS three times with 5 min each, and then blocked in 2.5% BSA (in PBS) for 20 min at room temperature. Afterwards, the DNA fibers were incubated with primary antibodies (anti-BrdU mouse 1:25 and antiBrdU rat 1:300, in 2.5% BSA in PBS) at room temperature for 2 h followed by the incubation with secondary antibodies (anti-mouse Alexa 555 and anti-rat Alexa 488, both 1:200 in 2.5% BSA in PBS) at room temperature for another 2 h with three times PBS washing in between (5 min each). Finally, the slides were washed with PBS and dried and mounted with 15 μl DAPI-containing mounting solution and sealed with nail polish for long-term storage at 4 °C in the dark.

3.2.16 Neutral comet assay

To test and visualize the DNA double strand breaks in different cell lines or under different situations, neutral comet assays were performed in this thesis. The procedures are as follow:

Slides pre-coating: 1.5 ml of boiled 0.8% solution of Agarose Standard in PBS was added on the Super Frost slide and cooled overnight to coat the agarose layer on the slide.

Cells preparation and Embedding: 150,000 of cells were collected and resuspended in 200 µl of 0.7% Low Melting Point (LMP) agarose solution in PBS. 65 µl of the mixture was dropped and covered by a coverslip on the pre-coated slides, duplicates were made for each sample. Slides were kept on ice for solidification and coverslips were removed and 75 µl of 0.7% LMP agarose solution in PBS was added on top with coverslip covered to form the upper layer. Slides were kept on ice and coverslips were removed after solidification.

Lysis and electrophoresis: Slides were covered by 1.5 ml neutral comet lysis buffer and lysed at 4 °C overnight in dark. Subsequently, slides were washed three times for 5 min with TE buffer and then the electrophoresis was preceded in TAE buffer with 0.5 V/cm for 1 h.

Fixation and staining: After twice washing with PBS for 10 min each, cells were fixed with 1 ml absolute ethanol twice with 10 min each and then dried in the dark for 3 h at room temperature. Afterwards, cells were stained by 50 µl ethidium bromide solution (2 µg/ml in ddH_2O) for microscopy.

3.2.17 Cut & Run

To study the interaction between DNA and proteins, the Cut & Run assays were performed in this thesis as it costs less cells (no more than 1 million) and shorter experimental time. The protocol was published previously (229) and the modified procedures are as follow:

Binding cells to beads: 1 million of 0.2% PFA fixed cells were washed once with 1 ml PBS and twice with 1 ml C & R Wash buffer by centrifugation at room temperature and 600 G for 3 min. pellets were resuspended in 1 ml C & R Wash buffer and 20 µl was taken as input. 40 µl of concanavalin A-coated beads (prewashed twice and resuspended in C & R Binding buffer) were added into each sample and the mixture was incubated at room temperature with rotation for 10 min.

Permeabilized cells and bind primary antibodies: Samples were washed once with 1 ml C & R Wash buffer and then resuspended in 150 µl C & R Antibody buffer and 1 µg antibody against protein of interest was added per sample and samples were incubated in a shaker at 4 °C and 800 rpm overnight.

Bind Protein-A/G-MNase fusion protein: Liquid was removed after centrifugation (4 °C, 600 G, 3 min) and washed twice with 1 ml C & R TritonX-Wash buffer. Subsequently, beads were incubated with Protein-A/G-MNase in 150 µl C & R TritonX-Wash buffer (1:2000) in a shaker at 4 °C and 800 rpm.

Chromatin digestion and release: Liquid was removed after centrifugation (4 °C, 600 G, 3 min) and washed twice with 1 ml C & R TritonX-Wash buffer and one more time with 1 ml C & R Low-Salt Rinse buffer. Subsequently, beads were incubated in 200 µl C & R Incubation buffer at 0 °C for 30 min. Afterwards, liquid was removed after centrifugation (4 °C, 600 G, 3 min) and beads were incubated in 200 µl C & R Stop buffer at 37 °C for 30 min to release DNA fragments.

DNA precipitation: Supernatant was transferred into a fresh DNA low binding tube with 2 ul 10% SDS and 5 ul proteinase K. Samples were well mixed and then incubated at 55 °C overnight. On the next day, 200 µl of phenol/chloroform/isoamyl alcohol was added and vortexed for 1 min to extract DNA. The aqua phase (around 200 µl) was transferred to a new DNA low binding tube after centrifugation (4 °C, 17000 G, 10 min) and well mixed with 500 µl prechilled absolute ethanol and 1 µl GlycoBlue and incubated at -20 °C overnight. Afterwards, the samples were centrifuged at 4 °C and 17000 G for 30 min and the blue DNA pellet could be seen at the bottom of the tube. The pellets were further washed once with 1 ml prechilled 75% ethanol and then air dried until they were dissolved in the elution buffer. These fragmented DNAs could be used for qPCR or prepared for the library for deep sequencing after quantification. DNAs in the elution buffer could be kept at -20 °C for long-term storage.

Input samples preparation: Input samples were sonicated in 200 µl TE buffer with 250 mM NaCl and 0.5% SDS at 4 °C to obtain the fragmented DNA with the following parameters: 100% cycle, 30% amplitude, 45 sec on/15 sec off for 10 min. After sonication, 1 µl of RNase A was added and the mixture was incubated at 50 °C for 2 h and then 2 µl of proteinase K in 200 µl TE buffer with 250 mM NaCl and 0.5% SDS was added into the samples and the mixture was incubated at 50 °C for 1 h and then warmed to 65 °C overnight. Afterwards, they were precipitated in phenol/chloroform/isoamyl alcohol in the same way as described above.

3.2.18 Data analysis

Immunoblotting: free software FIJI/ImageJ version 1.53f (https://imagej.net/software/fiji/) was used to scan the grayscale of proteins of interest from the blotting films. The results were further normalized to either loading control (Cycloheximide assay), total protein (DUB activity assay) or reference protein (Immunoprecipitation, His-Ub assay) first and then normalized to the control group for quantification.

Immunofluorescence: Images were analyzed automatically with the free software FIJI/ImageJ version 1.53f (https://imagej.net/software/fiji/). In brief, images were segmented based on nuclear areas in the DAPI channel and staining intensity (Immunofluorescence, EdU incorporation assay) in other channels or the number of PLA foci (PLA assay) was measured for each nucleus. For PLAs, several z-layers were combined to a single image by maximum intensity projection prior to counting the number of PLA foci using the "Find Maxima" command.

Neutral comet assay: Images were analyzed automatically with the free software FIJI/ImageJ version 1.53f (https://imagej.net/software/fiji/) with the free plugin ‘OpenComet’ (https://cometbio.org/)

DNA fiber assay: For quantification, DNA fiber lengths were measured by free software FIJI/ImageJ version 1.53f (https://imagej.net/software/fiji/)and converted to fork velocity using the following formula: 1 um = 2.59 kb.

Statistical analysis: Statistical analysis was done using GraphPad Prism 9 (GraphPad Software Inc.). Two-tailed, unpaired t tests were used to compare two groups and ordinary one-way ANOVA multiple comparisons were used to compare more than two groups. Non-linear fit model-one phase decay was used for protein half-life determination. Linear regression was used for correlation analysis. Sample sizes and P-values are shown in the figure legends and significance was considered as *P < 0.05. **P < 0.01, ***P < 0.001, ****P < 0.0001. ns denotes no significance (P > 0.05).

3.3 Molecular biology methods

3.3.1 RNA isolation and DNase I treatment

Cells were washed with PBS when they were still attached on the dish and TRI reagent (1 ml for a 10-cm dish) was directly added into the dish. The dish was incubated on a shaker at room temperature for a few minutes until cells were detached. Cell-containing TRI reagent was transferred into a DNA low binding tube and mixed with 0.1 ml 1-bromo-3-chloropropane. The liquid was well mixed via a vigorous vortex and then allowed to stand at room temperature for 15 min followed by a centrifugation at 4 °C and 17000 G for 15 min.

The upper aqua phase was transferred into a fresh DNA low binding tube and 0.5 ml of isopropanol was added and well mixed. The tube was allowed to stand at room temperature for 15 min followed by a centrifugation at 4 °C and 17000 G for 15 min. An RNA pellet should be visible at the bottom of the tube. The supernatant was carefully removed and the pellet was washed twice with 1 ml of prechilled 75% ethanol and RNA pellet was then air dried at room temperature for 5-10 min with the tube lid opened. Afterwards, the pellet was dissolved in 20 µl of ultra-pure water and concentration was measured for DNase I treatment.

To remove the remaining DNA from the newly isolated RNA, 20 µg of RNA was dissolved with 100 µl of ultra-pure water (include 10 µl of 10X DNase I Reaction Buffer and 1 µl of DNase I) and incubated at 37 °C for 10 min. Afterwards, RNA was extracted by mixing with 100 µl of phenol/chloroform/isoamyl alcohol and aqua phase was transferred and well mixed with 10 µl of 3 M sodium acetate (pH 5.2) and 250 µl of prechilled absolute ethanol and incubated at -20 °C for 2 h and then washed by prechilled 70% ethanol. The pellet was air dried at room temperature for 5-10 min with the tube lid opened. Afterwards, the pellet was dissolved in 10 µl of ultra-pure water and concentration was measured for cDNA synthesis and can be stored at -80 °C.

3.3.2 cDNA synthesis

Promega reverse transcriptase m-MLV and the corresponding kit was used for cDNA synthesis from isolated RNA. In brief, 2 µg of DNase I treated RNA was well mixed with 2 µl of random primer (500 µM). Ultra-pure water was added until 10 µl and the mixture was incubated at 70 °C for 5 min to denature and to anneal RNA and then kept the mixture on ice.

To this 10 µl of RNA-Primer mixture, the following reagents were added and well mixed: 25.5 µl of ultra-pure water, 10 µl of 5X m-MLV buffer, 1.25 µl of dNTPs (10 mM), 1.25 µl of RiboLock inhibitor and 2 µl of m-MLV reverse transcriptase. The mixture was heated at 25 °C for 10 min and then warmed to 37 °C for 1 h and then warmed to 70 °C for 15 min and finally kept on ice. Synthesized cDNA can be stored at -20 °C.

3.3.3 Polymerase Chain Reaction

Routine polymerase chain reaction: To obtain and amplify target DNA fragments from cDNA or plasmid DNA, polymerase chain reaction (PCR) was performed in this thesis. In brief, 2X NEBNext Ultra II Q5 Master Mix was incubated with template DNA (cDNA or plasmid DNA) and primers in Bio-Rad T100TM Thermal Cycler with the following program:

Step	Temperature	Duration	Cycle
Initial Denaturation	98 °C	30 sec	1
Denaturation	98 °C	5-10 sec	30-35
Annealing	50–72 °C	10-30 sec	
Extention	72 °C	20–30 sec/kb	
Final extention	72 °C	2-10 min	1

Index Polymerase chain reaction: For DNAs subjected for deep sequencing, index PCR was performed to label them with specific index. In brief, 2X NEBNext Ultra II Q5 Master Mix (for pure DNA) or 2X KAPA HiFi HotStart ReadyMix (for DNA binds on the beads) was mixed with i5/i7 index primers and the DNA for labeling, and the following program was applied:

NEBNext Ultra II Q5 Master Mix or KAPA HiFi HotStart ReadyMix			
Step	**Temperature**	**Duration**	**Cycle**
Initial Denaturation	95 °C	3 min	1
Denaturation	98 °C	20 sec	20-25
Annealing	65 °C	15 sec	
Extention	72 °C	20 sec	
Final extention	72 °C	7 min	1

Quantitative real-time PCR: To test the mRNA level or to check the abundance of the specific DNA fragments Cut & Run, quantitative real-time PCR (qPCR) was performed in this thesis. In brief, template DNA (cDNA synthesized from RNA or DNA from Cut & Run, 1:5-1:10 diluted with dd ultra-pure water) was mixed with 2X SYBR® Green JumpStart™ Taq ReadyMix™ and primer pairs and performed in the Bio-Rad CFX Connect Real-Time system with the following program:

Step	Temperature	Duration	Cycle
Initial denaturation	94 °C	5 min	1
Denaturation	94 °C	15 sec	45
Annealing	60 °C	1 min	
Extension			
Fluorescence reading		Not applicable	
Final extension	72 °C	10 min	1
Melting curve and fluorescence	60-95 °C, with 0.5 °C	1 min	1

For quantification, the Livak delta/delta CT method was applied and target gene mRNA level or target DNA abundance was normalized with beta-Actin or with the input group.

3.3.4 Agarose gel electrophoresis, DNA extraction and purification

To obtain the desired DNA with specific size, agarose gel electrophoresis was performed to separate different DNAs and Monarch® DNA Gel Extraction Kit was used to extract and purify target DNA in this thesis. The procedures are as follow:

Agarose gel electrophoresis: 0.8-3% Seakem® agarose was boiled in 1X TAE buffer and 8 µl of ethidium bromide (10 mg/ml) was added before pouring to the gel chamber with comb assembled. The agarose solution was kept at room temperature until completely polymerized. Afterwards, DNA samples (PCR products/restriction enzyme digestion mixture/index PCR product…) were mixed with 6X DNA loading dye and loaded into the gel with GeneRuler 1kb DNA Ladder. The electrophoresis was performed under 110 V for 35 min and DNAs were visualized under a UV transilluminator.

DNA extraction and purification: target DNA-containing agarose gel was cut under UV and incubated with 4X mass volume of dissolving buffer (for example, 100 µg of agarose gel with 400 µl of dissolving buffer) at 50 °C with interval vortexing until completely dissolved. Subsequently, sample solution was loaded into the column which preloaded into the collection tube. Samples were centrifuged at 4 °C and 17000 G for 1 min to remove the dissolving buffer. After all samples were loaded and centrifuged, 200 µl of washing buffer (diluted with 4 volumes of absolute ethanol) was loaded into the column and centrifuged at 4 °C and 17000 G for 1 min for washing. After one more washing step, the column was carefully removed into a fresh DNA low binding tube and 20 µl of elution buffer was added to the center of the matrix. Column was incubated at room temperature with the elution buffer for 1 min and then centrifuged at 4 °C and 17000 G for 1 min to elute target DNA (elution buffer containing target DNA may reload into the column and centrifuge one more time to increase the yield). DNA can be stored at -20 °C in the elution buffer for further study.

3.3.5 Nucleic acid quantification

To measure the concentration of nucleic acid, picogreen measurement and nanodrop measurement were performed in this thesis.

Picogreen: Double strand DNA (Cut & Run, DNA library…) concentration was measured with Quant-iT™ PicoGreen™ dsDNA reagent. In brief, 1 µl of DNA sample was diluted in 99 µl TE buffer in the well of a black 96-well plate, 100 µl of TE buffer (with 0.5% Quant-iT™ PicoGreen™ dsDNA reagent) was added and incubated at room temperature for 3 min follow by the detection of the fluorescence (Excitation: 480 nm, Emission: 520 nm) with a TECAN infinite M200 PRO Reader. The concentration of the measured sample was calculated with the standard formula.

Nanodrop: Routine DNA and RNA samples were measured with nanodrop. In brief, 1 µl of the nucleic acid sample was loaded on the nanodrop to measure the absorbance at 260 nm. The ratio of the absorbance at 260 and 280 nm should be between 1.8-2.

3.3.6 Target plasmid generation

Several novel plasmids were generated in this thesis to establish new cell lines and here are the procedures how to generate them:

Insert DNA preparation:

For shRNAs against h53bp1, 11.25 ul of each oligo (forward and reverse, both 0.1 nM/ul) were mixed with 2.5 ul of 10X annealing buffer and warmed up to 95 °C. Subsequently, heating was stopped and the sample was allowed to cool down naturally until room temperature on a rack (around 2-3 h) and then diluted in 0.5X annealing buffer (1:400) and stored at -20 °C.

For GFP-Usp28 overexpression, open reading frames (ORFs) were amplified from sfGFP plasmids and Usp28-WT plasmids via the routine PCR described above with the primers which have an overlap at the 3' end of GFP and the 5' end of Usp28-WT. After purification, these two parts were fused via another PCR with primers targeting the 5' end of GFP and 3' end of Usp28-WT. Product was verified and purified by agarose gel electrophoresis.

Backbone preparation:

For shRNAs, the pLKO1.puro vector was used as the backbone. In short, plasmids were incubated with restriction enzymes EcoRI and AgeI under corresponding buffer at 37 °C overnight and purified by agarose gel electrophoresis (a 1.9 kb stuffer should be seen after digestion and should be removed).

For overexpression, the pRRL-hygro vector was used as the backbone. In short, plasmids were incubated with restriction enzymes AgeI and SpeI under corresponding buffer at 37 °C overnight and purified by agarose gel electrophoresis.

Assembly:

For shRNAs, T4 DNA ligase was used for the ligation and the recipe is as follow:

Diluted oligo (or 0.5X annealing buffer as a negative	1 ul
Digested pLKO1.puro	1 ul (10-20 ng)
10X ligase buffer	1 ul
T4 DNA ligase	1 ul
Distilled water	6 ul

Incubated at room temperature for 1-3 h and the reaction products can be stored at -20 °C.

For overexpression, NEBuilder HiFi DNA Assembly Master Mix was used and the recipe is as follow:

Insert DNA (or equal water as negative control)	1 ul (0.134 pM)
Digested pRRL-hygro	0.5 ul (0.067 pM)
NEBuilder HiFi DNA Assembly Master Mix	1.5 ul

Incubated at 50 °C for 15 min and the reaction products can be stored at -20 °C.

3.3.7 Transformation, verification and amplification

Plasmids with insert DNA assembled were further transformed into NEB® 10-beta Competent E. coli (High Efficiency) bacteria with heat shock method. In brief, 1 ul of plasmids DNA (after T4 ligation or HiFi assembly) was well mixed with 5 ul of fresh thawed 10-beta competent E. coli cells by flicking. The mixture was incubated on ice for 30 min and then heat shock at 42 °C for exactly 30 sec followed by another 5 min incubation on ice. Subsequently, 150 ul of SOC medium was added and mixture was incubated at 37 °C for 1 h before spreading over prewarmed LB agar plates with 50 µg/ml Ampicillin. The agar plates were incubated upside down in a 37 °C incubator overnight.

Single colonies were picked and inoculated into 2 ml of SOC medium and plasmids were isolated with the GenElute HP Plasmid Miniprep Kit. Afterwards, plasmids were digested with restriction enzymes (XhoI for pLKO and EcoRI for pRRL) overnight and checked via agarose gel electrophoresis. Positive candidates were further sent for sequencing with specific primers for confirmation.

After sequencing, plasmids with correct insert DNA were transformed again into 10-beta competent cells and amplified into 1 l of LB medium with 50 µg/ml Ampicillin for amplification and plasmids were isolated with the GenElute HP Plasmid Midiprep Kit. Isolated plasmids can be stored at -20 °C for long-term storage after concentration measurement. Transformed plasmids in E. coli cells can also be stored at -80 °C in the mixture of SOC/glycine (50%/50% v/v).

3.4 Next generation sequencing

3.4.1 RNA sequencing

RNA sequencing was performed in this thesis to check the mRNA level of Myc target genes in different cell lines. In brief, total RNA was isolated as described above, then NEBNext Poly(A) mRNA Magnetic Isolation Module was used to isolate mRNA from 1 ug of total RNA according to the manufacturer's protocol. Afterwards, NEBNext® Ultra™ RNA Library Prep Kit for Illumina® was used for cDNA synthesis and Highprep PCR magnetic beads (Magbio) were used for cDNA purification.

Subsequently, NEBNext Ultra II DNA Library Prep Kit for Illumina and NEBNext Multiplex Oligos for Illumina (Index Primer Set 1 & 2) were used for the library preparation according to the manufacturer's protocol.

After index PCR, products were separated via the agarose gel electrophoresis.

3.4.2 RNA sequencing data analysis

Libraries were sequenced on the Illumina Novaseq 6000 instrument. Mapping of fastq files was performed with STAR (230) and differentially expressed genes were identified using EdgeR (231).

The RNA sequencing data discussed in this thesis have been deposited in NCBI's Gene Expression Omnibus and are accessible through GEO Series accession number GSE213892 (https://www.ncbi.nlm.nih.gov/geo/query/acc.cgi?acc=GSE213892).

4. Results

Part of this chapter is adapted from the manuscript 'Jin, C., Einig, E., Xu, W., Kollampally, R.B., Schlosser, A., Flentje, M. and Popov, N. (under revision) The dimeric deubiquitinase Usp28 integrates 53bp1 and Myc functions to limit DNA damage.' (1).

4.1 Dimerization of Usp28 controls Myc turnover

Deubiquitinase Usp28 regulates Myc stability and transcriptional function

The deubiquitinase Usp28 was identified as a key factor in regulation of the ubiquitination of Myc based on a retroviral short hairpin RNA (shRNA) library screen performed on U2OS osteosarcoma cells by our group (149), which means Usp28 can deubiquitinate Myc and thus stabilize Myc from degradation.

To check if Usp28 also can deubiquitinate and stabilize Myc in hepatocellular carcinoma (HCC) cells, we generated the Usp28 knockout HLF cell lines using CRISPR-Cas9 gene editing

Indeed, Myc protein levels were downregulated with the deletion of Usp28 in tested clones, while the deletion of a related DUB Usp25 did not affect Myc levels (Fig. 1A). Furthermore, the measurement of the Myc protein stability by the canonical cycloheximide assay showed a declined half-life of Myc without Usp28 (Fig. 1B). Taken together, Usp28 can regulate Myc stability in liver cancer cell line HLF and the loss of Usp28 destabilizes Myc.

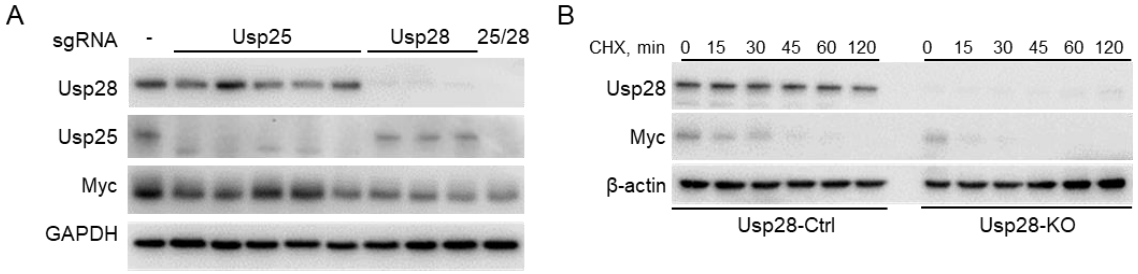

Figure 1. Usp28 stabilizes Myc in HLF cells

(A) Immunoblotting analysis of protein levels of Usp28, Usp25 and Myc in different clones of HLF cells with sgRNA against Usp28 and/or Usp25. The faint band that detected by the antibody against Usp28 in the Usp28-KO clones, is likely because of cross reactivity of the antibody with the highly homologous Usp25 protein, as the band is disappeared in the cells with sgRNA against both Usp28 and Usp25. **(B)** Immunoblotting analysis of protein levels of Myc in HLF Usp28-Ctrl and Usp28-KO cells, indicated time points show the durations of cycloheximide (100 µg/ml) treatment. Panels are adapted from the manuscript 'Jin, C., Einig, E., Xu, W., Kollampally, R.B., Schlosser, A., Flentje, M. and Popov, N. (under revision) The dimeric deubiquitinase Usp28 integrates 53bp1 and Myc functions to limit DNA damage.' (1).

The transcriptional function of Myc is regulated by ubiquitination, for instance, the complex of Myc and the elongation factor Paf1c can be disrupted by ubiquitination of Myc (118). Loss of Usp28 facilitates Myc ubiquitination (149), suggesting a weaken Myc-Paf1c interaction and reinforced Myc target genes expression in cells with Usp28 deletion. To test this idea, RNA-seq analysis was performed in HLF Usp28-WT and Usp28-KO cells. As the result showed, the knockout of Usp28 deregulated Myc-driven transcription – known Myc bound and -regulated genes were the top enriched groups among all 4205 deregulated genes, (Fig. 2A, B). This was also accompanied by the reduced interaction between Myc and Paf1c subunits Cdc73, Ctr9 and Paf1 (Fig. 2C), in line with previous observations (118).

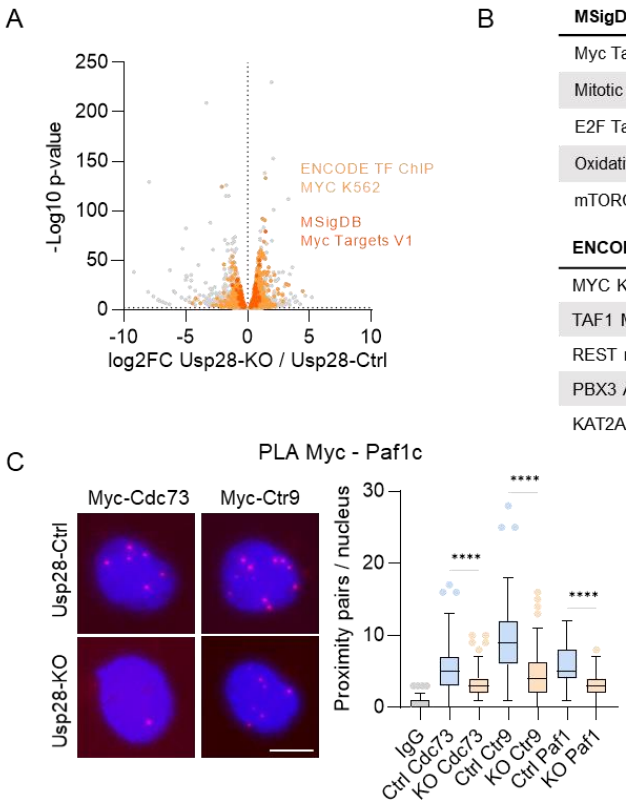

B

MSigDB Hallmark	adj p value
Myc Targets V1	2.6e-26
Mitotic Spindle	2.3e-20
E2F Targets	2.3e-20
Oxidative Phosphorylation	2.3e-20
mTORC1 Signaling	7.4e-20

ENCODE TF ChIP	adj p value
MYC K562 hg19	4.358e-69
TAF1 MCF-7 hg19	3.976e-46
REST myocyte mm9	2.399e-47
PBX3 A549 hg19	1.001e-45
KAT2A GM12878 hg19	2.643e-43

Figure 2. Usp28 regulates Myc transcriptional function via Paf1c

(A) RNA-seq analysis of gene expression in HLF Usp28-KO cells compared to HLF Control (Usp28-Ctrl) cells. Highlighted are the top enriched sets for the Encode TF ChIP and MsigDB datasets, based on the analysis by the Enrichr portal (232). **(B)** Top five gene sets for the indicated databases, enriched within the Usp28-deregulated genes based on the analysis of RNA-seq data in HLF Usp28-KO and HLF Usp28-Ctrl cells. Analysis by the Enrichr portal (232). **(C)** PLA assays with antibodies against Myc and Paf1c subunits (Cdc73/Ctr9/Paf1) or non-specific IgG control antibody (IgG) in HLF Usp28-Ctrl/KO cells with representative images. At least 71 cells were quantified. The data were analyzed with two-tailed, unpaired t test for each pair, ****p < 0.0001. Scale bar = 10 µm. Fig.2A was made by Prof. Nikita Popov and Elias Einig. Fig. 2B was processed by Prof. Nikita Popov. Panels and figure legends are adapted from the manuscript 'Jin, C., Einig, E., Xu, W., Kollampally, R.B., Schlosser, A., Flentje, M. and Popov, N. (under revision) The dimeric deubiquitinase Usp28 integrates 53bp1 and Myc functions to limit DNA damage.' (1).

Dimerization of Usp28 attenuates Myc ubiquitination

In the previous research, our collaborators and us have proved the Usp28 forms stable homodimers as its active state *in vitro* and in cells, and the key amino acid for the dimerization is the leucine which is located at the 545th in the dimerization interface. With a negative charged amino acid substituted, for example the glutamic acid, the dimerization is disrupted (196,197).

To study how Myc function is regulated by Usp28 dimerization, we generated the reconstituted cell lines which only express either the HA-tagged wildtype Usp28 (Usp28-WT) or the HA-tagged monomeric Usp28 (Usp28-M) alleles using lentiviral transduction based on the Usp28-KO HLF cells. An empty vector control cell line is also generated to avoid the potential transfection or infection or selection effects.

All three cell lines were first verified by immunoblotting in the Native PAGE under the nature condition to check the oligomerization states. As showed in the figure below, the dimer cells have a higher band against Usp28 antibodies than the monomer cells, which is due to the bigger molecular weight from the dimerization. In contrast, the empty vector cells, as a Usp28 knockout control, have no signal with the anti-Usp28 immunoblotting (Fig. 3A).

We further examined whether the two Usp28 variants had similar intracellular distribution and were able to interact with endogenous Myc. As the immunofluorescence staining showed, both Usp28 variants localized to the nucleus (Fig. 3B), and both were able to interacte with endogenous Myc, as determined by PLA assays with antibodies against Usp28 and Myc (Fig. 3C).

Interestingly, Myc is found more stable in the Usp28-M cells than in the Usp28-WT cells as checked by cycloheximide assay (Fig. 3D, E), similar result was also found in mouse liver cancer cells (Fig. 3F).

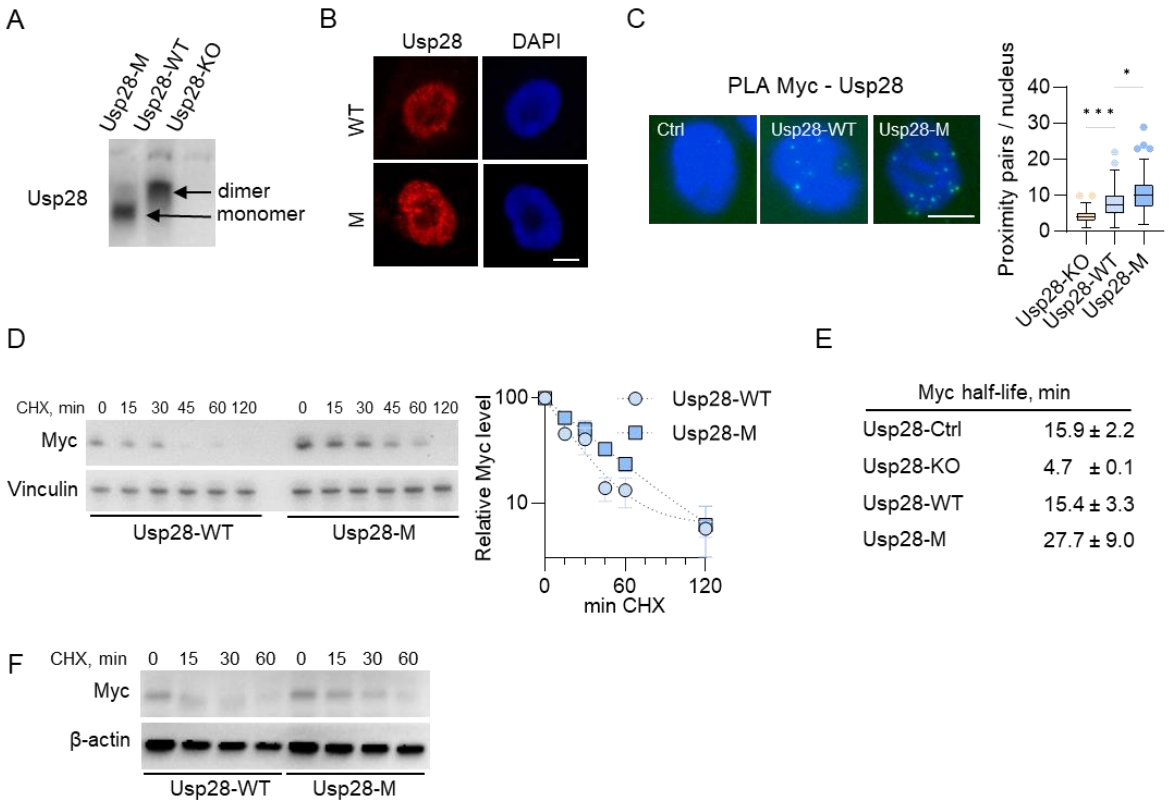

Figure 3. Reconstitution of Usp28-M stabilizes Myc in both HLF and p19$^{-/-}$Nras cells

(A) Immunoblotting analysis of Usp28-WT and Usp28-M expression in corresponding reconstituted HLF cells lines via Native PAGE. **(B)** Immunofluorescence analysis presenting nuclear localization of wildtype (WT) and monomeric (M) Usp28 in HLF cells. Scale bar = 10 µm. **(C)** PLA assays with antibodies against Myc and Usp28 in HLF Usp28-KO cells expressing Usp28-WT/Mono or a control vector with representative images. At least 30 cells were quantified. The data were analyzed with ordinary one-way ANOVA followed by Tukey's multiple comparisons test, *p < 0.05, ***p < 0.001. Scale bar = 10 µm. **(D)** Immunoblotting analysis of Usp28-KO HLF cells, expressing Usp28-WT or Usp28-M, indicated time points show the durations of cycloheximide (100 µg/ml) treatment. Myc protein half-life was determined by a non-linear fit model. Right panel shows a mean of three biological replicates. Error bars denote S.D. **(E)** The half-life of Myc in HLF Usp28-Ctrl, Usp28-KO or Usp28-KO cells, reconstituted with Usp28-WT or Usp28-M variants. The analysis is based on the data showed in panel **(D)**, Fig. 1B and replicate experiments. **(F)** Immunoblotting analysis of p19$^{-/-}$Nras cells, expressing Usp28-WT or Usp28-M, treated with cycloheximide (100 µg/ml) for the indicated time points. Original data of Fig.3F was provided by Ravi B Kollampaly. Part of the panels and figure legends are adapted from the manuscript 'Jin, C., Einig, E., Xu, W., Kollampally, R.B., Schlosser, A., Flentje, M. and Popov, N. (under revision) The dimeric deubiquitinase Usp28 integrates 53bp1 and Myc functions to limit DNA damage.' (1).

Since Myc is a substrate of Usp28 in terms of deubiquitination, this result indicated that dimerization can attenuate the deubiquitination activity of Usp28. To test this idea, we first did a cell based deubiquitination activity assay with DUB-reactive probes Ub-VME and Ub-VS (233,234). In short, the whole cell lysates of cells expressing Usp28-WT and Usp28-M were incubated with the Ub-VME and Ub-VS probes, which can be bound to the cystine in the catalytic domain of Usp28 covalently, mimics the binding between Usp28 and its

substrates. This covalently binding can be visualized as a higher band in immunoblotting. As it turned out, in the DMSO groups, we can only see a single band which is the original Usp28 itself. Strikingly, in the tested groups, Usp28 revealed a more complete conversion into the Ub-modified form for the Usp28-M than the Usp28-WT, indicates the deubiquitination activity of Usp28 is higher in Usp28-M cells than Usp28-WT cells (Fig. 4A).

Same results were also found via the ubiquitin pulldown assays from HeLa Usp28-KO cells transfected with vectors expressing Myc, His-tagged ubiquitin and different Usp28 variants. Immunoblotting showed that Usp28-M more potently promoted deubiquitination of Myc compared to wildtype Usp28 (Fig. 4B).

Since Usp28 is able to deubiquitinate degradative K48- and K11-linked ubiquitin chains (234,235), we compared the activity of Usp28 using pulldown assays with His-Ub variants bearing K48 or K11 as a sole internal ubiquitin acceptor. Interestingly, Usp28-M deubiquitinates Myc with K11-linked chains more potently than Usp28-WT, while Myc modified with K48-linked chains were deubiquitinated similarly by both variants (Fig. 4C), suggesting Usp28 dimerization primarily impairs the uncoupling of K11-linked chains on Myc.

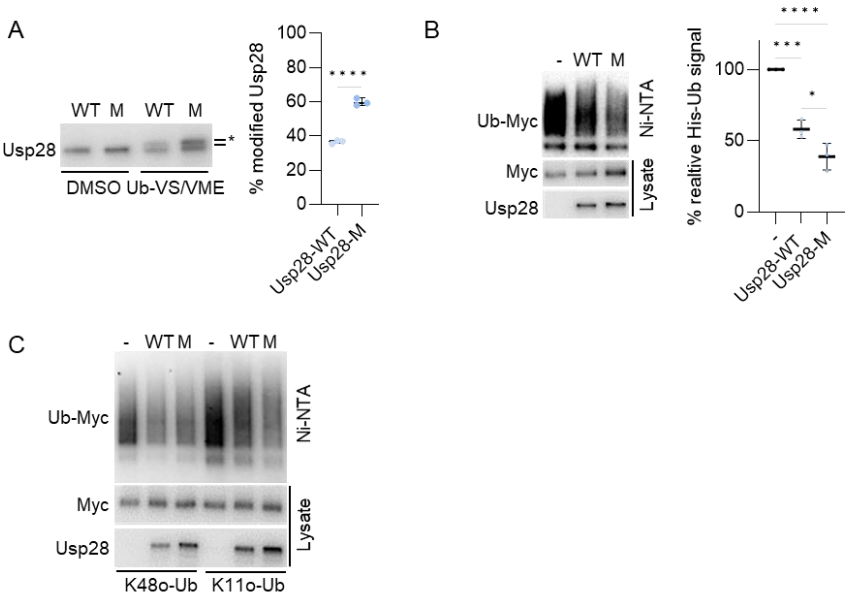

Fig 4. Usp28-M shows higher deubiquitination activity towards Myc in HLF cells

(A) DUB activity assays in whole cell lysates of HLF cells expressing Usp28-WT or Usp28-M. Right panel shows the average of three independent experiments. The data were analyzed with two-tailed, unpaired t test, ****p < 0.0001. **(B)** Ubiquitin pulldown assays with HeLa Usp28-KO cells expressing Myc, wildtype His-Ub and Usp28-WT/M. Right panel shows the average of three independent experiments. The data were analyzed with ordinary one-way ANOVA followed by Tukey's multiple comparisons test, *p < 0.05, ***p < 0.001, ****p < 0.0001. **(C)** Ubiquitin pulldown assays with HeLa Usp28-KO cells expressing Myc, K48-only or K11-only His-Ub and Usp28-WT/M. Panels and figure legends are adapted from the manuscript 'Jin, C., Einig, E., Xu, W., Kollampally, R.B., Schlosser, A., Flentje, M. and Popov, N. (under revision) The dimeric deubiquitinase Usp28 integrates 53bp1 and Myc functions to limit DNA damage.' (1).

4.2 Usp28 dimerization suppresses DNA replication

Dimerization of Usp28 weakens Myc-Paf1c interaction with non-transcriptional effect

In line with effects on Myc ubiquitination, PLA assays showed that the interaction between Myc and Paf1c was reinforced in cells expressing Usp28-M compared to Usp28-WT (Fig. 5A, B). Cut&Run assays with antibodies against Leo1, a subunit of Paf1c, showed a significantly increased recruitment to several Myc target promoters in cells expressing Usp28-M compared to Usp28-WT (Fig. 5C). However, transcriptome profiling showed that expression of Usp28-WT and Usp28-M in Usp28-KO cells have almost no difference in Myc target genes expression regulation (Fig. 5D), suggesting that ectopic stabilization of Myc by Usp28-M primarily has non-transcriptional functions.

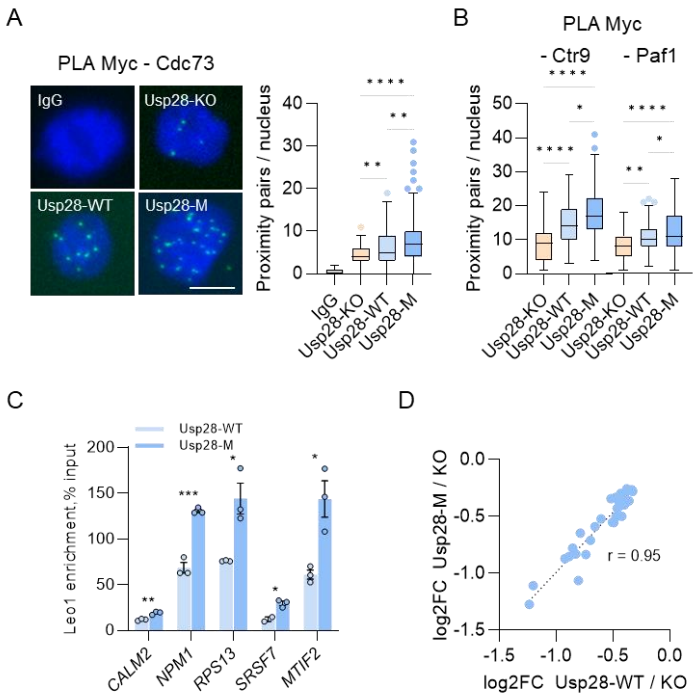

Fig 5. Usp28-M promotes Myc-Paf1c binding with non-transcriptional function

(A) and **(B)** PLA assays with antibodies against Myc, Cdc73/Ctr9/Paf1 or IgG in HLF Usp28-KO cells expressing Usp28-WT/M or a control vector with representative images. At least 67 cells were quantified. The data were analyzed with ordinary one-way ANOVA followed by Tukey's multiple comparisons test, **p < 0.01, ****p < 0.0001. Scale bar = 10 μm. **(C)** Cut&Run assay followed by qPCR analysis showing Paf1c subunit Leo1 abundance on Myc target promoters in HLF Usp28-KO cells expressing Usp28-WT or Usp28-M. The data were analyzed from three technical replicates with two-tailed, unpaired t test for each pair, *p < 0.05, **p < 0.01, ***p < 0.001. **(D)** Regulation (log2FC) of a subset of Myc target genes (MsigDB Hallmark set Myc targets V1) in HLF Usp28-KO cells expressing either Usp28-WT or Usp28-M. The pearson correlation coefficient r equals 0.95. Fig. 5D was made by Elias Einig. Panels and figure legends are adapted from the manuscript 'Jin, C., Einig, E., Xu, W., Kollampally, R.B., Schlosser, A., Flentje, M. and Popov, N. (under revision) The dimeric deubiquitinase Usp28 integrates 53bp1 and Myc functions to limit DNA damage.' (1).

Dimerization of Usp28 restrains DNA synthesis

Both Myc and Paf1c have transcription-independent functions in DNA replication (109,110,119). Paf1c facilitates resolution of transcription-replication conflicts (TRCs) - collisions between RNAPII and replisome and promotes DNA replication under stress (119).

To check TRCs, we performed PLA assays with antibodies against PCNA and pS5-RNAPII (236). Results showed that the TRCs are significantly reduced in cells expressing Usp28-M compared to Usp28-WT (Fig. 6), in line with reinforced recruitment of Paf1c.

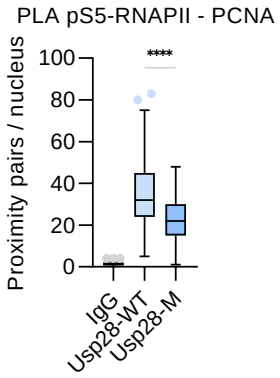

Fig 6. Usp28-M resolve TRCs in HLF cells

PLA assays with antibodies against pS5-RNAPII and PCNA or a control IgG in HLF Usp28-KO cells expressing Usp28-WT/M. At least 95 cells were quantified. The data were analyzed with two-tailed, unpaired t test, ****p < 0.0001. Panel and figure legends are adapted from the manuscript 'Jin, C., Einig, E., Xu, W., Kollampally, R.B., Schlosser, A., Flentje, M. and Popov, N. (under revision) The dimeric deubiquitinase Usp28 integrates 53bp1 and Myc functions to limit DNA damage.' (1).

To check if the reduced TRCs have an effect on DNA replication, we performed EdU incorporation assays in HLF cells with Usp28-WT or Usp28-M expressing. Indeed, with the resolution of TRCs, Usp28-M cells had a strongly increased DNA synthesis rate (Fig. 7A). unexpectedly, DNA fiber assays showed the replication fork progression rate in Usp28-M cells is reduced (Fig. 7B), indicating the increased DNA synthesis is due to the acceleration of replication origins firing.

To check the freshly replicated DNA, we performed nascent chromatin capture assays (237). In short, Usp28-WT and Usp28-M cells were treated with biotin-linked dUTP/dCTP and immunoprecipitation with streptavidin beads were done in these cells to pulldown the newly synthesized DNA which contains biotin. The subsequent immunoblotting showed an increased enrichment of both RNAPII and Ctr9 on nascent DNA obtained from Usp28-M cells (Fig. 7C), indicating that monomeric Usp28 enhances DNA synthesis near the RNAPII/Paf1c-bound sites. Accordingly, Ctr9 knockdown in Usp28-M cells prevented the

increasing of EdU incorporation (Fig. 7A, D), showing that Usp28 dimerization regulates DNA synthesis via Paf1c recruitment.

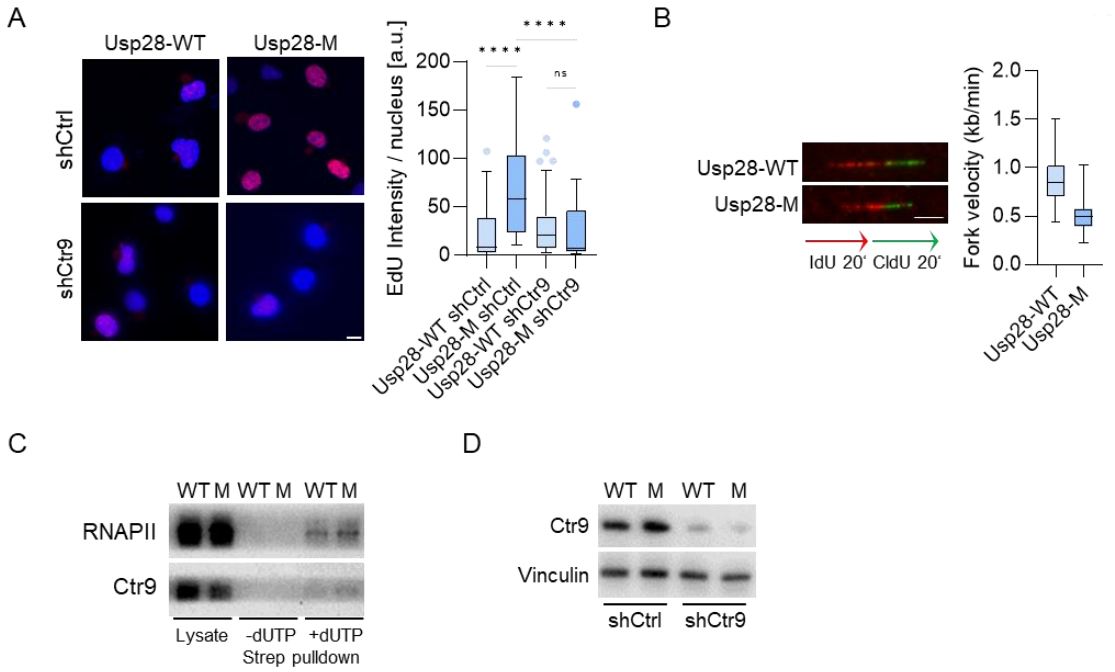

Figure 7. Usp28-M accelerates DNA replication via Paf1c recruitment

(A) EdU incorporation assays in HLF Usp28-WT or Usp28-M cells with shCtrl/shCtr9 with representative images. At least 72 cells were quantified. The data were analyzed with ordinary one-way ANOVA followed by Tukey's multiple comparisons test, ****p < 0.0001, ns p > 0.05. Scale bar = 10 µm. **(B)** DNA fiber assays in HLF Usp28-WT or Usp28-M cells with representative images. At least 70 fibers were quantified. The data were analyzed with two-tailed, unpaired t test, ****p < 0.0001. Scale bar = 5 µm. **(C)** Immunoblotting analysis of protein levels of RNAPII and Ctr9 on nascent chromatin captured from HLF Usp28-WT or Usp28-M cells. **(D)** Immunoblotting analysis verifying Ctr9 knockdown in HLF Usp28-WT or Usp28-M cells with shCtrl/shCtr9. Part of panels and figure legends are adapted from the manuscript 'Jin, C., Einig, E., Xu, W., Kollampally, R.B., Schlosser, A., Flentje, M. and Popov, N. (under revision) The dimeric deubiquitinase Usp28 integrates 53bp1 and Myc functions to limit DNA damage.' (1).

4.3 Monomeric Usp28 induces replication-dependent DNA damage

As deregulated DNA synthesis can lead to genomic instability (238,239) and Usp28-M can stimulate DNA replication, we compared the levels of pH2AX, a marker of DNA damage, in cells expressing Usp28-WT and Usp28-M using immunoblotting and immunofluorescence assays. Expression of Usp28-M significantly upregulated pH2AX levels compared to Usp28-WT, in both assays (Fig. 8A, B, C, D). Since the stimulation of DNA synthesis by Usp28-M was found involved with Paf1c recruitment, we further checked how Paf1c regulates DNA damage in Usp28-M and Usp28-WT cells. As showed below, with the depletion of Paf1c subunits Ctr9 and Cdc73, pH2AX levels were significantly decreased in Usp28-M cells only (Fig. 8A, B, C, D), similar with the effects on DNA replication (Fig. 7A).

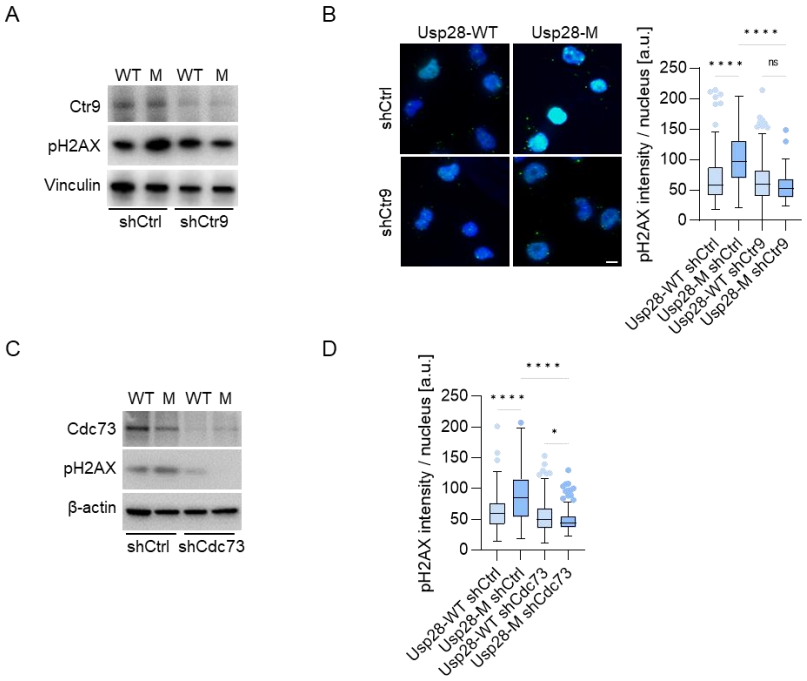

Figure 8. Paf1c depletion reduces DNA damage in HLF Usp28-M cells

(A) Immunoblotting analysis of protein levels of pH2AX in HLF Usp28-WT or Usp28-M cells with shCtrl/shCtr9. **(B)** Immunofluorescence analysis of intensity of pH2AX in HLF Usp28-WT or Usp28-M cells with shCtrl/shCtr9 with representative images. At least 122 cells were quantified. The data were analyzed with ordinary one-way ANOVA followed by Tukey's multiple comparisons test, ****p < 0.0001, ns p > 0.05. Scale bar = 10 μm. **(C)** Immunoblotting analysis of protein levels of pH2AX in HLF Usp28-WT or Usp28-M cells with shCtrl/shCdc73. **(D)** Immunofluorescence analysis of intensity of pH2AX in HLF Usp28-WT or Usp28-M cells with shCtrl/shCdc73. At least 104 cells were quantified. The data were analyzed with ordinary one-way ANOVA, Tukey's multiple comparisons test, *p < 0.05, ****p < 0.0001. Panels and figure legends are adapted from the manuscript 'Jin, C., Einig, E., Xu, W., Kollampally, R.B., Schlosser, A., Flentje, M. and Popov, N. (under revision) The dimeric deubiquitinase Usp28 integrates 53bp1 and Myc functions to limit DNA damage.' (1).

Considering the immunochemical staining of pH2AX represents the biological response to DNA damage, we further performed the neutral comet assays (240), which directly detects DNA double strand breaks (241). Consistent with pH2AX levels measured above, DNA DSBs were strongly increased in cells expressing Usp28-M compared to Usp28-WT while the depletion of Paf1c reverted this effect (Fig. 9A), suggesting that Paf1c recruitment contributes to the DNA DSBs in Usp28-M cells. Next, to check if Usp28-M induces DNA damage by deregulating DNA replication, we evaluated DNA breakage and pH2AX levels in Usp28-WT and Usp28-M cells treated with a high concentration (2 mM) of thymidine, which blocks DNA synthesis (242). Indeed, thymidine decreased DNA DSBs in both cell lines and reverted the increase in Usp28-M cells (Fig. 9B, C). Taken together, we concluded that monomeric Usp28 promotes TRCs resolution in a Paf1c-dependent manner and induces aberrant DNA synthesis leading to DNA damage.

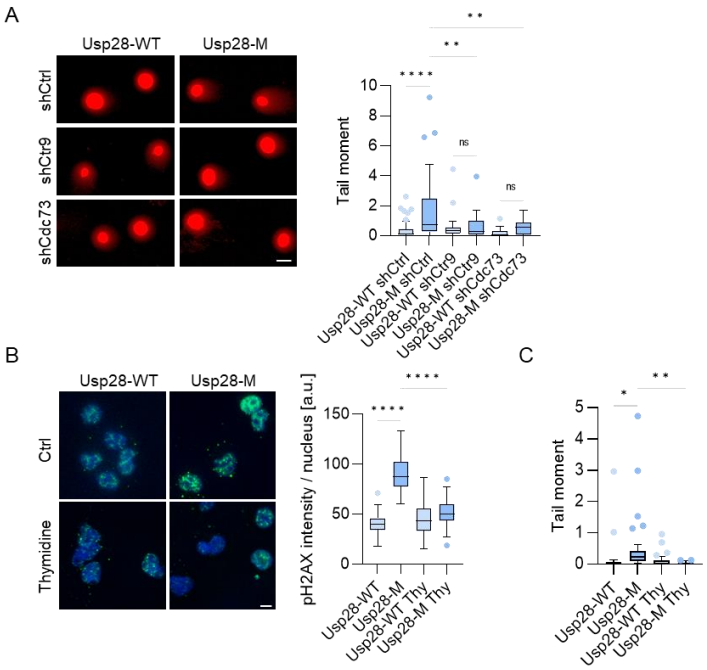

Figure 9. Paf1c depletion reverts Usp28-M induced replication-dependent DNA damage

(A) Neutral comet assays in Usp28-WT or Usp28-M cells with shCtrl/shCtr9/shCdc73 with representative images. At least 18 cells were quantified. The data were analyzed with ordinary one-way ANOVA followed by Tukey's multiple comparisons test, **p < 0.01, ****p < 0.0001, ns p > 0.05. Scale bar = 10 µm. **(B)** Immunofluorescence analysis with antibodies against pH2AX in Usp28-WT or Usp28-M cells treated with thymidine (2 mM) or vehicle control for 2 h with representative images. At least 47 cells were quantified. The data were analyzed with ordinary one-way ANOVA followed by Šídák's multiple comparisons test of selected pairs, ****p < 0.0001. Scale bar = 10 µm. **(C)** Neutral comet assays in Usp28-WT or Usp28-M cells treated with thymidine (2 mM) or vehicle control for 2 h. At least 27 cells were quantified. The data were analyzed with ordinary one-way ANOVA followed by Šídák's multiple comparisons test of selected pairs, *p < 0.05, **p < 0.01. Panels and figure legends are adapted from the manuscript 'Jin, C., Einig, E., Xu, W., Kollampally, R.B., Schlosser, A., Flentje, M. and Popov, N. (under revision) The dimeric deubiquitinase Usp28 integrates 53bp1 and Myc functions to limit DNA damage.' (1).

4.4 DNA damage disrupts Usp28 dimerization

Usp28 is activated upon DNA damage

Since the dimerization of Usp28 regulates DNA synthesis and mediates DNA replication-induced DNA damage, we would like to know the mechanisms that regulate Usp28 dimerization. Usp28 is known to be activated by DDR signaling while the mechanisms remain unknown (153,213,243). To test if Usp28 can also be activated by DDR in HLF cells, we treated them with etoposide, the topoisomerase II inhibitor, to induce DNA damage. Myc protein was found accumulated (Fig. 10A), in line with the previous research (244), while the mRNA level of Myc kept constant, excluding the transcriptional regulation (Fig. 10B). Interestingly, protein levels of Myc did not increase in cells with Usp28 knockout, indicating that the accumulation of Myc in response to etoposide induced DNA damage is Usp28-dependent (Fig. 10A).

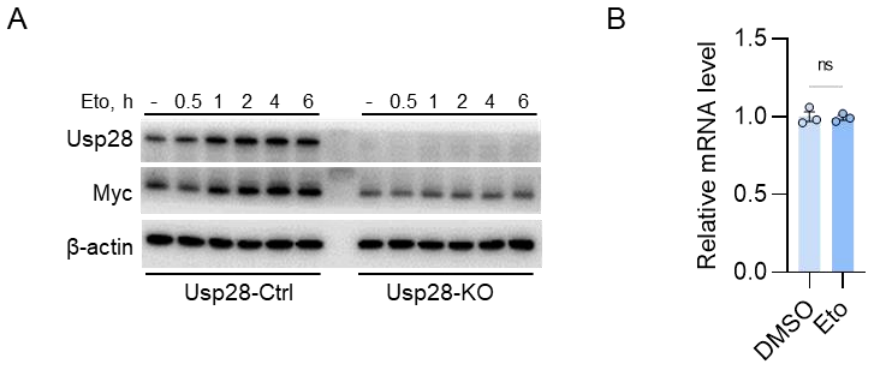

Figure 10. Myc is accumulated upon DNA damage in a Usp28-dependent manner

(A) Immunoblotting analysis of Myc protein levels in HLF Usp28-Ctrl and Usp28-KO cells with etoposide (5 μM) treatment for the indicated time points. **(B)** qPCR analysis of the Myc mRNA levels in HLF Usp28-WT cells with or without etoposide treatment (5 μM, 30 min). The data were analyzed from three technical replicates with two-tailed, unpaired t test, ns $p > 0.05$. Panels and figure legends are adapted from the manuscript 'Jin, C., Einig, E., Xu, W., Kollampally, R.B., Schlosser, A., Flentje, M. and Popov, N. (under revision) The dimeric deubiquitinase Usp28 integrates 53bp1 and Myc functions to limit DNA damage.' (1).

Less Myc ubiquitination was found with etoposide treatment from ubiquitin pulldown assays compared to DMSO-treated cells (Fig. 11A). besides, deubiquitination activity assays with Ub-VME/VS probes showed an enhanced Usp28 activity with etoposide treatment (Fig. 11B). Furthermore, etoposide did not accumulate Myc protein levels in Usp28-M cells, which had higher basal Myc levels (Fig. 11C, D), indicating that the accumulation of Myc in response to etoposide involves formation of Usp28 monomers, which underlies the activation of Usp28 upon DDR.

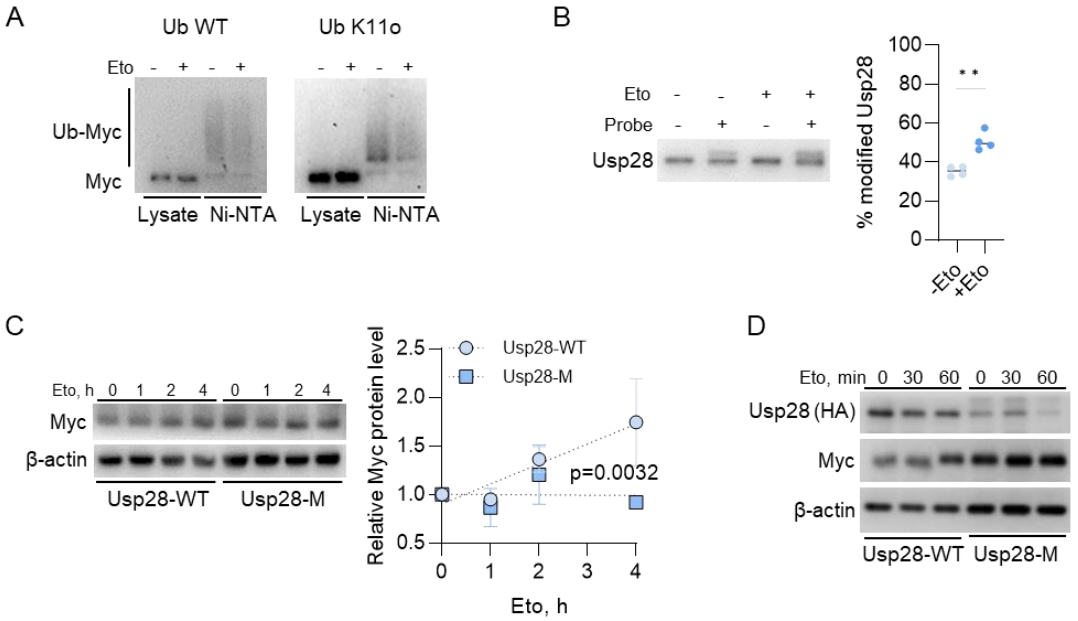

Figure 11. Usp28 deubiquitination activity is enhanced upon DNA damage

(A) Ubiquitin pulldown assay in HeLa cells transfected with Myc and WT or K11-only His-Ub before and after etoposide (5 μM, 30 min) treatment. **(B)** DUB activity assay in HLF Usp28-WT cells with or without etoposide (5 μM, 30 min) treatment. Right panel shows a mean of four biological replicates. The data were analyzed with two-tailed, unpaired t test, **p < 0.01. **(C)** Immunoblotting analysis of protein levels of Myc in HLF Usp28-WT and Usp28-M cells with etoposide (5 μM) for the indicated time points. Right panel shows a mean of three biological replicates. Linear regression analysis shows that the slopes of the regression lines differ significantly (p = 0.0032). Error bar denotes S.D. **(D)** Immunoblotting analysis of protein levels of Myc in p19$^{-/-}$Nras Usp28-WT and Usp28-M cells with etoposide (5 μM) for the indicated time points. Original data of Fig. 11D was provided by Ravi B Kollampaly. Panels and figure legends are adapted from the manuscript 'Jin, C., Einig, E., Xu, W., Kollampally, R.B., Schlosser, A., Flentje, M. and Popov, N. (under revision) The dimeric deubiquitinase Usp28 integrates 53bp1 and Myc functions to limit DNA damage.' (1).

Usp28 dimers are disrupted upon DNA damage

To confirm whether the formation of Usp28 monomers can underlie Usp28 activation during DDR, cells stably expressing HA- and GFP-tagged Usp28 proteins (Fig. 12A) were generated based on p19$^{-/-}$Nras cells to study the dimerization status of Usp28 before and after etoposide treatment.

PLA assays with antibodies against HA and GFP showed a strong signal in unstressed cells, which was dramatically decreased after etoposide treatment (Fig. 12B), indicating that Usp28 dimerization is blocked by DNA damage. Immunoprecipitation assays in p19$^{-/-}$Nras cells stably expressing HA- and GFP-tagged Usp28 alleles and in HeLa cells transiently transfected with HA- and FLAG-tagged Usp28 also showed similar results (Fig. 12C, D).

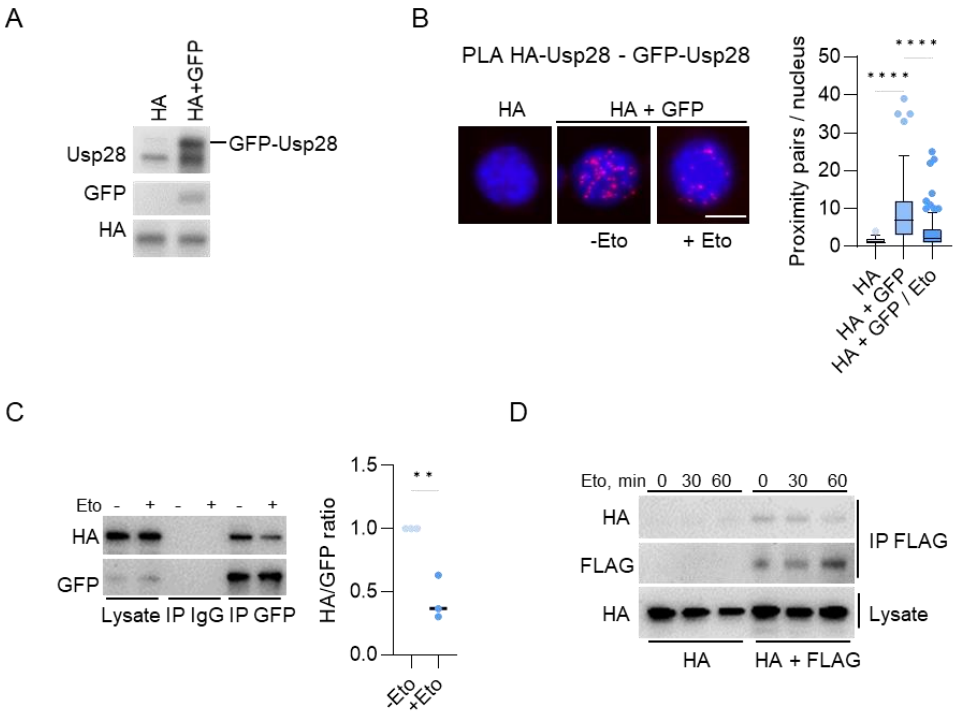

Figure 12. DNA damage induces monomeric Usp28 formation

(A) Immunoblotting analysis verifying the expression of GFP- and HA-tagged Usp28 proteins in p19$^{-/-}$Nras cells. **(B)** PLA assays with antibodies against GFP and HA-tag in p19$^{-/-}$Nras cells expressing GFP- and HA-tagged Usp28 with or without etoposide (5 μM, 30 min) treatment with representative images. At least 26 cells were quantified. The data were analyzed with ordinary one-way ANOVA, Tukey's multiple comparisons test, ****$p < 0.0001$. Scale bar = 10 μm. **(C)** Immunoprecipitation analysis with antibodies against GFP in p19$^{-/-}$Nras cells expressing HA- and GFP-tagged Usp28, treated with DMSO or etoposide (5 μM, 30 min). Right panel shows a mean of three biological replicates. The data were analyzed with two-tailed, unpaired t test, **$p < 0.01$. **(D)** Immunoprecipitation analysis with antibodies against FLAG from HeLa cells transient transfected with HA- and FLAG-tagged Usp28 before and after etoposide treatment (5 μM) for the indicated time points. Panels and figure legends are adapted from the manuscript 'Jin, C., Einig, E., Xu, W., Kollampally, R.B., Schlosser, A., Flentje, M. and Popov, N. (under revision) The dimeric deubiquitinase Usp28 integrates 53bp1 and Myc functions to limit DNA damage.' (1).

Taken together, these data indicate Usp28 is activated during DNA damage response due to the formation of monomeric Usp28 which has a higher catalytic activity.

4.5 53bp1 controls Usp28 dimerization and catalytic activity

53bp1 is a binding partner of Usp28 but only binds to Usp28 dimer

One major Usp28 binding partner is 53bp1 - a DDR mediator protein that can promote localization of Usp28 to DNA lesions. In turn, Usp28 can stabilize 53bp1 upon DNA damage (213,214). To check the binding between Usp28 and 53bp1 in our research model, mass spectrometry analysis was performed after immunoprecipitation with antibodies against Usp28 or 53bp1 in HeLa cells (Fig. 13A). Immunoprecipitation assays with the same antibodies were also done in HLF cells (Fig. 13B, C). Both results showed that Usp28 and 53bp1 can efficiently interact in unstressed cells, suggesting a role for Usp28-53bp1 during unperturbed cell cycle (213,245).

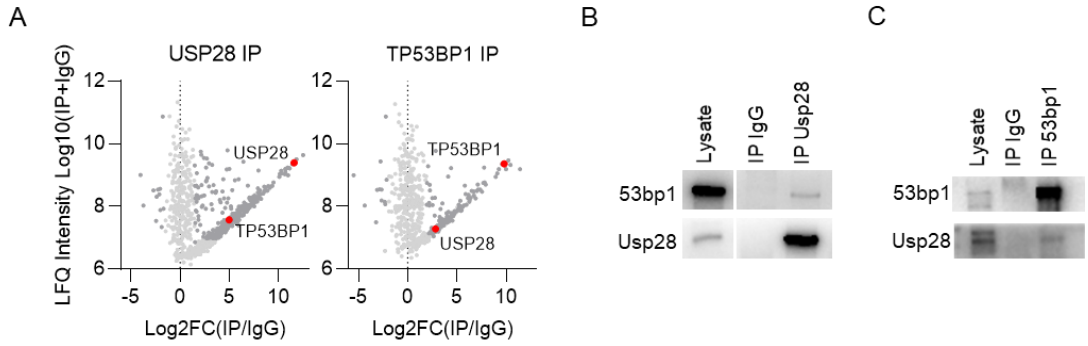

Figure 13. 53bp1 interacts with Usp28

(A) LC-MS/MS analysis of immunoprecipitations with antibodies against Usp28 and 53bp1 from HeLa cells showing reciprocal identification of Usp28 and 53bp1 interaction. Dark grey dots denote significant interactors of Usp28 or 53bp1. **(B)** Immunoprecipitation analysis with antibodies against Usp28 or control IgG from HLF cells. **(C)** Immunoprecipitation analysis with antibodies against 53bp1 or control IgG from HLF cells. Original samples of Fig. 13A were prepared by Ravi B Kollampaly. The assay was performed and the raw data was analyzed by Prof. Andreas Schlosser. The figure was made by Prof. Nikita Popov and Elias Einig. Panels and figure legends are adapted from the manuscript 'Jin, C., Einig, E., Xu, W., Kollampally, R.B., Schlosser, A., Flentje, M. and Popov, N. (under revision) The dimeric deubiquitinase Usp28 integrates 53bp1 and Myc functions to limit DNA damage.' (1).

Unexpectedly, immunoprecipitation showed that 53bp1 selectively binds wildtype but not monomeric Usp28 both in HLF and in $p19^{-/-}$Nras cell lines (Fig. 14A, B), PLA assays also showed the same result (Fig. 14C). Furthermore, etoposide treatment diminished the binding between 53bp1 and Usp28 (Fig. 14C), accompanied with the formation of Usp28 monomers (Fig. 12B, C, D), indicating that 53bp1 stabilizes dimeric Usp28 and the dissociation of Usp28 from 53bp1 upon DNA damage leads to the formation of Usp28 monomers and thus activates Usp28 catalytic function.

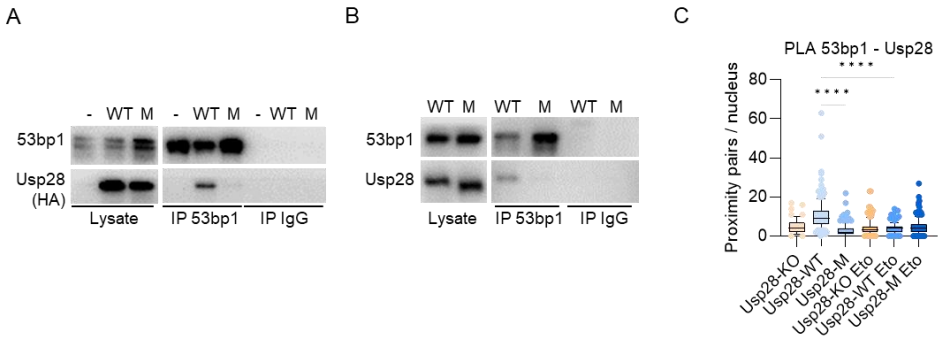

Figure 14. 53bp1 and Usp28-WT specific binding is disrupted by DNA damage

(A) Immunoprecipitation analysis with antibodies against 53bp1 or control IgG from HLF Usp28-KOWT/M cells. **(B)** Immunoprecipitation analysis with antibodies against 53bp1 or control IgG from p19$^{-/-}$Nras Usp28-WT/M cells. **(C)** PLA assays with antibodies against 53bp1 and HA-tag in HLF Usp28-KO/WT/M cells treated with DMSO or etoposide (5 μM, 30 min). At least 71 cells were quantified. The data were analyzed with ordinary one-way ANOVA followed by Tukey's multiple comparisons test, ****p < 0.0001. Original data of Fig. 14B was provided by Ravi B Kollampaly. Panels and figure legends are adapted from the manuscript 'Jin, C., Einig, E., Xu, W., Kollampally, R.B., Schlosser, A., Flentje, M. and Popov, N. (under revision) The dimeric deubiquitinase Usp28 integrates 53bp1 and Myc functions to limit DNA damage.' (1).

Depletion of 53bp1 activates Usp28

To test if 53bp1 is a key factor in regulating Usp28 dimerization in response to DNA damage, we generated 53bp1 depleted cells in the HLF cells and p19$^{-/-}$Nras cells with different shRNAs against 53bp1 (Fig. 15A, B). As expected, Usp28 dimerization was significantly diminished with the depletion of 53bp1 (Fig. 15C), phenocopying the effect of etoposide (Fig. 12B, C, D).

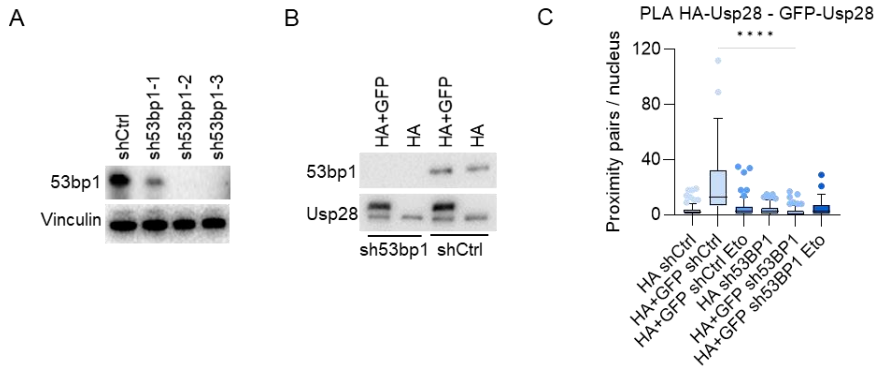

Figure 15. 53bp1 depletion diminishes Usp28 dimerization

(A) Immunoblotting analysis verifying the depletion of 53bp1 in HLF cells with different shRNAs against 53bp1. **(B)** Immunoblotting analysis verifying the depletion of 53bp1 in p19$^{-/-}$Nras cells with HA- and/or GFP-tagged Usp28. **(C)** PLA assays with antibodies against GFP and HA-tag in p19$^{-/-}$Nras cells with shCtrl/sh53bp1 treated with DMSO or etoposide (5 μM, 30 min). At least 42 cells were quantified. The data were analyzed with ordinary one-way ANOVA followed by Tukey's multiple comparisons test, ****p < 0.0001. Panels and figure legends are adapted from the manuscript 'Jin, C., Einig, E., Xu, W., Kollampally, R.B., Schlosser, A., Flentje, M. and Popov, N. (under revision) The dimeric deubiquitinase Usp28 integrates 53bp1 and Myc functions to limit DNA damage.' (1).

Since Usp28 monomers are more active towards Myc deubiquitination, we compared Usp28 catalytic activity in shCtrl and sh53bp1 cells. Deubiquitination activity assays with the Ub-VME/Ub-VS probes showed that depletion of 53bp1 stimulated Usp28 deubiquitinase activity (Fig. 16A). Furthermore, ubiquitin pulldown assays revealed less Myc ubiquitination in 53bp1-deficient cells (Fig. 16B). In accord, depletion of 53bp1 increased steady state Myc levels and enhanced Myc protein stability while Myc mRNA was reduced (Fig. 16C, D, E). We concluded that depletion of 53bp1 promotes formation of Usp28 monomers and stabilizes Myc.

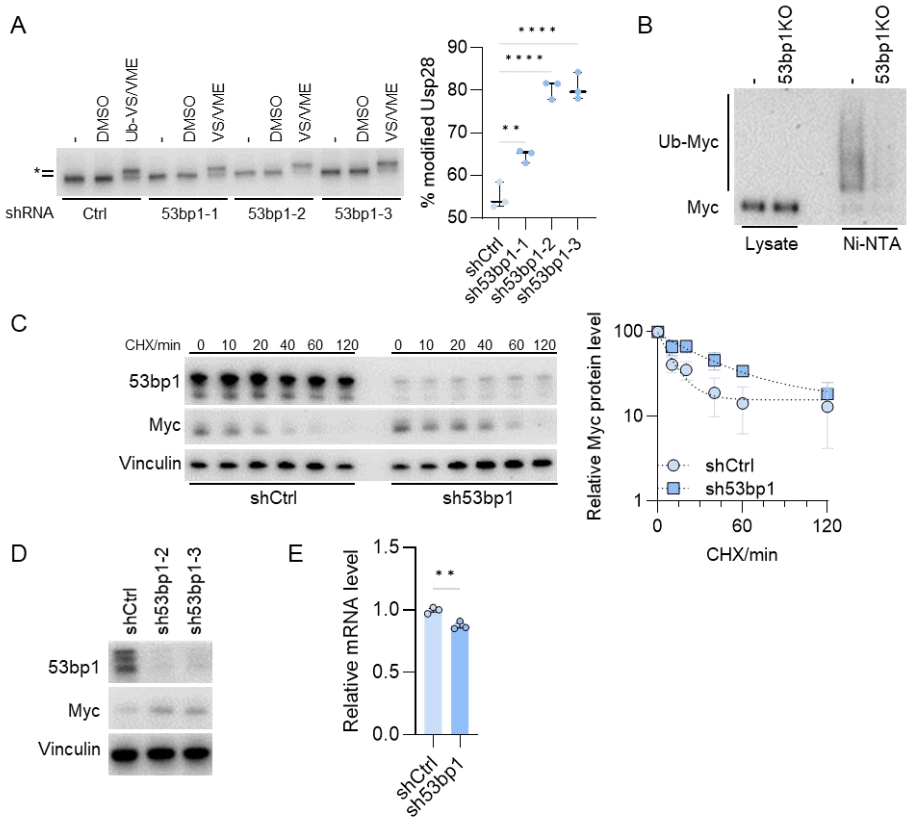

Figure 16. 53bp1 depletion stabilizes Myc via Usp28 activation

(A) DUB activity assay in HLF sh53bp1 cells. Right panel shows a mean of three biological replicates. The data were analyzed with ordinary one-way ANOVA followed by Tukey's multiple comparisons test, **p < 0.01, ****p < 0.0001. **(B)** Ubiquitin pulldown assay in HeLa cells transfected with Myc, wildtype His-Ub showing the deubiquitination activity of Usp28 with or without 53bp1 knockout. **(C)** Immunoblotting analysis with antibodies against 53bp1 and Myc showing Myc protein levels in HLF shCtrl/sh53bp1 cells. The indicated time points indicate the durations of cycloheximide (100 µg/ml) treatment. Right panel shows a mean of three biological replicates. Error bar denotes S.D. **(D)** Immunoblotting analysis with antibodies against 53bp1 and Myc showing 53bp1 and Myc protein levels in HLF cells with different shRNAs. **(E)** qPCR showing the mRNA levels of Myc in HLF shCtrl/sh53bp1 cells. The data were analyzed from three technical replicates with two-tailed, unpaired t test, **p < 0.01. Panels and figure legends are adapted from the manuscript 'Jin, C., Einig, E., Xu, W., Kollampally, R.B., Schlosser, A., Flentje, M. and Popov, N. (under revision) The dimeric deubiquitinase Usp28 integrates 53bp1 and Myc functions to limit DNA damage.' (1).

4.6 Depletion of 53bp1 diminishes TRCs and induces replication-associated DNA damage

Depletion of 53bp1 enhanced the recruitment of Paf1c to Myc and RNAPII

Opposite to the effects of Usp28 knockout, 53bp1 depletion stimulated Myc-Paf1c binding in HLF cells (Fig. 17A, B); importantly, this effect was disappeared in sh53bp1cells with Usp28 deletion, indicating that activation of Usp28 in the absence of 53bp1 underlies enhanced Myc-Paf1c interaction.

PLA assay with antibodies against pS5-RNAPII and Paf1 also showed an enhanced pS5-RNAPII-Paf1 binding (Fig. 17C), indicating 53bp1 restrains the recruitment of Paf1 at transcriptionally active chromatin.

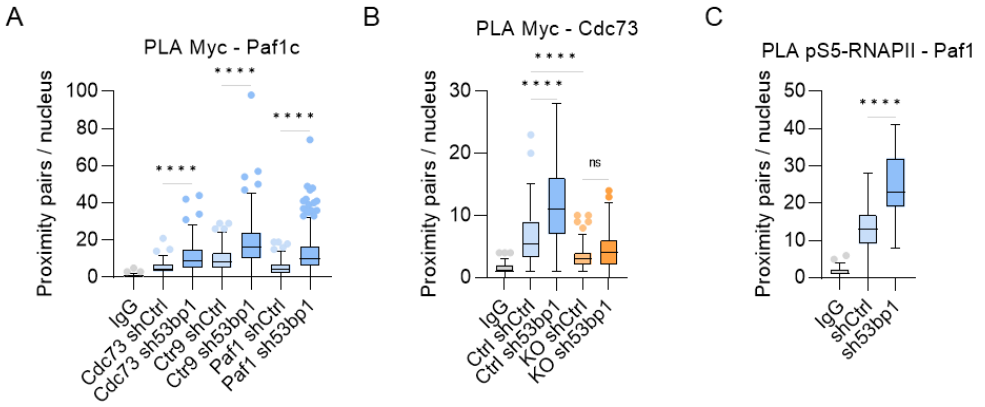

Figure 17. 53bp1 knockdown promotes Paf1c binding with Myc and pS5-RNAPII

(A) PLA assays with antibodies against Myc and Paf1c subunits (Cdc73/Ctr9/Paf1) or IgG in HLF cells with shCtrl/sh53bp1. At least 130 cells were quantified. The data were analyzed with two-tailed, unpaired t test for each pair, ****p < 0.0001. **(B)** PLA assays with antibodies against Myc and Cdc73 or IgG in HLF Usp28-Ctrl/KO cells with shCtrl/sh53bp1. At least 70 cells were quantified. The data were analyzed with ordinary one-way ANOVA, Šídák's multiple comparisons test of selected pairs, ****p < 0.0001, ns p > 0.05. **(C)** PLA assays with antibodies against pS5-RNAPII and Paf1 or IgG in HLF shCtrl/sh53bp1 cells. At least 55 cells were quantified. The data were analyzed with two-tailed, unpaired t test, ****p < 0.0001. Panels and figure legends are adapted from the manuscript 'Jin, C., Einig, E., Xu, W., Kollampally, R.B., Schlosser, A., Flentje, M. and Popov, N. (under revision) The dimeric deubiquitinase Usp28 integrates 53bp1 and Myc functions to limit DNA damage.' (1).

Depletion of 53bp1 reduces TRCs and stimulates DNA replication

Consistent with the recruitment of Paf1c in 53bp1 depletion cells, PLA assays with antibodies against pS5-RNAPII and PCNA showed a strong reduction in the number of proximity pairs compared to the control cells (Fig. 18A), indicating the rapid resolution of TRCs without 53bp1.

Accompanied with the resolution of TRCs in sh53bp1 cells, DNA replication was detected significantly stimulated compared to shCtrl cells by EdU incorporation assays (Fig. 18B). However, DNA fiber assays showed a reduced progression rate of DNA replication forks (Fig. 18C), indicating that loss of 53bp1 stimulates replication origins firing, mimicking the phenotype of Usp28-M cells (Fig. 7A, B).

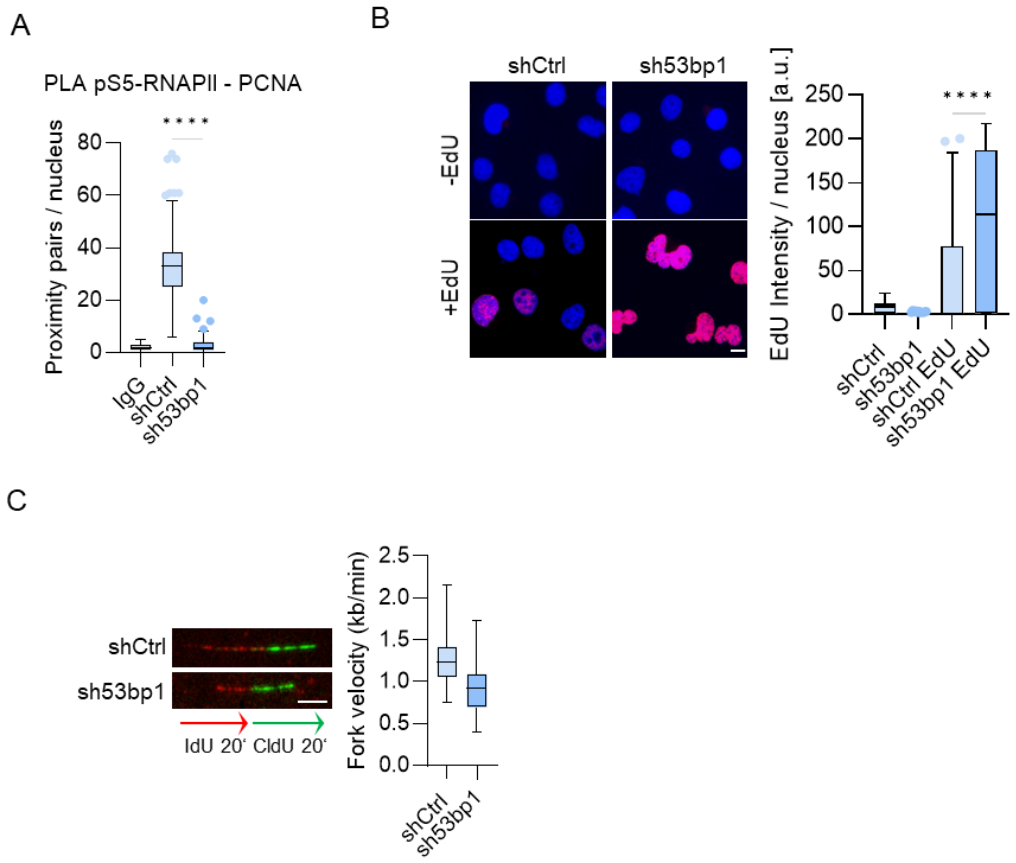

Figure 18. 53bp1 knockdown reduces TRCs and promotes DNA synthesis

(A) PLA assays with antibodies against pS5-RNAPII and PCNA or IgG in HLF shCtrl/sh53bp1 cells. At least 101 cells were quantified. The data were analyzed with two-tailed, unpaired t test, ****p < 0.0001. **(B)** EdU incorporation assays in HLF shCtrl/sh53bp1 cells with representative images. At least 69 cells were quantified. The data were analyzed with ordinary one-way ANOVA, Tukey's multiple comparisons test, ****p < 0.0001. Scale bar = 10 µm. **(C)** DNA fiber assays in HLF shCtrl/sh53bp1 cells with representative images. At least 94 fibers were quantified. The data were analyzed with two-tailed, unpaired t test, **** p < 0.0001. Scale bar = 5 µm. Part of the panels and figure legends are adapted from the manuscript 'Jin, C., Einig, E., Xu, W., Kollampally, R.B., Schlosser, A., Flentje, M. and Popov, N. (under revision) The dimeric deubiquitinase Usp28 integrates 53bp1 and Myc functions to limit DNA damage.' (1).

Depletion of 53bp1 induces replication-associated DNA damage

As discussed above, deregulated DNA replication is associated with replicative stress and genomic instability (238,239), loss of 53bp1 may lead to replication-associated DNA damage. In line with this idea, immunofluorescence analysis with antibodies against pH2AX showed increased pH2AX levels in sh53bp1 cells (Fig. 19A), which was further reverted by DNA replication inhibition under thymidine treatment (Fig. 19A), indicative of increased replication-dependent DNA damage. Similarly, neutral comet assays revealed an accumulation of DNA DSBs in sh53bp1 cells (Fig. 19B), which was also rescued by the incubation with thymidine (Fig. 19B).

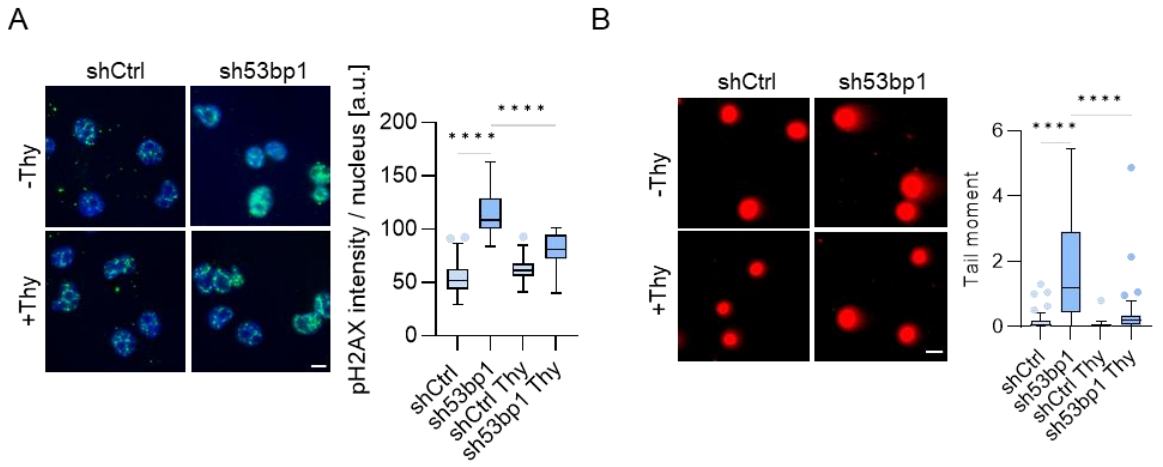

Figure 19. 53bp1 knockdown raises replication-associated DNA damage

(A) Immunofluorescence analysis with antibodies against pH2AX in HLF shCtrl/sh53bp1 cells with or without thymidine treatment (2 mM, 2 h) with representative images. At least 60 cells were quantified. The data were analyzed with ordinary one-way ANOVA, Tukey's multiple comparisons test, ****p < 0.0001. Scale bar = 10 µm. **(B)** Neutral comet assays showing the DSBs in HLF shCtrl/sh53bp1 cells with or without thymidine treatment (2 mM, 2 h) with representative images. At least 34 cells were quantified. The data were analyzed with ordinary one-way ANOVA followed by Tukey's multiple comparisons test, ****p < 0.0001. Scale bar = 10 µm. Panels and figure legends are adapted from the manuscript 'Jin, C., Einig, E., Xu, W., Kollampally, R.B., Schlosser, A., Flentje, M. and Popov, N. (under revision) The dimeric deubiquitinase Usp28 integrates 53bp1 and Myc functions to limit DNA damage.' (1).

4.7 Etoposide triggers a transient replicative response

DNA replication is stimulated at an early stage of DDR

In line with impaired formation of 53bp1-Usp28 complexes and Usp28 dimers, etoposide enhanced Paf1c recruitment to Myc in shCtrl cells but not in sh53bp1 or Usp28-KO cells (Fig. 20A). Furthermore, etoposide decreased TRCs in shCtrl cells but not in sh53bp1 cells (Fig. 20B), indicating that etoposide reduces TRCs by disrupting 53bp1-Usp28 complexes.

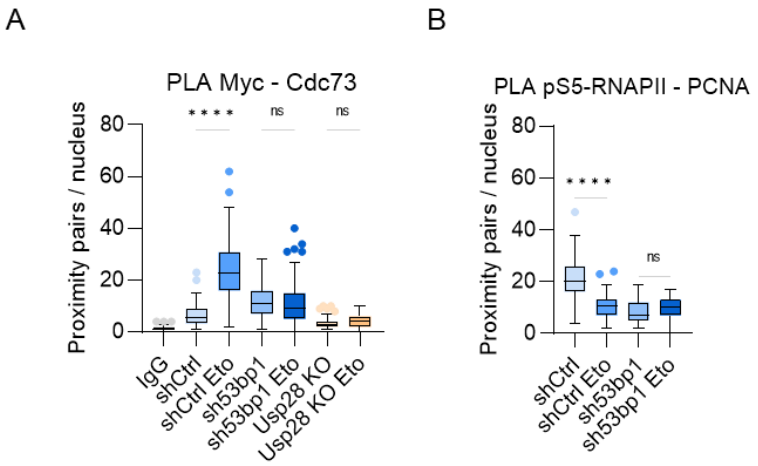

Figure 20. DNA damage promotes Myc-Paf1c binding and TRCs resolutions

(A) PLA assays with antibodies against Myc and Cdc73 or IgG in HLF shCtrl/sh53bp1 or Usp28-KO cells with or without etoposide treatment (5 μM, 30 min). At least 41 cells were quantified. The data were analyzed with ordinary one-way ANOVA followed by Šídák's multiple comparisons test of selected pairs, ****p < 0.0001, ns p > 0.05. **(B)** PLA assays with antibodies against pS5-RNAPII and PCNA in HLF shCtrl/sh53bp1 cells with or without etoposide treatment (5 μM, 30 min). At least 44 cells were quantified. The data were analyzed with ordinary one-way ANOVA followed by Tukey's multiple comparisons test, ****p < 0.0001, ns p > 0.05. Panels and figure legends are adapted from the manuscript 'Jin, C., Einig, E., Xu, W., Kollampally, R.B., Schlosser, A., Flentje, M. and Popov, N. (under revision) The dimeric deubiquitinase Usp28 integrates 53bp1 and Myc functions to limit DNA damage.' (1).

Since the reduced TRCs in Usp28-M and sh53bp1 cells is accompanied by stimulated DNA replication, we checked EdU incorporation in HLF cells at different timepoints after a short (30 min) treatment of etoposide. DNA synthesis was reduced at 16 h after etoposide incubation (Fig. 21A), likely due to the cell cycle arrest-induced by DNA damage. Strikingly, right after etoposide treatment, EdU incorporation signal was significantly increased compared to unstressed cells (Fig. 21A), suggesting etoposide-induced DNA synthesis stimulation is a transient response at an early stage of DDR. DNA fiber assays showed that replication fork progression was slowed by etoposide (Fig. 21B). However, the fraction of new origin fibers (228), strongly increased upon treatment (Fig. 21C), indicating

that etoposide-induced EdU incorporation is due to ectopic origin firing. Etoposide did not stimulate DNA synthesis in sh53bp1 or Usp28-M cells, which had an elevated basal rate of EdU incorporation (Fig. 21D, E). Besides, knockout of 53bp1 also abolished etoposide-induced DNA synthesis in HeLa cells (Fig. 21F), suggesting that genotoxic stress can induce DNA synthesis in a 53bp1-dependent manner in different cellular contexts.

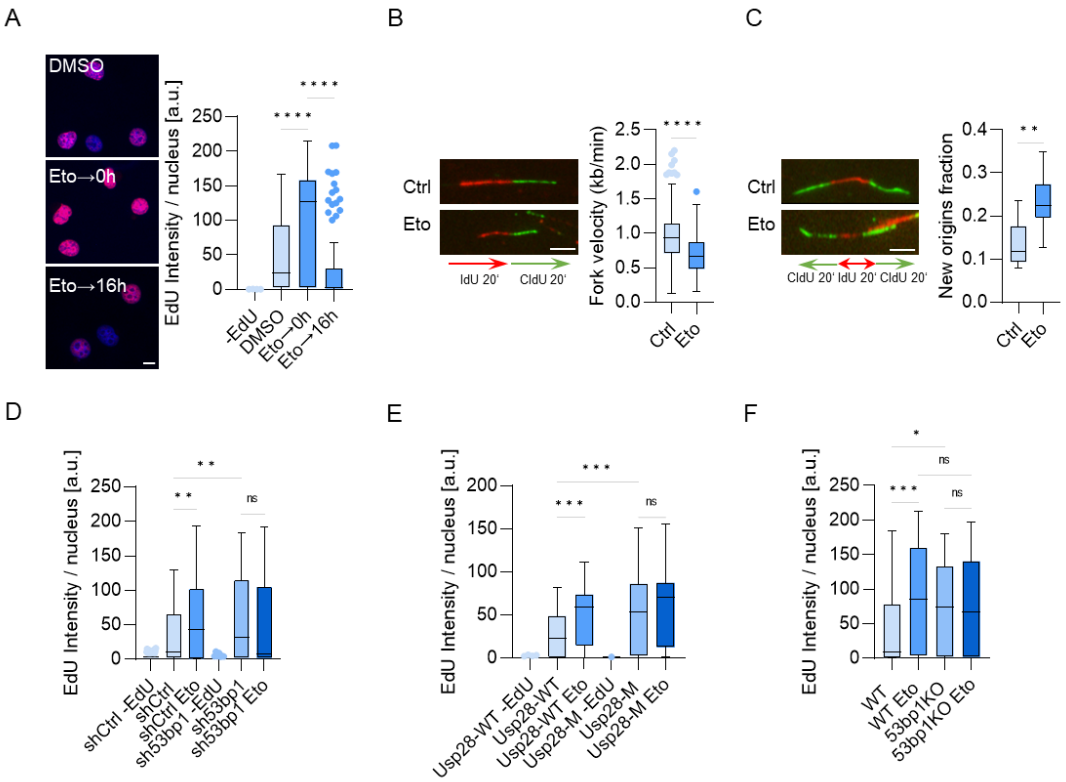

Figure 21. DNA synthesis is transient accelerated in a 53bp1-dependent manner

(A) EdU incorporation assays in HLF cells with DMSO or etoposide treatment (5 μM, 30 min) with or without release (16 h) with representative images. At least 69 cells were quantified. The data were analyzed with ordinary one-way ANOVA followed by Tukey's multiple comparisons test, ****p < 0.0001. Scale bar = 10 μm. **(B)** DNA fiber assays in HLF cells with or without etoposide treatment (5 μM, 30 min). At least 263 fibers were quantified. The data were analyzed with two-tailed, unpaired t test, ****p < 0.0001. Scale bar = 5 μm. **(C)** Quantification of new origins fraction from data showed in panel **(B)**. The data were analyzed with two-tailed, unpaired t test, **p < 0.01. Scale bar = 5 μm. **(D)** EdU incorporation assays in HLF shCtrl/sh53bp1 cells with or without etoposide treatment (5μM, 30 min). At least 82 cells were quantified. The data were analyzed with ordinary one-way ANOVA, Šídák's multiple comparisons test, **p < 0.01, ns p > 0.05. **(E)** EdU incorporation assays in HLF Usp28-WT or Usp28-M cells with or without etoposide treatment (5 μM, 30 min). At least 43 cells were quantified. The data were analyzed with ordinary one-way ANOVA, Šídák's multiple comparisons test ***p < 0.001, ns p > 0.05. **(F)** EdU incorporation assays in HeLa WT or 53bp1KO cells with or without etoposide treatment (5 μM, 30 min). At least 59 cells were quantified. The data were analyzed with ordinary one-way ANOVA, Tukey's multiple comparisons test, *p < 0.05, ***p < 0.001, ns p > 0.05. Panels and figure legends are adapted from the manuscript 'Jin, C., Einig, E., Xu, W., Kollampally, R.B., Schlosser, A., Flentje, M. and Popov, N. (under revision) The dimeric deubiquitinase Usp28 integrates 53bp1 and Myc functions to limit DNA damage.' (1).

Etoposide promotes DNA replication via Paf1c recruitment on Myc

To confirm if etoposide promotes DNA replication by Paf1c recruitment on Myc, we performed EdU incorporation assays in HLF Usp28-WT and Usp28-M cell with shCtrl/shCtr9/shCdc73 with or without etoposide treatment. As quantification showed, with the depletion of Paf1c subunits Ctr9 and Cdc73, the etoposide-induced DNA synthesis was eliminated (Fig. 22A, B). Furthermore, incubation with compound 10074-G5 (246), a known Myc inhibitor, can also partially down regulate the DNA synthesis stimulated by etoposide (Fig. 22C). In addition, depletion of Myc with different shRNAs in HCT116 cells also showed the similar result (Fig. 22D). Consistently, RNAPII and Ctr9 were found accumulated on newly synthesized DNA upon etoposide treatment in Usp28-WT cells from nascent chromatin capture assays (Fig. 22E). Based on these results, we concluded that Paf1c recruitment by Myc is important for etoposide-induced stimulation of DNA replication.

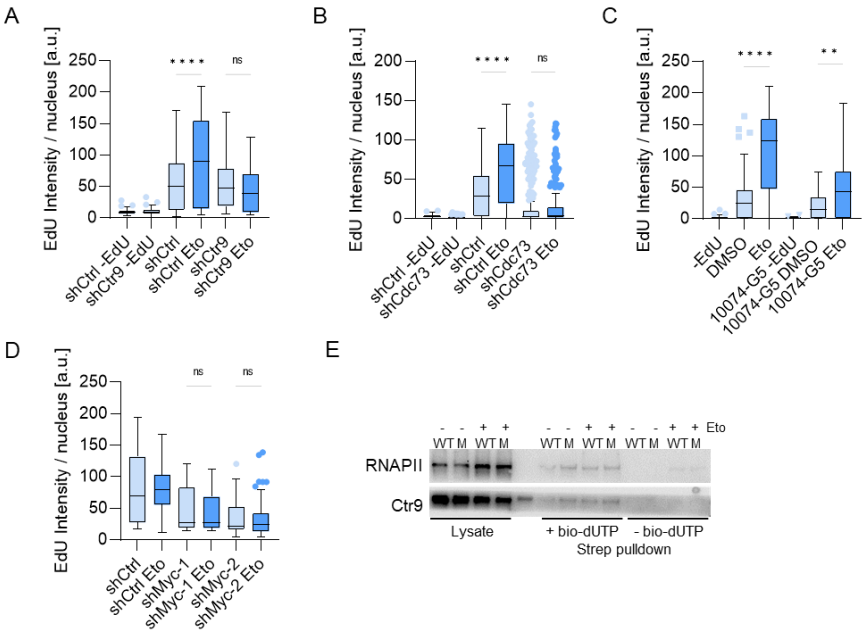

Figure 22. Suppression of Paf1c/Myc rescues DNA damage induced DNA synthesis

(A) and **(B)** EdU incorporation assays in HLF shCtrl/shCtr9/shCdc73 cells with or without etoposide treatment (5 μM, 30 min). At least 164 and 102 cells were quantified. The data were analyzed with ordinary one-way ANOVA, Tukey's multiple comparisons test, ****p < 0.001, ns p > 0.05. **(C)** EdU incorporation assays in HLF cells treated with 10074-G5 (10 μM, 2 h) and etoposide (5 μM, 30 min) alone or combined. At least 43 cells were quantified. The data were analyzed with ordinary one-way ANOVA, Tukey's multiple comparisons test, **p < 0.01, ****p < 0.0001. **(D)** EdU incorporation assays in HCT116 shCtrl/shMyc cells with or without etoposide treatment (5 μM, 30 min). At least 50 cells were quantified. The data were analyzed with ordinary one-way ANOVA, Tukey's multiple comparisons test, ns p > 0.05. **(E)** Immunoblotting analysis with antibodies against RNAPII and Ctr9 showing protein levels of RNAPII and Ctr9 on nascent chromatin captured from HLF Usp28-WT/M cells with or without etoposide treatment (5 μM, 30 min). Panels and figure legends are adapted from the manuscript 'Jin, C., Einig, E., Xu, W., Kollampally, R.B., Schlosser, A., Flentje, M. and Popov, N. (under revision) The dimeric deubiquitinase Usp28 integrates 53bp1 and Myc functions to limit DNA damage.' (1).

We then tested the effect of other genotoxins on DNA replication. Treatment of HLF cells with either topotecan or zeocin, which induce single and double strand breaks, respectively, significantly stimulated EdU incorporation (Fig. 23), indicating that stimulation of DNA replication is a common early response to genotoxic stress.

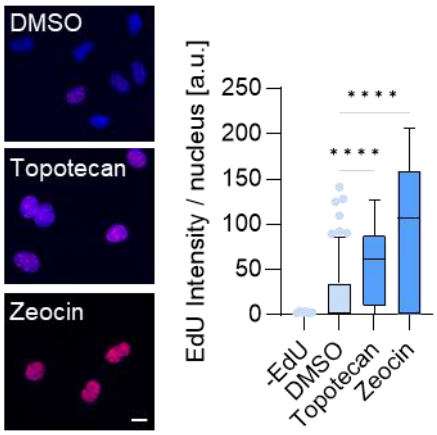

Figure 23. DNA replication stimulation is a common response to genotoxic stress

EdU incorporation assays in HLF cells with or without topotecan (1 μM, 30 min) or zeocin treatment (100 μg/ml, 30 min). At least 81 cells were quantified. The data were analyzed with ordinary one-way ANOVA, Šídák's multiple comparisons test, ****p < 0.0001. Scale bar = 10 μm. Panels and figure legends are adapted from the manuscript 'Jin, C., Einig, E., Xu, W., Kollampally, R.B., Schlosser, A., Flentje, M. and Popov, N. (under revision) The dimeric deubiquitinase Usp28 integrates 53bp1 and Myc functions to limit DNA damage.' (1).

4.8 Etoposide-induced DNA synthesis propagates DNA damage

Stimulation of DNA synthesis upon etoposide treatment may lead to accumulation of DNA damage, as observed in sh53bp1 and Usp28-M cells (Fig. 8, 19). To test this hypothesis, we treated cells with etoposide alone or in combination with DNA synthesis inhibitor thymidine and checked DNA damage levels. Immunofluorescence analysis showed that co-treatment with thymidine decreased etoposide-induced increase in pH2AX levels (Fig. 24A). Neutral comet assays revealed a strongly DNA breakage reduction in cells co-treated with thymidine (Fig. 24B), indicating that aberrant stimulation of DNA synthesis by etoposide propagates DNA damage. Thymidine also strongly decreased etoposide-induced cytotoxicity and promoted long term survival of HLF and HeLa cells (Fig. 24C), suggesting that the early replicative response to genotoxic stress exacerbates DNA breakage and impairs cell viability.

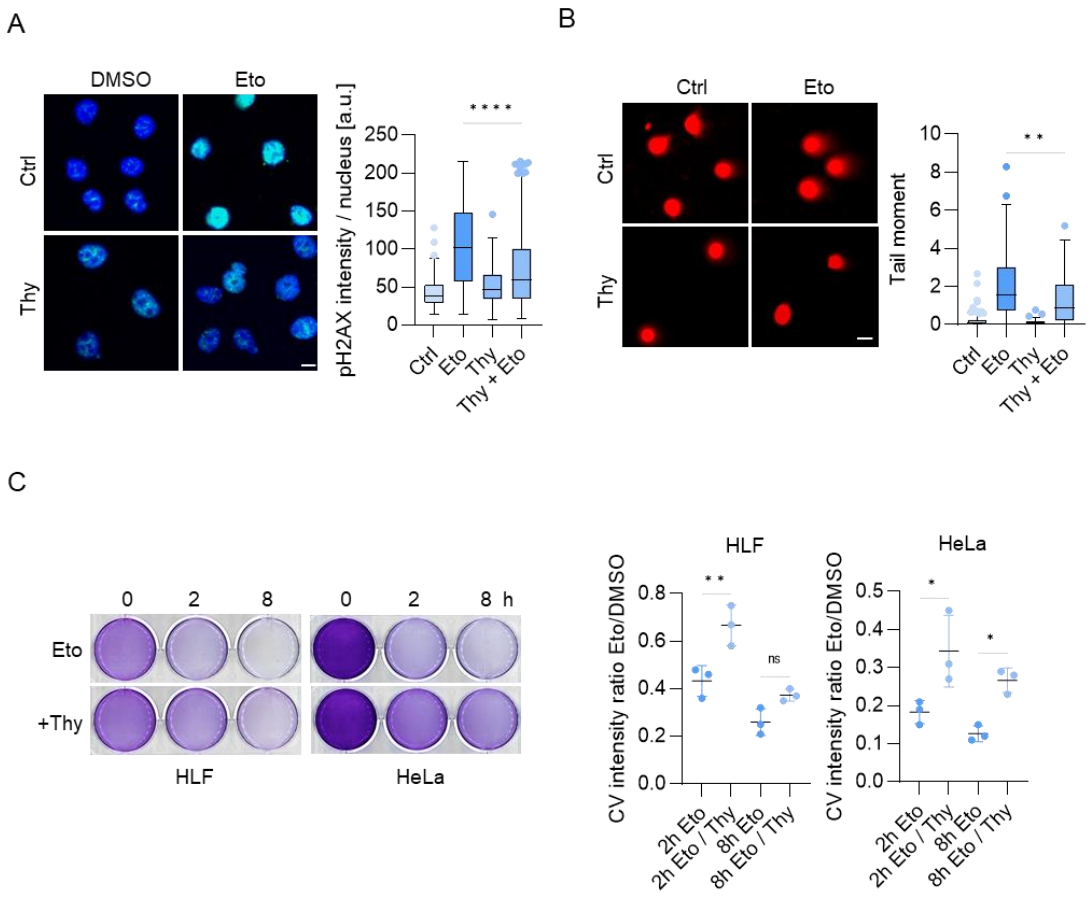

Figure 24. Etoposide-induced DNA synthesis propagates DNA damage

(A) Immunofluorescence analysis with antibodies against pH2AX showing pH2AX intensity in HLF cells with etoposide (5 µM, 30 min) and thymidine (2 mM, 2 h) alone or combined treatment with representative images. At least 77 cells were quantified; the data were analyzed with ordinary one-way ANOVA, Tukey's multiple comparisons test, ****p < 0.0001. Scale bar = 10 µm. **(B)** Neutral comet assays showing the DSBs in HLF cells with etoposide (5 µM, 30 min) and thymidine (2 mM, 2 h) alone or combined treatment with representative images. At least 33 cells were quantified. The data were analyzed with ordinary one-way ANOVA, Tukey's multiple comparisons test, **p < 0.01. Scale bar = 10 µm. **(C)** Crystal violet staining showing etoposide (5 µM) treated HLF and HeLa cells with indicated time points with or without thymidine (2 mM, 1 h prior etoposide treatment). Right panel shows a mean of three biological replicates. The data were analyzed with ordinary one-way ANOVA, Tukey's multiple comparisons test, *p < 0.05, **p < 0.01, ns p > 0.05. Error bar denotes S.D. The HeLa data in Fig. 24C was provided by Prof. Nikita Popov. Panels and figure legends are adapted from the manuscript 'Jin, C., Einig, E., Xu, W., Kollampally, R.B., Schlosser, A., Flentje, M. and Popov, N. (under revision) The dimeric deubiquitinase Usp28 integrates 53bp1 and Myc functions to limit DNA damage.' (1).

5. Discussion

Part of this chapter is adapted from the manuscript 'Jin, C., Einig, E., Xu, W., Kollampally, R.B., Schlosser, A., Flentje, M. and Popov, N. (under revision) The dimeric deubiquitinase Usp28 integrates 53bp1 and Myc functions to limit DNA damage.' (1).

The transcription factor Myc is well known for its role in tumorigenesis, in fact, it is deregulated in almost all human cancers. Many studies have been done to confirm Myc is essential for tumor progression and thus inactivation of Myc exhibits the potentiality as a promising anti-cancer strategy. The Usp28 has identified as a deubiquitinase targets the oncogenic transcription factor Myc and thereby has a prominent function in RNA Polymerase II-driven transcription, cell proliferation and tumorigenesis. Recent studies suggest Usp28 forms dimer physiologically while the biological function of Usp28 dimerization remains unknown. In this thesis, we explored the role of dimerization in biological functions of Usp28. We provide evidence that Usp28 dimerization attenuates deubiquitination of Myc and limits recruitment of the elongation factor Paf1c but with a non-transcriptional effect. Furthermore, Usp28 dimers are disassembled upon genotoxic stress into monomeric Usp28, in a 53bp1 dependent manner, leading to the transient stimulation of unscheduled DNA replication, accompanied with the replication-associated DNA damage.

Our findings provide a basis for further analysis of replicative responses to genotoxins and can be instructive for the development of combinatorial antineoplastic therapies.

5.1 Myc is stabilized by monomeric Usp28 but its transcriptional function remains unchanged

The deubiquitinase Usp28 is confirmed to exist predominantly as dimers in cells and *in vitro* from recent study (197), however, our DUB activity assays and ubiquitin pulldown assays showed that the monomeric Usp28 has a higher deubiquitination activity towards its oncogenic substrate Myc for stabilization (Fig. 3D; Fig. 4A, B), raising the question that why the Usp28 monomers are more catalytically active?

One possibility might come from the oligomerization, a common property of proteins and it happens ubiquitously in all biological systems. As a matter of fact, it is believed that more than 35% of all proteins are oligomeric, ranging from dimer to higher order structure (247-249). Oligomerization can play a versatile role in regulating the function of proteins, for example the catalytic activity of an enzyme or the binding affinity and specificity of a transcription factor (250).

In the case of Usp28, obviously, dimerization will strongly reduce Usp28 in molecular concentration, which further undermines the deubiquitination function of Usp28 on its target substrates. In addition, dimerization may also sterically block the catalytic domain of Usp28 to impair the binding between Usp28 and the substrates, since the catalytic domain of Usp28 may be covered by another Usp28 and therefore has less chances to bind with its substrates.

However, the evidence from the structural and biochemical study (197) showed that the speculations mentioned above may not be the only explanation for the higher activity of monomeric Usp28. First of all, although dimerization of Usp28 can decrease the concentration of Usp28, crystal structure of Usp28 demonstrated the two catalytic domains from the same Usp28 dimer are separated with a 56 Å distance (measured between catalytic center Cys171 residues) spatially. Besides, co-crystallization of Usp28 dimer and ubiquitin probes revealed that both two catalytic domains are able to be modified by ubiquitin probes, ruling out the possibility of steric restriction of substrate binding due to dimerization. furthermore, co-expression of Usp28 and its substrate LSD1, revealed that both dimeric and monomeric Usp28 are able to stabilize LSD1 to the same extend.

Another explanation for higher catalytic activity of monomeric Usp28 may be the substrate specificity.

Usp28 interacts with Myc and other oncogenic transcription factors, such as Jun and Notch, via the common ubiquitin ligase SCF(Fbw7) that recognizes specific phosphodegrons (251). Recent studies also showed that Usp28 can bind substrates directly or via other adaptor proteins (153). For example, Usp28 can directly bind to Myc in the absence of Fbw7 because it can recognize the same motif on Myc which also recognized by Fbw7, but unphosphorylated (151).

The single ubiquitin modification on the substrates can be further extended via the self-ubiquitination on its lysine residues, to form chains. Depend on the specific ubiquitination site, different ubiquitin chains are generated responsible for different biological functions. In general, K48-linked chains are able to lead the substrates proteasomal degradation; K11-linked chains are known to play a role in DDR (252), moreover, these atypical chains are also reported to regulate cell division and as well as proteasomal degradation (170,253).

While Fbw7 primarily assembles K48-linked ubiquitin chains, other Myc ubiquitin ligases can conjugate different types of chains, including K63 and K11 (251,254-259). In light of that Usp28 has the capacity to disassemble both degradative K11- and K48-linked polyubiquitin chains, in this thesis, we tested the deubiquitination activity of both dimeric Usp28 and monomeric Usp28 against Myc via the ubiquitin pulldown assay co-transfected with K11- or K48-linked ubiquitin, and surprisingly, we found that monomeric Usp28 is selectively active towards K11-linked chains (Fig. 4C), suggesting that such chains contribute to constitutive Myc turnover during unperturbed cell cycle.

K11 chains are predominantly assembled by the anaphase-promoting complex Apc/c, but also by other ligases that target Myc including Huwe1, RNF4, RNF8 and beta-TrCP (254,257,258,260-262). Usp28 monomers may antagonize ubiquitination of Myc by these enzymes, analogously to the mechanism described for Apc/c-mediated turnover of Claspin (263).

Besides regulating the stability of Myc via proteasomal degradation, ubiquitination is essential for the transcriptional function of Myc (146,256,264). For example, the Skp2 mediated ubiquitination of Myc is important for Myc transcriptional activity and transformation. In contrast, inhibition of this transcriptional domain ubiquitination by the competitive interaction with tumor suppressor ARF not only leads to the suppression of Myc's canonical transcriptional function but also induces the expression of the noncanonical target gene of Myc which further induces apoptosis in a p53-independent manner (265).

In particular, ubiquitination of Myc promotes histone acetylation, recruitment of elongation factors pTEFb and Paf1c, and the transfer of Paf1c from Myc onto RNAPII (118). Paf1c is a multivalent complex controlling transcriptional pausing, processive elongation, RNA maturation and nuclear export (266,267), this indicates that Usp28 may play an important role in Myc-dependent transcription.

Indeed, our RNA-seq analysis of HLF Usp28-WT and Usp28-KO cells showed a strong enrichment of Myc-regulated genes demonstrating that Usp28 regulates Myc-dependent transcription (Fig. 2A, B). Meanwhile the PLA assay also showed a strong reduction of Myc binding with Paf1c in the absence of Usp28 (Fig. 2C).

Since Usp28 is verified a key factor in Myc-dependent transcription regulation, and monomeric Usp28 revealed a stimulation of Myc-Paf1c binding in HLF cells, we would like to check how Usp2 dimerization regulates Myc-dependent transcription. Unexpectedly, RNA-seq analysis showed both two Usp28 variants regulated the expression of Myc target genes almost equally, indicating that ectopic stabilization of Myc by Usp28-M primarily does not have a transcriptional effect.

One potential explanation is, the regulation of ubiquitin on Myc-driven transcription depends only on if Myc is ubiquitinated, but not on to what extend Myc is ubiquitinated. This explains why monomeric Usp28 can only stabilize Myc without simultaneously regulating Myc-dependent transcription.

Furthermore, another speculation might be, the regulation of ubiquitin on Myc-driven transcription is ubiquitin chain type dependent.

As discussed above, different ubiquitin chains responsible for different biological functions, and our ubiquitin pulldown assay showed that Usp28-M is selectively active towards K11-linked chains but has a similar activity as Usp-WT in K48-linked chains deubiquitinating (Fig. 4B, C). Previous studies demonstrated that ubiquitination regulates

Myc transcriptional effects by utilizing K-less Myc, a variant in which all potential ubiquitinated lysine sites are mutated, without examining the effects of different types of ubiquitin chains on Myc mediated transcription (118).

Huwe1 facilitates Paf1c transfer to RNAPII from Myc to regulate Myc-dependent transcription, probably via the ubiquitination of Myc, as the blockade of Huwe1 suppressed Myc mediated transcription, phenocopying the effect with K-less Myc (117). As an E3 ligase, Huwe1 is able to modify its substrates with K6-, K11-, K48- and K63-linked polyubiquitin chains (268), validation studies showed Huwe1 primarily generates K48-linked polyubiquitin chains in N-Myc, the isoform of c-Myc, in glioblastoma multiforme (GBM) cells (269).

Based on the evidence presented above, we can speculate that the regulation of Huwe1 on Myc-dependent transcription in HLF cells is K48-linked polyubiquitin chain dependent, while the ectopic stabilization of Myc by monomeric Usp28 majorly depend on its deubiquitination on K11-linked polyubiquitin chains.

And for the reinforced Myc-Paf1c binding, since PLA can only show the proximity between Myc and Paf1c in the nucleus, it cannot exclude the possibility that the enhanced binding does not happen on active Myc promoters so that the enhanced Paf1c recruitment on Myc does not regulate Myc mediated transcription.

However, then comes the new concern as the qPCR analysis after Cut&Run assay with Paf1c subunit Leo1 antibody does show an upregulated Leo1 abundance on Myc target promoters, at least on the tested 5 genes, in Usp28-M expressing HLF cells, and this hints us that monomeric Usp28 promotes Paf1c binding on Myc might have extra effects independent of transcription.

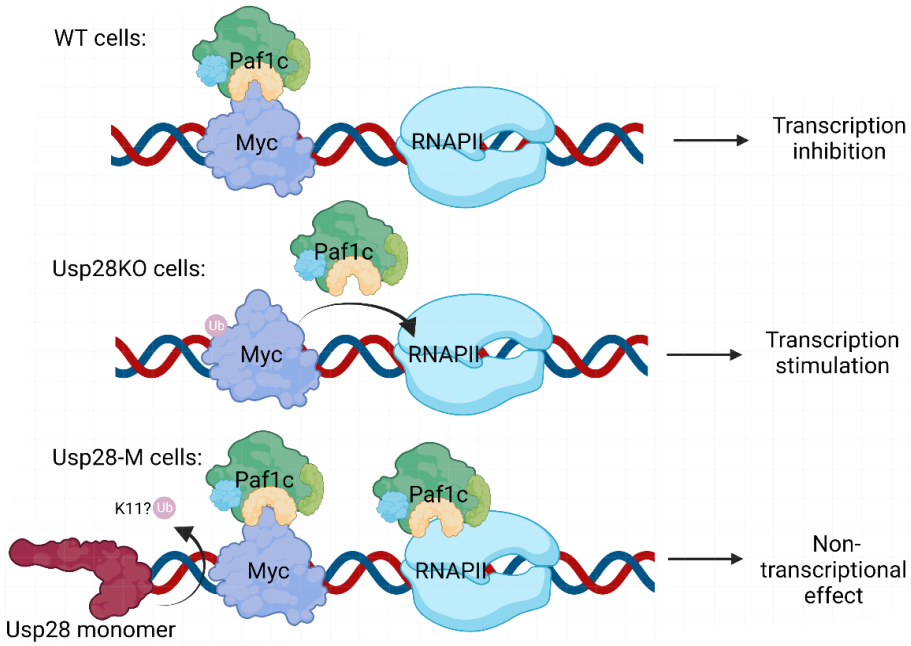

Proposed schematic: Usp28-M stabilizes Myc via deubiquitination but has non-transcriptional effect (Created with BioRender.com.)

5.2 Monomeric Usp28 recruits Paf1c on Myc to reduce TRCs and to accelerate DNA replication

The Paf1c protein complex exhibits versatility as it regulates all steps of the RNAPII transcription cycle, including transcription initiation, elongation, termination, and RNA 3'-end formation (267).

Nonetheless, our research findings demonstrated that the increased recruitment of Paf1c on Myc by monomeric Usp28 does not significantly impact the expression of Myc target genes. This suggests that the recruitment of Paf1c on Myc serves a non-transcriptional function in HLF cells expressing Usp28-M.

Both Myc and Paf1c have been implicated in transcription-independent functions related to DNA replication (109,110,119). Studies showed that Myc facilitates the resolution of R-loops and restricts collisions between RNAPII and the replisome, thereby reducing TRCs. This is achieved through the recruitment of Brca1 and the exosome complex, which contribute to the maintenance of genomic stability (115,116).

In addition, Myc is known for its ability to regulate the activity of DNA replication origins. Myc can bind directly to or in close proximity to DNA replication origins, and the absence of Myc leads to compromised origin activity, likely attributed to Myc's regulatory role during the origin selection step following the assembly of the pre-replicative complex. Moreover, this impairment can be rescued by the overexpression of full-length Myc, suggesting that the ectopic stabilization of Myc by monomeric Usp28 may impact (upregulate) (109).

Furthermore, the recruitment of Paf1c by Myc plays a crucial role in the resolution of TRCs. Additionally, this Paf1c recruitment has been found to facilitate DNA repair (117-119,270,271) at transcription start sites via the ubiquitination of histone H2B (120), which conversely stabilizes replication forks and promotes HR. Besides, Paf1c also exhibits the ability to stimulate DNA replication under stress (119).

However, contrasting findings suggest that Paf1c can have an opposing effect. These studies found that Paf1c is associated with the accumulation of R-loops and can stimulate ATR signaling, thereby exacerbating replicative stress and eventually contributing to genomic instability (121,122).

In this thesis, we showed that the ectopic stabilization of Myc by monomeric Usp28 leads to the recruitment of Paf1c. Surprisingly, this recruitment did not have an impact on the expression of Myc target genes. In contrast, PLA data revealed that monomeric Usp28 promotes the resolution of TRCs (Fig. 6). Additionally, EdU incorporation assay demonstrated an increased level of DNA synthesis in Usp28-M HLF cells (Fig. 7A). These

findings were further supported by the nascent DNA capture assay, which demonstrated enriched levels of RNAPII and the Paf1c subunit Ctr9 in these cells (Fig. 7C). Moreover, the depletion of Ctr9 using shRNAs led to a downregulation of the increased EdU signals in Usp28-M HLF cells, bringing them to the same level as in Usp28-WT cells (Fig. 7A). Collectively, these results in line with known functions of Paf1c and Myc in response to replicative stress and in DNA replication (109,110,114,119).

Interestingly, DNA fiber assay indicated a reduced rate of replication fork progression in Usp28-M cells (Fig. 7B), which appears contradictory to the observed increase in DNA replication.

One possible explanation for this phenomenon is that the deceleration of replication fork speed may be a self-protective mechanism in these rapidly replicating HLF cells. It is known that accelerated replication fork progression can induce replicative stress and DNA damage. Therefore, reducing the speed of replication forks is a major strategy employed by cells, especially highly proliferative cells, to avoid replicative stress and maintain genome integrity (239,272).

In line with this, immunoblotting, immunofluorescence, and comet assays consistently revealed elevated levels of DNA damage in HLF cells expressing monomeric Usp28 (Fig. 8, 9). Notably, these increased DNA damages could be further blocked with thymidine treatment (Fig. 9B, C), a known inhibitor of DNA synthesis. This suggests that the DNA damage detected in Usp28-M cells arises from rapid DNA synthesis and it is reasonable for these cells to exhibit slowed replication forks as a protective response.

Another speculation to explain the reinforced net DNA synthesis with decelerated forks is the firing of dormant origins, which are believed to localize in the vicinity of transcription start sites (273-275). Previous studies showed that the firing of dormant origins during recovery from stress serves as a mechanism to facilitate the completion of DNA replication for fragments that become trapped between broken replication forks (276,277).

However, to make sure whether this phenomenon is indeed a result of accelerated firing of replication origins, further experiments need to be done. For example, performing EdU sequencing in HLF Usp28-WT and Usp28-M cells could be conducted after synchronization to monitor the firing of origins (278).

5.3 DNA damage disrupts Usp28 dimerization

Both Myc and its deubiquitinase Usp28 are known to play critical roles in response to DNA damage.

Myc, on one hand, is required to activate some of the DDR factors, for example the ATM-dependent DDR checkpoints. Studies have shown that the kinase ATM and its substrate H2AX are downregulated in response to ionizing radiation in the absence of Myc in murine cells; also, in the human cell line HCT116, ATM and phosphorylated Chk2 were also decreased with the knocking down of the endogenous Myc upon DNA damage induced by irradiation (279). Myc is also essential for the DNA damage induced apoptosis regulated by the tumor suppressor p53 (280). On the other hand, Myc itself can induce DNA damage. Overexpression of Myc in normal human fibroblasts, for instance, increases reactive oxygen species levels and impairs p53-dependent cell cycle arrest in response to DNA damage. This events collectively leads to genomic instability and further contributes to the progression of tumors (281).

Usp28 was identified as a key regulator of cellular response to ionizing irradiation-induced DNA damage. It promotes the ATM signal pathway via the stabilization of 53bp1 and Chk2, besides, it can also facilitate the ATR-mediated Chk1 activation via the stabilization of Claspin and G2 arrest (213).

Usp28 is known to be activated upon DNA damage while the mechanism remains unknown. Some argue the activation of Usp28 is due to the phosphorylation of Usp28 at S67 and S417 mediated by ATM/ATR upon cisplatin induced DNA damage (153). In HLF cells, we did find accumulated Myc upon DNA damage induced by etoposide whereas did not appear in Usp28-KO HLF cells (Fig. 10A), showing the accumulation of Myc is Usp28-dependent, together with the unchanged Myc mRNA (Fig. 10B), indicating the activation of Usp28. However, this Myc accumulation only happens in Usp28-WT cells but not in Usp28-M cells, which have an elevated basal level of Myc (Fig. 11C, D), suggesting the formation of Usp28 monomers may be responsible for the activation of Usp28 after DNA damage in HLF cells.

To check the oligomerization states of Usp28 in cells upon DNA damage with regular immunoblotting, we generated $p19^{-/-}$Nras cells express both HA-tagged Usp28 and GFP-tagged Usp28 so that we can easily confirm the monomer/dimer ratio by detecting one tag after co-immunoprecipitating with antibodies against another tag, as describe previously (196). We can also perform PLA assays with antibodies against these tags which can serve as a proxy for Usp28 dimerization.

As the PLA and immunoprecipitation assays showed, Usp28 dimerization is disrupted and monomeric Usp28 is formed rapidly after DNA damage initiated (Fig. 12B, C), similar result is also found from HeLa cells transient transfected with HA- and Flag-tagged Usp28 (Fig. 12D), indicating DNA damage controls Usp28 dimerization.

Next, we aimed to investigate the key mediator responsible for regulating Usp28 dimerization, especially in the context of DDR. Remarkably, our findings revealed that 53bp1 plays a crucial role in orchestrating this process.

53bp1 was identified as the binding partner of the tumor suppressor p53 (282); subsequent studies showed that it plays a critical role in cellular response to DNA damage and replicative stress (213,283-286). For example, 53bp1 stimulates non-homologous end-joining (NHEJ) (287,288). 53bp1 was also found as a binding partner of Usp28 (213), which is further confirmed by our mass spectrometry analysis (Fig. 13A) and immunoprecipitation assays (Fig. 13B, C).

Unexpectedly, immunoprecipitation of 53bp1 in HLF cells shows that it does not interacts with monomeric Usp28 but selectively binds to dimeric Usp28 (Fig. 14A), which is confirmed by PLA assays with antibodies against HA-tag (Usp28) and 53bp1 (Fig. 14C). Similar result is also found via immunoprecipitation from $p19^{-/-}$Nras cells with Usp28-WT or Usp28-M expression (Fig. 14B). Furthermore, this specific binding is disrupted upon DNA damage induced by etoposide (Fig. 14C)

To explain the specific binding between 53bp1 and dimeric Usp28, one speculation might be that oligomerization state modulates binding affinity and specificity, especially given that 53bp1 is known to be capable of dimerization.

And for the disruption of Usp28 dimerization upon DNA damage, one potential explanation might be the oligomerization state of 53bp1. 53bp1 is known to be rapidly recruited at the DSB sites upon DNA damage via the directly binding between the Tudor domain and UDR domain on 53bp1 and the methylated H4K20 and ubiquitylated H2AK15 adjacent to the damaged chromatin (289). Usp28 is also recruited to the break sites via the binding with the tandem BRCT domains at the C-terminal of 53bp1 (214). Interestingly, 53bp1 is recruited as a dimer onto the damage sites and this dimerization is important for its DNA repair functions (285,290). However, after moving to the damage sites, 53bp1 dimers will continue assembly as oligomers, namely 53bp1 foci (291). Since 53bp1 selectively interacts with dimeric Usp28, it might be possible that after forming 53bp1 foci, the binding between Usp28 dimers and 53bp1 is disrupted due to some possible reasons, for example the spatial conformational constraints, and release Usp28 as monomers as a result.

The other simple hypothesis might be that the recruitment of 53bp1 to DSB may directly disassociate its binding with Usp28 and release Usp28 as monomers. Indeed, 53bp1 is recruited to damage sites ranging from 5-60 min after damage induced by ionizing

radiation or 4-Hydroxytamoxifen (291-293), and coincidentally, in our PLA assays, we did find that the disassociation occurs at 30 min after etoposide treatment (Fig. 14C), correlating with the formation of Usp28 monomers (Fig. 12B, C, D).

One more mechanism of the disassembly of 53bp1-Usp28 complexes upon DNA damage might involve the proteasomal degradation of 53bp1.

Several studies propose an alternative mechanism where, instead of recruiting all 53bp1 molecules to sites of DSB, the bulk of 53bp1 in the nucleoplasm is degraded in an RNF8/RNF168-dependent manner. Meanwhile, a pool of 53bp1 binds specifically to the damage site and subsequently recruits RIF1, a key factor in DNA repair, in response to IR induced DNA damage (294). Based on this, one can argue that the degradation of 53bp1 upon DDR may lead to the disassociation with dimeric Usp28 and the formation of monomeric Usp28.

To confirm that 53bp1 controls Usp28 dimerization, we depleted 53bp1 with different shRNAs in HLF and $p19^{-/-}$Nras cells. Knockdown of 53bp1 leads to formation of Usp28 monomers (Fig. 15C), suggesting that 53bp1 stabilizes the dimeric conformation of Usp28.

Consistently, loss of 53bp1 mimics the expression of monomeric Usp28 with enhanced Usp28 catalytic activity (Fig. 16), increased Paf1c recruitment (Fig. 17) and accumulated replication-dependent DNA damage (Fig. 18, 19).

The 53bp1-Usp28 interaction is diminished upon genotoxic stress tested in different cell lines (Fig. 21E) and with different genotoxins (Fig. 23), leading to formation of Usp28 monomers and acceleration of DNA replication. This can provide a simple mechanism for the activation of Usp28 upon DNA damage and other stresses, such as prolonged mitosis and disruption of centrosomes (204-206,213,214,243). This activation of Usp28 and the further reinforced DNA replication exacerbates DNA breakage and impairs cell viability (Fig. 24), suggesting the dimerization of Usp28 may act as a safeguard to limit anomalous DNA synthesis and the subsequent replication-associated damage.

5.4 Conclusions and prospects

In this thesis, we elucidated the biological function, at least partially, of Usp28 dimerization. We proved the monomeric Usp28 is more active in stabilizing its substrate Myc but has no transcriptional effect, instead, it can facilitate the DNA replication and accumulate DNA damage. We further found 53bp1, the key DDR factor, as well as a known interactor of Usp28, controls Usp28 dimerization and thus regulates DNA replication via Paf1c.

Based on these results, we put forward a model that dimerization of Usp28 provides a mechanism to limit unscheduled DNA replication at transcriptionally active loci via Myc-dependent recruitment of Paf1c.

We propose that during a normal cell cycle, DDR signaling due to endogenous DNA lesions or fork stalling would disrupt Usp28 dimers to induce transient Usp28 activation and coordinate DNA replication with RNAPII activity. By contrast, constitutive activation of Usp28 by mutation of the dimer interface or upon loss of 53bp1 leads to chronic stimulation of DNA synthesis accompanied by the accumulation of DNA damage.

This mechanism is also perturbed by genotoxic stress, which triggers Paf1c recruitment and transiently stimulates DNA synthesis. Since the same conditions slow progression of replication forks, the net stimulation of DNA replication is most likely due to firing of dormant origins that localize adjacent to the transcription start sites. However, in order to verify this hypothesis, additional assays, for example EdU sequencing in cells after synchronization, need to be done.

In our experiments, inhibition of DNA replication concomitantly with genotoxin treatment reduces DNA damage and promotes cell viability. These observations indicate that stabilization of Myc and acute DNA replication are early pathological effects of genotoxic stress rather than a programmed rescue mechanism. Our findings thus provide a basis for further analysis of replicative responses to genotoxins and can be instructive for the development of combinatorial antineoplastic therapies.

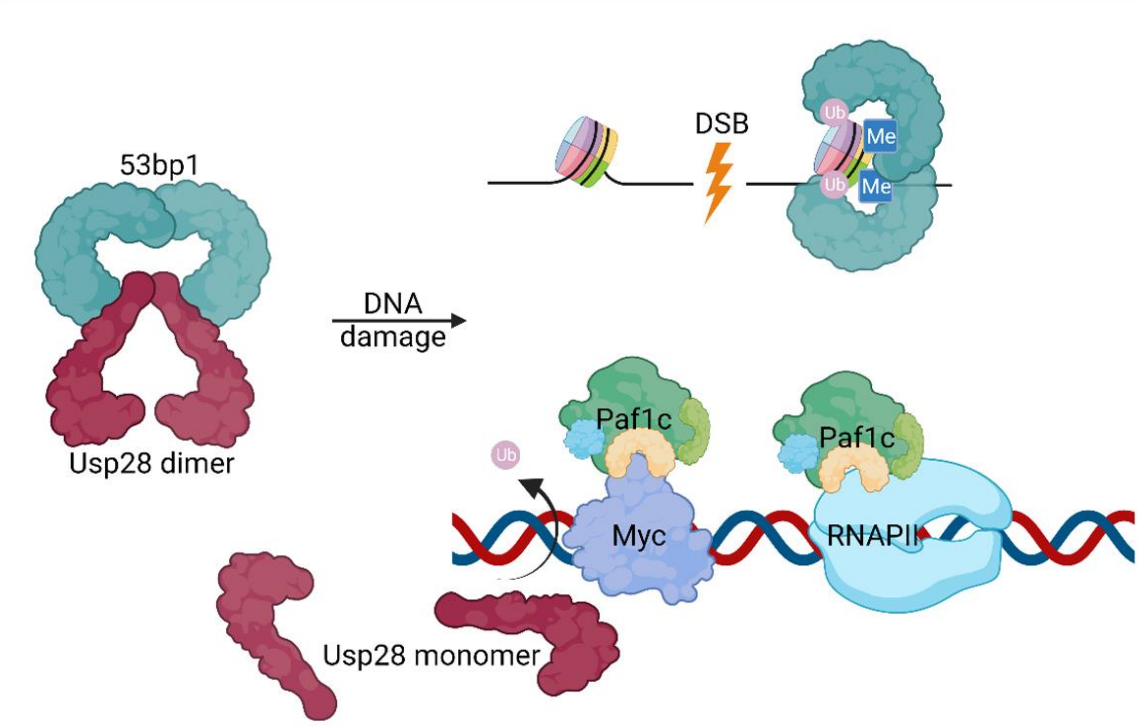

Proposed schematic: 53bp1 stabilizes Usp28 in dimer comformation
(Created with BioRender.com.)

References

1. Jin, C., Einig, E., Xu, W., Kollampally, R.B., Schlosser, A., Flentje, M. and Popov, N. (under revision) The dimeric deubiquitinase Usp28 integrates 53bp1 and Myc functions to limit DNA damage.
2. Martin, L.J. (2008) DNA damage and repair: relevance to mechanisms of neurodegeneration. *J Neuropathol Exp Neurol*, **67**, 377-387.
3. Alhmoud, J.F., Woolley, J.F., Al Moustafa, A.E. and Malki, M.I. (2020) DNA Damage/Repair Management in Cancers. *Cancers (Basel)*, **12**.
4. Hanahan, D. and Weinberg, R.A. (2011) Hallmarks of cancer: the next generation. *Cell*, **144**, 646-674.
5. Chatterjee, N. and Walker, G.C. (2017) Mechanisms of DNA damage, repair, and mutagenesis. *Environ Mol Mutagen*, **58**, 235-263.
6. Kunkel, T.A. (2009) Evolving views of DNA replication (in)fidelity. *Cold Spring Harb Symp Quant Biol*, **74**, 91-101.
7. Vignard, J., Mirey, G. and Salles, B. (2013) Ionizing-radiation induced DNA double-strand breaks: a direct and indirect lighting up. *Radiother Oncol*, **108**, 362-369.
8. Lomax, M.E., Folkes, L.K. and O'Neill, P. (2013) Biological consequences of radiation-induced DNA damage: relevance to radiotherapy. *Clin Oncol (R Coll Radiol)*, **25**, 578-585.
9. Gentil, A., Le Page, F., Margot, A., Lawrence, C.W., Borden, A. and Sarasin, A. (1996) Mutagenicity of a unique thymine-thymine dimer or thymine-thymine pyrimidine pyrimidone (6-4) photoproduct in mammalian cells. *Nucleic Acids Res*, **24**, 1837-1840.
10. Reuvers, T.G.A., Kanaar, R. and Nonnekens, J. (2020) DNA Damage-Inducing Anticancer Therapies: From Global to Precision Damage. *Cancers (Basel)*, **12**.
11. Harper, J.W. and Elledge, S.J. (2007) The DNA damage response: ten years after. *Mol Cell*, **28**, 739-745.
12. Qiu, Z., Oleinick, N.L. and Zhang, J. (2018) ATR/CHK1 inhibitors and cancer therapy. *Radiother Oncol*, **126**, 450-464.
13. Cortez, D. (2015) Preventing replication fork collapse to maintain genome integrity. *DNA Repair (Amst)*, **32**, 149-157.
14. Wang, H., Wang, H., Powell, S.N., Iliakis, G. and Wang, Y. (2004) ATR affecting cell radiosensitivity is dependent on homologous recombination repair but independent of nonhomologous end joining. *Cancer Res*, **64**, 7139-7143.
15. Lukas, C., Falck, J., Bartkova, J., Bartek, J. and Lukas, J. (2003) Distinct spatiotemporal dynamics of mammalian checkpoint regulators induced by DNA damage. *Nat Cell Biol*, **5**, 255-260.
16. Mimitou, E.P. and Symington, L.S. (2009) DNA end resection: many nucleases make light work. *DNA Repair (Amst)*, **8**, 983-995.
17. Sedgwick, B., Bates, P.A., Paik, J., Jacobs, S.C. and Lindahl, T. (2007) Repair of alkylated DNA: recent advances. *DNA Repair (Amst)*, **6**, 429-442.

18. Petruseva, I.O., Evdokimov, A.N. and Lavrik, O.I. (2014) Molecular mechanism of global genome nucleotide excision repair. *Acta Naturae*, **6**, 23-34.
19. Panier, S. and Boulton, S.J. (2014) Double-strand break repair: 53BP1 comes into focus. *Nat Rev Mol Cell Biol*, **15**, 7-18.
20. Huen, M.S., Huang, J., Leung, J.W., Sy, S.M., Leung, K.M., Ching, Y.P., Tsao, S.W. and Chen, J. (2010) Regulation of chromatin architecture by the PWWP domain-containing DNA damage-responsive factor EXPAND1/MUM1. *Mol Cell*, **37**, 854-864.
21. Silverman, J., Takai, H., Buonomo, S.B., Eisenhaber, F. and de Lange, T. (2004) Human Rif1, ortholog of a yeast telomeric protein, is regulated by ATM and 53BP1 and functions in the S-phase checkpoint. *Genes Dev*, **18**, 2108-2119.
22. DiTullio, R.A., Jr., Mochan, T.A., Venere, M., Bartkova, J., Sehested, M., Bartek, J. and Halazonetis, T.D. (2002) 53BP1 functions in an ATM-dependent checkpoint pathway that is constitutively activated in human cancer. *Nat Cell Biol*, **4**, 998-1002.
23. Wang, B., Matsuoka, S., Carpenter, P.B. and Elledge, S.J. (2002) 53BP1, a mediator of the DNA damage checkpoint. *Science*, **298**, 1435-1438.
24. Pommier, Y., Tanizawa, A. and Kohn, K.W. (1994) Mechanisms of topoisomerase I inhibition by anticancer drugs. *Adv Pharmacol*, **29B**, 73-92.
25. Chankova, S.G., Dimova, E., Dimitrova, M. and Bryant, P.E. (2007) Induction of DNA double-strand breaks by zeocin in Chlamydomonas reinhardtii and the role of increased DNA double-strand breaks rejoining in the formation of an adaptive response. *Radiat Environ Biophys*, **46**, 409-416.
26. Fong, P.C., Boss, D.S., Yap, T.A., Tutt, A., Wu, P., Mergui-Roelvink, M., Mortimer, P., Swaisland, H., Lau, A., O'Connor, M.J. *et al.* (2009) Inhibition of poly(ADP-ribose) polymerase in tumors from BRCA mutation carriers. *N Engl J Med*, **361**, 123-134.
27. Hickson, I., Zhao, Y., Richardson, C.J., Green, S.J., Martin, N.M., Orr, A.I., Reaper, P.M., Jackson, S.P., Curtin, N.J. and Smith, G.C. (2004) Identification and characterization of a novel and specific inhibitor of the ataxia-telangiectasia mutated kinase ATM. *Cancer Res*, **64**, 9152-9159.
28. Foote, K.M., Nissink, J.W.M., McGuire, T., Turner, P., Guichard, S., Yates, J.W.T., Lau, A., Blades, K., Heathcote, D., Odedra, R. *et al.* (2018) Discovery and Characterization of AZD6738, a Potent Inhibitor of Ataxia Telangiectasia Mutated and Rad3 Related (ATR) Kinase with Application as an Anticancer Agent. *J Med Chem*, **61**, 9889-9907.
29. Dang, C.V., O'Donnell, K.A., Zeller, K.I., Nguyen, T., Osthus, R.C. and Li, F. (2006) The c-Myc target gene network. *Semin Cancer Biol*, **16**, 253-264.
30. Meyer, N. and Penn, L.Z. (2008) Reflecting on 25 years with MYC. *Nat Rev Cancer*, **8**, 976-990.
31. Lancho, O. and Herranz, D. (2018) The MYC Enhancer-ome: Long-Range Transcriptional Regulation of MYC in Cancer. *Trends Cancer*, **4**, 810-822.
32. Lin, C.P., Liu, C.R., Lee, C.N., Chan, T.S. and Liu, H.E. (2010) Targeting c-Myc as a novel approach for hepatocellular carcinoma. *World J Hepatol*, **2**, 16-20.
33. Min, Z., Xunlei, Z., Haizhen, C., Wenjing, Z., Haiyan, Y., Xiaoyun, L., Jianyun, Z., Xudong, C. and Aiguo, S. (2021) The Clinicopathologic and Prognostic

Significance of c-Myc Expression in Hepatocellular Carcinoma: A Meta-Analysis. *Front Bioinform*, **1**, 706835.
34. Dalla-Favera, R., Bregni, M., Erikson, J., Patterson, D., Gallo, R.C. and Croce, C.M. (1982) Human c-myc onc gene is located on the region of chromosome 8 that is translocated in Burkitt lymphoma cells. *Proc Natl Acad Sci U S A*, **79**, 7824-7827.
35. Nau, M.M., Brooks, B.J., Battey, J., Sausville, E., Gazdar, A.F., Kirsch, I.R., McBride, O.W., Bertness, V., Hollis, G.F. and Minna, J.D. (1985) L-myc, a new myc-related gene amplified and expressed in human small cell lung cancer. *Nature*, **318**, 69-73.
36. Rickman, D.S., Schulte, J.H. and Eilers, M. (2018) The Expanding World of N-MYC-Driven Tumors. *Cancer Discov*, **8**, 150-163.
37. Chen, H., Liu, H. and Qing, G. (2018) Targeting oncogenic Myc as a strategy for cancer treatment. *Signal Transduct Target Ther*, **3**, 5.
38. Xu, L., Morgenbesser, S.D. and DePinho, R.A. (1991) Complex transcriptional regulation of myc family gene expression in the developing mouse brain and liver. *Mol Cell Biol*, **11**, 6007-6015.
39. Hirning, U., Schmid, P., Schulz, W.A., Rettenberger, G. and Hameister, H. (1991) A comparative analysis of N-myc and c-myc expression and cellular proliferation in mouse organogenesis. *Mech Dev*, **33**, 119-125.
40. Dang, C.V. (2016) A Time for MYC: Metabolism and Therapy. *Cold Spring Harb Symp Quant Biol*, **81**, 79-83.
41. Duffy, M.J., O'Grady, S., Tang, M. and Crown, J. (2021) MYC as a target for cancer treatment. *Cancer Treat Rev*, **94**, 102154.
42. Conacci-Sorrell, M., McFerrin, L. and Eisenman, R.N. (2014) An overview of MYC and its interactome. *Cold Spring Harb Perspect Med*, **4**, a014357.
43. Kalkat, M., Resetca, D., Lourenco, C., Chan, P.K., Wei, Y., Shiah, Y.J., Vitkin, N., Tong, Y., Sunnerhagen, M., Done, S.J. *et al.* (2018) MYC Protein Interactome Profiling Reveals Functionally Distinct Regions that Cooperate to Drive Tumorigenesis. *Mol Cell*, **72**, 836-848 e837.
44. Welcker, M., Orian, A., Jin, J., Grim, J.E., Harper, J.W., Eisenman, R.N. and Clurman, B.E. (2004) The Fbw7 tumor suppressor regulates glycogen synthase kinase 3 phosphorylation-dependent c-Myc protein degradation. *Proc Natl Acad Sci U S A*, **101**, 9085-9090.
45. Yada, M., Hatakeyama, S., Kamura, T., Nishiyama, M., Tsunematsu, R., Imaki, H., Ishida, N., Okumura, F., Nakayama, K. and Nakayama, K.I. (2004) Phosphorylation-dependent degradation of c-Myc is mediated by the F-box protein Fbw7. *EMBO J*, **23**, 2116-2125.
46. McMahon, S.B., Van Buskirk, H.A., Dugan, K.A., Copeland, T.D. and Cole, M.D. (1998) The novel ATM-related protein TRRAP is an essential cofactor for the c-Myc and E2F oncoproteins. *Cell*, **94**, 363-374.
47. Herbst, A., Hemann, M.T., Tworkowski, K.A., Salghetti, S.E., Lowe, S.W. and Tansey, W.P. (2005) A conserved element in Myc that negatively regulates its proapoptotic activity. *EMBO Rep*, **6**, 177-183.
48. Thomas, L.R., Adams, C.M., Wang, J., Weissmiller, A.M., Creighton, J., Lorey, S.L., Liu, Q., Fesik, S.W., Eischen, C.M. and Tansey, W.P. (2019) Interaction of the oncoprotein transcription factor MYC with its chromatin cofactor WDR5 is essential for tumor maintenance. *Proc Natl Acad Sci U S A*, **116**, 25260-25268.

49. Cowling, V.H., Chandriani, S., Whitfield, M.L. and Cole, M.D. (2006) A conserved Myc protein domain, MBIV, regulates DNA binding, apoptosis, transformation, and G2 arrest. *Mol Cell Biol*, **26**, 4226-4239.
50. Blackwood, E.M. and Eisenman, R.N. (1991) Max: a helix-loop-helix zipper protein that forms a sequence-specific DNA-binding complex with Myc. *Science*, **251**, 1211-1217.
51. Bedard, M., Maltais, L., Montagne, M. and Lavigne, P. (2017) Miz-1 and Max compete to engage c-Myc: implication for the mechanism of inhibition of c-Myc transcriptional activity by Miz-1. *Proteins*, **85**, 199-206.
52. Li, Z., Van Calcar, S., Qu, C., Cavenee, W.K., Zhang, M.Q. and Ren, B. (2003) A global transcriptional regulatory role for c-Myc in Burkitt's lymphoma cells. *Proc Natl Acad Sci U S A*, **100**, 8164-8169.
53. Fernandez, P.C., Frank, S.R., Wang, L., Schroeder, M., Liu, S., Greene, J., Cocito, A. and Amati, B. (2003) Genomic targets of the human c-Myc protein. *Genes Dev*, **17**, 1115-1129.
54. Arabi, A., Wu, S., Ridderstrale, K., Bierhoff, H., Shiue, C., Fatyol, K., Fahlen, S., Hydbring, P., Soderberg, O., Grummt, I. *et al.* (2005) c-Myc associates with ribosomal DNA and activates RNA polymerase I transcription. *Nat Cell Biol*, **7**, 303-310.
55. Grandori, C., Gomez-Roman, N., Felton-Edkins, Z.A., Ngouenet, C., Galloway, D.A., Eisenman, R.N. and White, R.J. (2005) c-Myc binds to human ribosomal DNA and stimulates transcription of rRNA genes by RNA polymerase I. *Nat Cell Biol*, **7**, 311-318.
56. Gomez-Roman, N., Grandori, C., Eisenman, R.N. and White, R.J. (2003) Direct activation of RNA polymerase III transcription by c-Myc. *Nature*, **421**, 290-294.
57. Eilers, M. and Eisenman, R.N. (2008) Myc's broad reach. *Genes Dev*, **22**, 2755-2766.
58. Hann, S.R. and Eisenman, R.N. (1984) Proteins encoded by the human c-myc oncogene: differential expression in neoplastic cells. *Mol Cell Biol*, **4**, 2486-2497.
59. Schaub, F.X., Dhankani, V., Berger, A.C., Trivedi, M., Richardson, A.B., Shaw, R., Zhao, W., Zhang, X., Ventura, A., Liu, Y. *et al.* (2018) Pan-cancer Alterations of the MYC Oncogene and Its Proximal Network across the Cancer Genome Atlas. *Cell Syst*, **6**, 282-300 e282.
60. Schick, M., Habringer, S., Nilsson, J.A. and Keller, U. (2017) Pathogenesis and therapeutic targeting of aberrant MYC expression in haematological cancers. *Br J Haematol*, **179**, 724-738.
61. Zhou, Y., Gao, X., Yuan, M., Yang, B., He, Q. and Cao, J. (2021) Targeting Myc Interacting Proteins as a Winding Path in Cancer Therapy. *Front Pharmacol*, **12**, 748852.
62. Luscher, B. and Larsson, L.G. (1999) The basic region/helix-loop-helix/leucine zipper domain of Myc proto-oncoproteins: function and regulation. *Oncogene*, **18**, 2955-2966.
63. Castell, A., Yan, Q., Fawkner, K., Hydbring, P., Zhang, F., Verschut, V., Franco, M., Zakaria, S.M., Bazzar, W., Goodwin, J. *et al.* (2018) A selective high affinity MYC-binding compound inhibits MYC:MAX interaction and MYC-dependent tumor cell proliferation. *Sci Rep*, **8**, 10064.
64. Agarwal, S., Milazzo, G., Rajapakshe, K., Bernardi, R., Chen, Z., Barbieri, E., Koster, J., Perini, G., Coarfa, C. and Shohet, J.M. (2018) MYCN acts as a

direct co-regulator of p53 in MYCN amplified neuroblastoma. *Oncotarget*, **9**, 20323-20338.

65. Cogne, B., Ehresmann, S., Beauregard-Lacroix, E., Rousseau, J., Besnard, T., Garcia, T., Petrovski, S., Avni, S., McWalter, K., Blackburn, P.R. *et al.* (2019) Missense Variants in the Histone Acetyltransferase Complex Component Gene TRRAP Cause Autism and Syndromic Intellectual Disability. *Am J Hum Genet*, **104**, 530-541.
66. Liu, X., Tesfai, J., Evrard, Y.A., Dent, S.Y. and Martinez, E. (2003) c-Myc transformation domain recruits the human STAGA complex and requires TRRAP and GCN5 acetylase activity for transcription activation. *J Biol Chem*, **278**, 20405-20412.
67. Feris, E.J., Hinds, J.W. and Cole, M.D. (2019) Formation of a structurally-stable conformation by the intrinsically disordered MYC:TRRAP complex. *PLoS One*, **14**, e0225784.
68. McMahon, S.B., Wood, M.A. and Cole, M.D. (2000) The essential cofactor TRRAP recruits the histone acetyltransferase hGCN5 to c-Myc. *Mol Cell Biol*, **20**, 556-562.
69. Nikiforov, M.A., Chandriani, S., Park, J., Kotenko, I., Matheos, D., Johnsson, A., McMahon, S.B. and Cole, M.D. (2002) TRRAP-dependent and TRRAP-independent transcriptional activation by Myc family oncoproteins. *Mol Cell Biol*, **22**, 5054-5063.
70. Ullius, A., Luscher-Firzlaff, J., Costa, I.G., Walsemann, G., Forst, A.H., Gusmao, E.G., Kapelle, K., Kleine, H., Kremmer, E., Vervoorts, J. *et al.* (2014) The interaction of MYC with the trithorax protein ASH2L promotes gene transcription by regulating H3K27 modification. *Nucleic Acids Res*, **42**, 6901-6920.
71. Thomas, L.R., Foshage, A.M., Weissmiller, A.M. and Tansey, W.P. (2015) The MYC-WDR5 Nexus and Cancer. *Cancer Res*, **75**, 4012-4015.
72. Chen, T., Li, K., Liu, Z., Liu, J., Wang, Y., Sun, R., Li, Z., Qiu, B., Zhang, X., Ren, G. *et al.* (2021) WDR5 facilitates EMT and metastasis of CCA by increasing HIF-1alpha accumulation in Myc-dependent and independent pathways. *Mol Ther*, **29**, 2134-2150.
73. Carugo, A., Genovese, G., Seth, S., Nezi, L., Rose, J.L., Bossi, D., Cicalese, A., Shah, P.K., Viale, A., Pettazzoni, P.F. *et al.* (2016) In Vivo Functional Platform Targeting Patient-Derived Xenografts Identifies WDR5-Myc Association as a Critical Determinant of Pancreatic Cancer. *Cell Rep*, **16**, 133-147.
74. Kanazawa, S., Soucek, L., Evan, G., Okamoto, T. and Peterlin, B.M. (2003) c-Myc recruits P-TEFb for transcription, cellular proliferation and apoptosis. *Oncogene*, **22**, 5707-5711.
75. Eberhardy, S.R. and Farnham, P.J. (2002) Myc recruits P-TEFb to mediate the final step in the transcriptional activation of the cad promoter. *J Biol Chem*, **277**, 40156-40162.
76. Rahl, P.B., Lin, C.Y., Seila, A.C., Flynn, R.A., McCuine, S., Burge, C.B., Sharp, P.A. and Young, R.A. (2010) c-Myc regulates transcriptional pause release. *Cell*, **141**, 432-445.
77. Baluapuri, A., Hofstetter, J., Dudvarski Stankovic, N., Endres, T., Bhandare, P., Vos, S.M., Adhikari, B., Schwarz, J.D., Narain, A., Vogt, M. *et al.* (2019) MYC Recruits SPT5 to RNA Polymerase II to Promote Processive Transcription Elongation. *Mol Cell*, **74**, 674-687 e611.

78. Fujinaga, K. (2020) P-TEFb as A Promising Therapeutic Target. *Molecules*, **25**.
79. Walz, S., Lorenzin, F., Morton, J., Wiese, K.E., von Eyss, B., Herold, S., Rycak, L., Dumay-Odelot, H., Karim, S., Bartkuhn, M. *et al.* (2014) Activation and repression by oncogenic MYC shape tumour-specific gene expression profiles. *Nature*, **511**, 483-487.
80. Otto, T., Horn, S., Brockmann, M., Eilers, U., Schuttrumpf, L., Popov, N., Kenney, A.M., Schulte, J.H., Beijersbergen, R., Christiansen, H. *et al.* (2009) Stabilization of N-Myc is a critical function of Aurora A in human neuroblastoma. *Cancer Cell*, **15**, 67-78.
81. Richards, M.W., Burgess, S.G., Poon, E., Carstensen, A., Eilers, M., Chesler, L. and Bayliss, R. (2016) Structural basis of N-Myc binding by Aurora-A and its destabilization by kinase inhibitors. *Proc Natl Acad Sci U S A*, **113**, 13726-13731.
82. den Hollander, J., Rimpi, S., Doherty, J.R., Rudelius, M., Buck, A., Hoellein, A., Kremer, M., Graf, N., Scheerer, M., Hall, M.A. *et al.* (2010) Aurora kinases A and B are up-regulated by Myc and are essential for maintenance of the malignant state. *Blood*, **116**, 1498-1505.
83. Yang, S., He, S., Zhou, X., Liu, M., Zhu, H., Wang, Y., Zhang, W., Yan, S., Quan, L., Bai, J. *et al.* (2010) Suppression of Aurora-A oncogenic potential by c-Myc downregulation. *Exp Mol Med*, **42**, 759-767.
84. Moroy, T., Saba, I. and Kosan, C. (2011) The role of the transcription factor Miz-1 in lymphocyte development and lymphomagenesis-Binding Myc makes the difference. *Semin Immunol*, **23**, 379-387.
85. Basu, S., Liu, Q., Qiu, Y. and Dong, F. (2009) Gfi-1 represses CDKN2B encoding p15INK4B through interaction with Miz-1. *Proc Natl Acad Sci U S A*, **106**, 1433-1438.
86. Liu, Q., Basu, S., Qiu, Y., Tang, F. and Dong, F. (2010) A role of Miz-1 in Gfi-1-mediated transcriptional repression of CDKN1A. *Oncogene*, **29**, 2843-2852.
87. Aesoy, R., Gradin, K., Aasrud, K.S., Hoivik, E.A., Ruas, J.L., Poellinger, L. and Bakke, M. (2014) Regulation of CDKN2B expression by interaction of Arnt with Miz-1--a basis for functional integration between the HIF and Myc gene regulatory pathways. *Mol Cancer*, **13**, 54.
88. Seoane, J., Le, H.V. and Massague, J. (2002) Myc suppression of the p21(Cip1) Cdk inhibitor influences the outcome of the p53 response to DNA damage. *Nature*, **419**, 729-734.
89. Qi, Y., Li, X., Chang, C., Xu, F., He, Q., Zhao, Y. and Wu, L. (2017) Ribosomal protein L23 negatively regulates cellular apoptosis via the RPL23/Miz-1/c-Myc circuit in higher-risk myelodysplastic syndrome. *Sci Rep*, **7**, 2323.
90. Queva, C., Hurlin, P.J., Foley, K.P. and Eisenman, R.N. (1998) Sequential expression of the MAD family of transcriptional repressors during differentiation and development. *Oncogene*, **16**, 967-977.
91. Zhang, X., Chen, X., Lin, J., Lwin, T., Wright, G., Moscinski, L.C., Dalton, W.S., Seto, E., Wright, K., Sotomayor, E. *et al.* (2012) Myc represses miR-15a/miR-16-1 expression through recruitment of HDAC3 in mantle cell and other non-Hodgkin B-cell lymphomas. *Oncogene*, **31**, 3002-3008.
92. Yang, Z., Jiang, X., Zhang, Z., Zhao, Z., Xing, W., Liu, Y., Jiang, X. and Zhao, H. (2021) HDAC3-dependent transcriptional repression of FOXA2 regulates FTO/m6A/MYC signaling to contribute to the development of gastric cancer. *Cancer Gene Ther*, **28**, 141-155.

93. Chen, W.L., Sun, H.P., Li, D.D., Wang, Z.H., You, Q.D. and Guo, X.K. (2017) G9a - An Appealing Antineoplastic Target. *Curr Cancer Drug Targets*, **17**, 555-568.
94. Cao, H., Li, L., Yang, D., Zeng, L., Yewei, X., Yu, B., Liao, G. and Chen, J. (2019) Recent progress in histone methyltransferase (G9a) inhibitors as anticancer agents. *Eur J Med Chem*, **179**, 537-546.
95. Tu, W.B., Shiah, Y.J., Lourenco, C., Mullen, P.J., Dingar, D., Redel, C., Tamachi, A., Ba-Alawi, W., Aman, A., Al-Awar, R. *et al.* (2018) MYC Interacts with the G9a Histone Methyltransferase to Drive Transcriptional Repression and Tumorigenesis. *Cancer Cell*, **34**, 579-595 e578.
96. Ke, X.X., Zhang, R., Zhong, X., Zhang, L. and Cui, H. (2020) Deficiency of G9a Inhibits Cell Proliferation and Activates Autophagy via Transcriptionally Regulating c-Myc Expression in Glioblastoma. *Front Cell Dev Biol*, **8**, 593964.
97. Cole, M.D. and Cowling, V.H. (2008) Transcription-independent functions of MYC: regulation of translation and DNA replication. *Nat Rev Mol Cell Biol*, **9**, 810-815.
98. Schwer, B., Mao, X. and Shuman, S. (1998) Accelerated mRNA decay in conditional mutants of yeast mRNA capping enzyme. *Nucleic Acids Res*, **26**, 2050-2057.
99. Bentley, D.L. (2005) Rules of engagement: co-transcriptional recruitment of pre-mRNA processing factors. *Curr Opin Cell Biol*, **17**, 251-256.
100. Shatkin, A.J. (1976) Capping of eucaryotic mRNAs. *Cell*, **9**, 645-653.
101. Shuman, S. (2002) What messenger RNA capping tells us about eukaryotic evolution. *Nat Rev Mol Cell Biol*, **3**, 619-625.
102. Knoepfler, P.S., Zhang, X.Y., Cheng, P.F., Gafken, P.R., McMahon, S.B. and Eisenman, R.N. (2006) Myc influences global chromatin structure. *EMBO J*, **25**, 2723-2734.
103. Cowling, V.H. and Cole, M.D. (2007) The Myc transactivation domain promotes global phosphorylation of the RNA polymerase II carboxy-terminal domain independently of direct DNA binding. *Mol Cell Biol*, **27**, 2059-2073.
104. Kress, T.R., Sabo, A. and Amati, B. (2015) MYC: connecting selective transcriptional control to global RNA production. *Nat Rev Cancer*, **15**, 593-607.
105. Dominguez-Sola, D. and Gautier, J. (2014) MYC and the control of DNA replication. *Cold Spring Harb Perspect Med*, **4**.
106. Bretones, G., Delgado, M.D. and Leon, J. (2015) Myc and cell cycle control. *Biochim Biophys Acta*, **1849**, 506-516.
107. Perna, D., Faga, G., Verrecchia, A., Gorski, M.M., Barozzi, I., Narang, V., Khng, J., Lim, K.C., Sung, W.K., Sanges, R. *et al.* (2012) Genome-wide mapping of Myc binding and gene regulation in serum-stimulated fibroblasts. *Oncogene*, **31**, 1695-1709.
108. Liu, Y.C., Li, F., Handler, J., Huang, C.R., Xiang, Y., Neretti, N., Sedivy, J.M., Zeller, K.I. and Dang, C.V. (2008) Global regulation of nucleotide biosynthetic genes by c-Myc. *PLoS One*, **3**, e2722.
109. Dominguez-Sola, D., Ying, C.Y., Grandori, C., Ruggiero, L., Chen, B., Li, M., Galloway, D.A., Gu, W., Gautier, J. and Dalla-Favera, R. (2007) Non-transcriptional control of DNA replication by c-Myc. *Nature*, **448**, 445-451.
110. Nepon-Sixt, B.S., Bryant, V.L. and Alexandrow, M.G. (2019) Myc-driven chromatin accessibility regulates Cdc45 assembly into CMG helicases. *Commun Biol*, **2**, 110.

111. Swarnalatha, M., Singh, A.K. and Kumar, V. (2012) The epigenetic control of E-box and Myc-dependent chromatin modifications regulate the licensing of lamin B2 origin during cell cycle. *Nucleic Acids Res*, **40**, 9021-9035.
112. Macheret, M. and Halazonetis, T.D. (2018) Intragenic origins due to short G1 phases underlie oncogene-induced DNA replication stress. *Nature*, **555**, 112-116.
113. Curti, L. and Campaner, S. (2021) MYC-Induced Replicative Stress: A Double-Edged Sword for Cancer Development and Treatment. *Int J Mol Sci*, **22**.
114. Srinivasan, S.V., Dominguez-Sola, D., Wang, L.C., Hyrien, O. and Gautier, J. (2013) Cdc45 is a critical effector of myc-dependent DNA replication stress. *Cell Rep*, **3**, 1629-1639.
115. Herold, S., Kalb, J., Buchel, G., Ade, C.P., Baluapuri, A., Xu, J., Koster, J., Solvie, D., Carstensen, A., Klotz, C. *et al.* (2019) Recruitment of BRCA1 limits MYCN-driven accumulation of stalled RNA polymerase. *Nature*, **567**, 545-549.
116. Papadopoulos, D., Solvie, D., Baluapuri, A., Endres, T., Ha, S.A., Herold, S., Kalb, J., Giansanti, C., Schulein-Volk, C., Ade, C.P. *et al.* (2022) MYCN recruits the nuclear exosome complex to RNA polymerase II to prevent transcription-replication conflicts. *Mol Cell*, **82**, 159-176 e112.
117. Endres, T., Solvie, D., Heidelberger, J.B., Andrioletti, V., Baluapuri, A., Ade, C.P., Muhar, M., Eilers, U., Vos, S.M., Cramer, P. *et al.* (2021) Ubiquitylation of MYC couples transcription elongation with double-strand break repair at active promoters. *Mol Cell*, **81**, 830-844 e813.
118. Jaenicke, L.A., von Eyss, B., Carstensen, A., Wolf, E., Xu, W., Greifenberg, A.K., Geyer, M., Eilers, M. and Popov, N. (2016) Ubiquitin-Dependent Turnover of MYC Antagonizes MYC/PAF1C Complex Accumulation to Drive Transcriptional Elongation. *Mol Cell*, **61**, 54-67.
119. Poli, J., Gerhold, C.B., Tosi, A., Hustedt, N., Seeber, A., Sack, R., Herzog, F., Pasero, P., Shimada, K., Hopfner, K.P. *et al.* (2016) Mec1, INO80, and the PAF1 complex cooperate to limit transcription replication conflicts through RNAPII removal during replication stress. *Genes Dev*, **30**, 337-354.
120. Wood, A., Schneider, J., Dover, J., Johnston, M. and Shilatifard, A. (2003) The Paf1 complex is essential for histone monoubiquitination by the Rad6-Bre1 complex, which signals for histone methylation by COMPASS and Dot1p. *J Biol Chem*, **278**, 34739-34742.
121. Landsverk, H.B., Sandquist, L.E., Sridhara, S.C., Rodland, G.E., Sabino, J.C., de Almeida, S.F., Grallert, B., Trinkle-Mulcahy, L. and Syljuasen, R.G. (2019) Regulation of ATR activity via the RNA polymerase II associated factors CDC73 and PNUTS-PP1. *Nucleic Acids Res*, **47**, 1797-1813.
122. van Bijsterveldt, L., Landsverk, H.B., Nähse, V., Durley, S.C., Sarkar, S.S., Syljuåsen, R.G. and Humphrey, T.C. (2021) R-loop-induced p21 expression following CDC73, CTR9, and PAF1 loss protects cancer cells against replicative catastrophe following WEE1 inhibition. *bioRxiv*.
123. Soucek, L., Whitfield, J., Martins, C.P., Finch, A.J., Murphy, D.J., Sodir, N.M., Karnezis, A.N., Swigart, L.B., Nasi, S. and Evan, G.I. (2008) Modelling Myc inhibition as a cancer therapy. *Nature*, **455**, 679-683.
124. Haynes, S.R., Dollard, C., Winston, F., Beck, S., Trowsdale, J. and Dawid, I.B. (1992) The bromodomain: a conserved sequence found in human, Drosophila and yeast proteins. *Nucleic Acids Res*, **20**, 2603.

125. Yang, Z., Yik, J.H., Chen, R., He, N., Jang, M.K., Ozato, K. and Zhou, Q. (2005) Recruitment of P-TEFb for stimulation of transcriptional elongation by the bromodomain protein Brd4. *Mol Cell*, **19**, 535-545.
126. Kwiatkowski, N., Zhang, T., Rahl, P.B., Abraham, B.J., Reddy, J., Ficarro, S.B., Dastur, A., Amzallag, A., Ramaswamy, S., Tesar, B. *et al.* (2014) Targeting transcription regulation in cancer with a covalent CDK7 inhibitor. *Nature*, **511**, 616-620.
127. Garcia-Cuellar, M.P., Fuller, E., Mathner, E., Breitinger, C., Hetzner, K., Zeitlmann, L., Borkhardt, A. and Slany, R.K. (2014) Efficacy of cyclin-dependent-kinase 9 inhibitors in a murine model of mixed-lineage leukemia. *Leukemia*, **28**, 1427-1435.
128. Sklar, M.D., Thompson, E., Welsh, M.J., Liebert, M., Harney, J., Grossman, H.B., Smith, M. and Prochownik, E.V. (1991) Depletion of c-myc with specific antisense sequences reverses the transformed phenotype in ras oncogene-transformed NIH 3T3 cells. *Mol Cell Biol*, **11**, 3699-3710.
129. Li, Y., Zhang, B., Zhang, H., Zhu, X., Feng, D., Zhang, D., Zhuo, B., Li, L. and Zheng, J. (2013) Oncolytic adenovirus armed with shRNA targeting MYCN gene inhibits neuroblastoma cell proliferation and in vivo xenograft tumor growth. *J Cancer Res Clin Oncol*, **139**, 933-941.
130. Kim, D.H., Sarbassov, D.D., Ali, S.M., King, J.E., Latek, R.R., Erdjument-Bromage, H., Tempst, P. and Sabatini, D.M. (2002) mTOR interacts with raptor to form a nutrient-sensitive complex that signals to the cell growth machinery. *Cell*, **110**, 163-175.
131. Wullschleger, S., Loewith, R. and Hall, M.N. (2006) TOR signaling in growth and metabolism. *Cell*, **124**, 471-484.
132. Bjornsti, M.A. and Houghton, P.J. (2004) The TOR pathway: a target for cancer therapy. *Nat Rev Cancer*, **4**, 335-348.
133. Frost, P., Moatamed, F., Hoang, B., Shi, Y., Gera, J., Yan, H., Frost, P., Gibbons, J. and Lichtenstein, A. (2004) In vivo antitumor effects of the mTOR inhibitor CCI-779 against human multiple myeloma cells in a xenograft model. *Blood*, **104**, 4181-4187.
134. Chapuis, N., Tamburini, J., Green, A.S., Vignon, C., Bardet, V., Neyret, A., Pannetier, M., Willems, L., Park, S., Macone, A. *et al.* (2010) Dual inhibition of PI3K and mTORC1/2 signaling by NVP-BEZ235 as a new therapeutic strategy for acute myeloid leukemia. *Clin Cancer Res*, **16**, 5424-5435.
135. Cascon, A. and Robledo, M. (2012) MAX and MYC: a heritable breakup. *Cancer Res*, **72**, 3119-3124.
136. Wang, H., Hammoudeh, D.I., Follis, A.V., Reese, B.E., Lazo, J.S., Metallo, S.J. and Prochownik, E.V. (2007) Improved low molecular weight Myc-Max inhibitors. *Mol Cancer Ther*, **6**, 2399-2408.
137. Han, H., Jain, A.D., Truica, M.I., Izquierdo-Ferrer, J., Anker, J.F., Lysy, B., Sagar, V., Luan, Y., Chalmers, Z.R., Unno, K. *et al.* (2019) Small-Molecule MYC Inhibitors Suppress Tumor Growth and Enhance Immunotherapy. *Cancer Cell*, **36**, 483-497 e415.
138. Soucek, L., Nasi, S. and Evan, G.I. (2004) Omomyc expression in skin prevents Myc-induced papillomatosis. *Cell Death Differ*, **11**, 1038-1045.
139. Demma, M.J., Mapelli, C., Sun, A., Bodea, S., Ruprecht, B., Javaid, S., Wiswell, D., Muise, E., Chen, S., Zelina, J. *et al.* (2019) Omomyc Reveals New Mechanisms To Inhibit the MYC Oncogene. *Mol Cell Biol*, **39**.

140. Sun, Y., Bell, J.L., Carter, D., Gherardi, S., Poulos, R.C., Milazzo, G., Wong, J.W., Al-Awar, R., Tee, A.E., Liu, P.Y. *et al.* (2015) WDR5 Supports an N-Myc Transcriptional Complex That Drives a Protumorigenic Gene Expression Signature in Neuroblastoma. *Cancer Res*, **75**, 5143-5154.
141. Chacon Simon, S., Wang, F., Thomas, L.R., Phan, J., Zhao, B., Olejniczak, E.T., Macdonald, J.D., Shaw, J.G., Schlund, C., Payne, W. *et al.* (2020) Discovery of WD Repeat-Containing Protein 5 (WDR5)-MYC Inhibitors Using Fragment-Based Methods and Structure-Based Design. *J Med Chem*, **63**, 4315-4333.
142. Tian, J., Teuscher, K.B., Aho, E.R., Alvarado, J.R., Mills, J.J., Meyers, K.M., Gogliotti, R.D., Han, C., Macdonald, J.D., Sai, J. *et al.* (2020) Discovery and Structure-Based Optimization of Potent and Selective WD Repeat Domain 5 (WDR5) Inhibitors Containing a Dihydroisoquinolinone Bicyclic Core. *J Med Chem*, **63**, 656-675.
143. Mudgapalli, N., Nallasamy, P., Chava, H., Chava, S., Pathania, A.S., Gunda, V., Gorantla, S., Pandey, M.K., Gupta, S.C. and Challagundla, K.B. (2019) The role of exosomes and MYC in therapy resistance of acute myeloid leukemia: Challenges and opportunities. *Mol Aspects Med*, **70**, 21-32.
144. King, B., Trimarchi, T., Reavie, L., Xu, L., Mullenders, J., Ntziachristos, P., Aranda-Orgilles, B., Perez-Garcia, A., Shi, J., Vakoc, C. *et al.* (2013) The ubiquitin ligase FBXW7 modulates leukemia-initiating cell activity by regulating MYC stability. *Cell*, **153**, 1552-1566.
145. Wang, J., Wang, H., Peters, M., Ding, N., Ribback, S., Utpatel, K., Cigliano, A., Dombrowski, F., Xu, M., Chen, X. *et al.* (2019) Loss of Fbxw7 synergizes with activated Akt signaling to promote c-Myc dependent cholangiocarcinogenesis. *J Hepatol*, **71**, 742-752.
146. Sun, X.X., He, X., Yin, L., Komada, M., Sears, R.C. and Dai, M.S. (2015) The nucleolar ubiquitin-specific protease USP36 deubiquitinates and stabilizes c-Myc. *Proc Natl Acad Sci U S A*, **112**, 3734-3739.
147. Tavana, O., Li, D., Dai, C., Lopez, G., Banerjee, D., Kon, N., Chen, C., Califano, A., Yamashiro, D.J., Sun, H. *et al.* (2016) HAUSP deubiquitinates and stabilizes N-Myc in neuroblastoma. *Nat Med*, **22**, 1180-1186.
148. Popov, N., Wanzel, M., Madiredjo, M., Zhang, D., Beijersbergen, R., Bernards, R., Moll, R., Elledge, S.J. and Eilers, M. (2007) The ubiquitin-specific protease USP28 is required for MYC stability. *Nat Cell Biol*, **9**, 765-774.
149. Schulein-Volk, C., Wolf, E., Zhu, J., Xu, W., Taranets, L., Hellmann, A., Janicke, L.A., Diefenbacher, M.E., Behrens, A., Eilers, M. *et al.* (2014) Dual regulation of Fbw7 function and oncogenic transformation by Usp28. *Cell Rep*, **9**, 1099-1109.
150. Diefenbacher, M.E., Popov, N., Blake, S.M., Schulein-Volk, C., Nye, E., Spencer-Dene, B., Jaenicke, L.A., Eilers, M. and Behrens, A. (2014) The deubiquitinase USP28 controls intestinal homeostasis and promotes colorectal cancer. *J Clin Invest*, **124**, 3407-3418.
151. Diefenbacher, M.E., Chakraborty, A., Blake, S.M., Mitter, R., Popov, N., Eilers, M. and Behrens, A. (2015) Usp28 counteracts Fbw7 in intestinal homeostasis and cancer. *Cancer Res*, **75**, 1181-1186.
152. Wrigley, J.D., Gavory, G., Simpson, I., Preston, M., Plant, H., Bradley, J., Goeppert, A.U., Rozycka, E., Davies, G., Walsh, J. *et al.* (2017) Identification and Characterization of Dual Inhibitors of the USP25/28 Deubiquitinating Enzyme Subfamily. *ACS Chem Biol*, **12**, 3113-3125.

153. Prieto-Garcia, C., Hartmann, O., Reissland, M., Fischer, T., Maier, C.R., Rosenfeldt, M., Schulein-Volk, C., Klann, K., Kalb, R., Dikic, I. *et al.* (2022) Inhibition of USP28 overcomes Cisplatin-resistance of squamous tumors by suppression of the Fanconi anemia pathway. *Cell Death Differ*, **29**, 568-584.
154. Sakamoto, K.M., Kim, K.B., Kumagai, A., Mercurio, F., Crews, C.M. and Deshaies, R.J. (2001) Protacs: chimeric molecules that target proteins to the Skp1-Cullin-F box complex for ubiquitination and degradation. *Proc Natl Acad Sci U S A*, **98**, 8554-8559.
155. Wang, C., Zhang, J., Yin, J., Gan, Y., Xu, S., Gu, Y. and Huang, W. (2021) Alternative approaches to target Myc for cancer treatment. *Signal Transduct Target Ther*, **6**, 117.
156. Llombart, V. and Mansour, M.R. (2022) Therapeutic targeting of "undruggable" MYC. *EBioMedicine*, **75**, 103756.
157. Goldstein, G., Scheid, M., Hammerling, U., Schlesinger, D.H., Niall, H.D. and Boyse, E.A. (1975) Isolation of a polypeptide that has lymphocyte-differentiating properties and is probably represented universally in living cells. *Proc Natl Acad Sci U S A*, **72**, 11-15.
158. Pickart, C.M. (2001) Mechanisms underlying ubiquitination. *Annu Rev Biochem*, **70**, 503-533.
159. Schulman, B.A. and Harper, J.W. (2009) Ubiquitin-like protein activation by E1 enzymes: the apex for downstream signalling pathways. *Nat Rev Mol Cell Biol*, **10**, 319-331.
160. van Wijk, S.J. and Timmers, H.T. (2010) The family of ubiquitin-conjugating enzymes (E2s): deciding between life and death of proteins. *Faseb J*, **24**, 981-993.
161. Hoege, C., Pfander, B., Moldovan, G.L., Pyrowolakis, G. and Jentsch, S. (2002) RAD6-dependent DNA repair is linked to modification of PCNA by ubiquitin and SUMO. *Nature*, **419**, 135-141.
162. Carter, S., Bischof, O., Dejean, A. and Vousden, K.H. (2007) C-terminal modifications regulate MDM2 dissociation and nuclear export of p53. *Nat Cell Biol*, **9**, 428-435.
163. Haglund, K., Sigismund, S., Polo, S., Szymkiewicz, I., Di Fiore, P.P. and Dikic, I. (2003) Multiple monoubiquitination of RTKs is sufficient for their endocytosis and degradation. *Nat Cell Biol*, **5**, 461-466.
164. Koegl, M., Hoppe, T., Schlenker, S., Ulrich, H.D., Mayer, T.U. and Jentsch, S. (1999) A novel ubiquitination factor, E4, is involved in multiubiquitin chain assembly. *Cell*, **96**, 635-644.
165. Peng, J., Schwartz, D., Elias, J.E., Thoreen, C.C., Cheng, D., Marsischky, G., Roelofs, J., Finley, D. and Gygi, S.P. (2003) A proteomics approach to understanding protein ubiquitination. *Nat Biotechnol*, **21**, 921-926.
166. Xu, P., Duong, D.M., Seyfried, N.T., Cheng, D., Xie, Y., Robert, J., Rush, J., Hochstrasser, M., Finley, D. and Peng, J. (2009) Quantitative proteomics reveals the function of unconventional ubiquitin chains in proteasomal degradation. *Cell*, **137**, 133-145.
167. Hershko, A. and Ciechanover, A. (1998) The ubiquitin system. *Annu Rev Biochem*, **67**, 425-479.
168. Chen, Z.J. and Sun, L.J. (2009) Nonproteolytic functions of ubiquitin in cell signaling. *Mol Cell*, **33**, 275-286.
169. Nishikawa, H., Ooka, S., Sato, K., Arima, K., Okamoto, J., Klevit, R.E., Fukuda, M. and Ohta, T. (2004) Mass spectrometric and mutational analyses

reveal Lys-6-linked polyubiquitin chains catalyzed by BRCA1-BARD1 ubiquitin ligase. *J Biol Chem*, **279**, 3916-3924.
170. Wickliffe, K.E., Williamson, A., Meyer, H.J., Kelly, A. and Rape, M. (2011) K11-linked ubiquitin chains as novel regulators of cell division. *Trends Cell Biol*, **21**, 656-663.
171. Grice, G.L., Lobb, I.T., Weekes, M.P., Gygi, S.P., Antrobus, R. and Nathan, J.A. (2015) The Proteasome Distinguishes between Heterotypic and Homotypic Lysine-11-Linked Polyubiquitin Chains. *Cell Rep*, **12**, 545-553.
172. Chastagner, P., Israel, A. and Brou, C. (2006) Itch/AIP4 mediates Deltex degradation through the formation of K29-linked polyubiquitin chains. *EMBO Rep*, **7**, 1147-1153.
173. Al-Hakim, A.K., Zagorska, A., Chapman, L., Deak, M., Peggie, M. and Alessi, D.R. (2008) Control of AMPK-related kinases by USP9X and atypical Lys(29)/Lys(33)-linked polyubiquitin chains. *Biochem J*, **411**, 249-260.
174. Flick, K., Raasi, S., Zhang, H., Yen, J.L. and Kaiser, P. (2006) A ubiquitin-interacting motif protects polyubiquitinated Met4 from degradation by the 26S proteasome. *Nat Cell Biol*, **8**, 509-515.
175. Ohtake, F., Tsuchiya, H., Saeki, Y. and Tanaka, K. (2018) K63 ubiquitylation triggers proteasomal degradation by seeding branched ubiquitin chains. *Proc Natl Acad Sci U S A*, **115**, E1401-E1408.
176. Tanaka, K. (2009) The proteasome: overview of structure and functions. *Proc Jpn Acad Ser B Phys Biol Sci*, **85**, 12-36.
177. Groettrup, M., Pelzer, C., Schmidtke, G. and Hofmann, K. (2008) Activating the ubiquitin family: UBA6 challenges the field. *Trends Biochem Sci*, **33**, 230-237.
178. Stewart, M.D., Ritterhoff, T., Klevit, R.E. and Brzovic, P.S. (2016) E2 enzymes: more than just middle men. *Cell Res*, **26**, 423-440.
179. Deshaies, R.J. and Joazeiro, C.A. (2009) RING domain E3 ubiquitin ligases. *Annu Rev Biochem*, **78**, 399-434.
180. Zheng, N. and Shabek, N. (2017) Ubiquitin Ligases: Structure, Function, and Regulation. *Annu Rev Biochem*, **86**, 129-157.
181. Yang, Q., Zhao, J., Chen, D. and Wang, Y. (2021) E3 ubiquitin ligases: styles, structures and functions. *Mol Biomed*, **2**, 23.
182. Xie, J., Jin, Y. and Wang, G. (2019) The role of SCF ubiquitin-ligase complex at the beginning of life. *Reprod Biol Endocrinol*, **17**, 101.
183. Bai, C., Sen, P., Hofmann, K., Ma, L., Goebl, M., Harper, J.W. and Elledge, S.J. (1996) SKP1 connects cell cycle regulators to the ubiquitin proteolysis machinery through a novel motif, the F-box. *Cell*, **86**, 263-274.
184. Skaar, J.R., Pagan, J.K. and Pagano, M. (2014) SCF ubiquitin ligase-targeted therapies. *Nat Rev Drug Discov*, **13**, 889-903.
185. Sluimer, J. and Distel, B. (2018) Regulating the human HECT E3 ligases. *Cell Mol Life Sci*, **75**, 3121-3141.
186. Rotin, D. and Kumar, S. (2009) Physiological functions of the HECT family of ubiquitin ligases. *Nat Rev Mol Cell Biol*, **10**, 398-409.
187. Hu, H., Dong, C., Sun, D., Hu, Y. and Xie, J. (2018) Genome-Wide Identification and Analysis of U-Box E3 Ubiquitin(-)Protein Ligase Gene Family in Banana. *Int J Mol Sci*, **19**.
188. Hatakeyama, S., Yada, M., Matsumoto, M., Ishida, N. and Nakayama, K.I. (2001) U box proteins as a new family of ubiquitin-protein ligases. *J Biol Chem*, **276**, 33111-33120.

189. Aguilera, M., Oliveros, M., Martinez-Padron, M., Barbas, J.A. and Ferrus, A. (2000) Ariadne-1: a vital Drosophila gene is required in development and defines a new conserved family of ring-finger proteins. *Genetics*, **155**, 1231-1244.
190. Mevissen, T.E.T. and Komander, D. (2017) Mechanisms of Deubiquitinase Specificity and Regulation. *Annu Rev Biochem*, **86**, 159-192.
191. Trulsson, F., Akimov, V., Robu, M., van Overbeek, N., Berrocal, D.A.P., Shah, R.G., Cox, J., Shah, G.M., Blagoev, B. and Vertegaal, A.C.O. (2022) Deubiquitinating enzymes and the proteasome regulate preferential sets of ubiquitin substrates. *Nat Commun*, **13**, 2736.
192. Fraile, J.M., Quesada, V., Rodriguez, D., Freije, J.M. and Lopez-Otin, C. (2012) Deubiquitinases in cancer: new functions and therapeutic options. *Oncogene*, **31**, 2373-2388.
193. Komander, D., Clague, M.J. and Urbe, S. (2009) Breaking the chains: structure and function of the deubiquitinases. *Nat Rev Mol Cell Biol*, **10**, 550-563.
194. Valero, R., Bayes, M., Francisca Sanchez-Font, M., Gonzalez-Angulo, O., Gonzalez-Duarte, R. and Marfany, G. (2001) Characterization of alternatively spliced products and tissue-specific isoforms of USP28 and USP25. *Genome Biol*, **2**, RESEARCH0043.
195. Wen, Y., Cui, R., Zhang, H. and Zhang, N. (2014) (1)H, (1)(3)C and (1)(5)N backbone and side-chain resonance assignments of the N-terminal ubiquitin-binding domains of the human deubiquitinase Usp28. *Biomol NMR Assign*, **8**, 251-254.
196. Sauer, F., Klemm, T., Kollampally, R.B., Tessmer, I., Nair, R.K., Popov, N. and Kisker, C. (2019) Differential Oligomerization of the Deubiquitinases USP25 and USP28 Regulates Their Activities. *Mol Cell*, **74**, 421-435 e410.
197. Gersch, M., Wagstaff, J.L., Toms, A.V., Graves, B., Freund, S.M.V. and Komander, D. (2019) Distinct USP25 and USP28 Oligomerization States Regulate Deubiquitinating Activity. *Mol Cell*, **74**, 436-451 e437.
198. Sun, X., Cai, M., Wu, L., Zhen, X., Chen, Y., Peng, J., Han, S. and Zhang, P. (2022) Ubiquitin-specific protease 28 deubiquitinates TCF7L2 to govern the action of the Wnt signaling pathway in hepatic carcinoma. *Cancer Sci*, **113**, 3463-3475.
199. Guo, G., Xu, Y., Gong, M., Cao, Y. and An, R. (2014) USP28 is a potential prognostic marker for bladder cancer. *Tumour Biol*, **35**, 4017-4022.
200. Wu, Y., Wang, Y., Yang, X.H., Kang, T., Zhao, Y., Wang, C., Evers, B.M. and Zhou, B.P. (2013) The deubiquitinase USP28 stabilizes LSD1 and confers stem-cell-like traits to breast cancer cells. *Cell Rep*, **5**, 224-236.
201. Zhang, L., Xu, B., Qiang, Y., Huang, H., Wang, C., Li, D. and Qian, J. (2015) Overexpression of deubiquitinating enzyme USP28 promoted non-small cell lung cancer growth. *J Cell Mol Med*, **19**, 799-805.
202. Wang, Z., Song, Q., Xue, J., Zhao, Y. and Qin, S. (2016) Ubiquitin-specific protease 28 is overexpressed in human glioblastomas and contributes to glioma tumorigenicity by regulating MYC expression. *Exp Biol Med (Maywood)*, **241**, 255-264.
203. Muller, I., Strozyk, E., Schindler, S., Beissert, S., Oo, H.Z., Sauter, T., Lucarelli, P., Raeth, S., Hausser, A., Al Nakouzi, N. *et al.* (2020) Cancer Cells Employ Nuclear Caspase-8 to Overcome the p53-Dependent G2/M Checkpoint through Cleavage of USP28. *Mol Cell*, **77**, 970-984 e977.

204. Meitinger, F., Anzola, J.V., Kaulich, M., Richardson, A., Stender, J.D., Benner, C., Glass, C.K., Dowdy, S.F., Desai, A., Shiau, A.K. *et al.* (2016) 53BP1 and USP28 mediate p53 activation and G1 arrest after centrosome loss or extended mitotic duration. *J Cell Biol*, **214**, 155-166.
205. Fong, C.S., Mazo, G., Das, T., Goodman, J., Kim, M., O'Rourke, B.P., Izquierdo, D. and Tsou, M.F. (2016) 53BP1 and USP28 mediate p53-dependent cell cycle arrest in response to centrosome loss and prolonged mitosis. *Elife*, **5**.
206. Lambrus, B.G., Daggubati, V., Uetake, Y., Scott, P.M., Clutario, K.M., Sluder, G. and Holland, A.J. (2016) A USP28-53BP1-p53-p21 signaling axis arrests growth after centrosome loss or prolonged mitosis. *J Cell Biol*, **214**, 143-153.
207. Bohgaki, M., Hakem, A., Halaby, M.J., Bohgaki, T., Li, Q., Bissey, P.A., Shloush, J., Kislinger, T., Sanchez, O., Sheng, Y. *et al.* (2013) The E3 ligase PIRH2 polyubiquitylates CHK2 and regulates its turnover. *Cell Death Differ*, **20**, 812-822.
208. Amati, B. and Sanchez-Arevalo Lobo, V.J. (2007) MYC degradation: deubiquitinating enzymes enter the dance. *Nat Cell Biol*, **9**, 729-731.
209. Prieto-Garcia, C., Hartmann, O., Reissland, M., Braun, F., Fischer, T., Walz, S., Schulein-Volk, C., Eilers, U., Ade, C.P., Calzado, M.A. *et al.* (2020) Maintaining protein stability of ΔNp63 via USP28 is required by squamous cancer cells. *EMBO Mol Med*, **12**, e11101.
210. Parrales, A. and Iwakuma, T. (2015) Targeting Oncogenic Mutant p53 for Cancer Therapy. *Front Oncol*, **5**, 288.
211. Bakkenist, C.J. and Kastan, M.B. (2004) Initiating cellular stress responses. *Cell*, **118**, 9-17.
212. Zhou, B.B. and Elledge, S.J. (2000) The DNA damage response: putting checkpoints in perspective. *Nature*, **408**, 433-439.
213. Zhang, D., Zaugg, K., Mak, T.W. and Elledge, S.J. (2006) A role for the deubiquitinating enzyme USP28 in control of the DNA-damage response. *Cell*, **126**, 529-542.
214. Knobel, P.A., Belotserkovskaya, R., Galanty, Y., Schmidt, C.K., Jackson, S.P. and Stracker, T.H. (2014) USP28 is recruited to sites of DNA damage by the tandem BRCT domains of 53BP1 but plays a minor role in double-strand break metabolism. *Mol Cell Biol*, **34**, 2062-2074.
215. Lin, S.Y., Li, K., Stewart, G.S. and Elledge, S.J. (2004) Human Claspin works with BRCA1 to both positively and negatively regulate cell proliferation. *Proc Natl Acad Sci U S A*, **101**, 6484-6489.
216. Wang, X., Liu, Z., Zhang, L., Yang, Z., Chen, X., Luo, J., Zhou, Z., Mei, X., Yu, X., Shao, Z. *et al.* (2018) Targeting deubiquitinase USP28 for cancer therapy. *Cell Death Dis*, **9**, 186.
217. Hinds, P.W., Mittnacht, S., Dulic, V., Arnold, A., Reed, S.I. and Weinberg, R.A. (1992) Regulation of retinoblastoma protein functions by ectopic expression of human cyclins. *Cell*, **70**, 993-1006.
218. Donnellan, R. and Chetty, R. (1999) Cyclin E in human cancers. *Faseb J*, **13**, 773-780.
219. Richardson, P.G., Hideshima, T. and Anderson, K.C. (2003) Bortezomib (PS-341): a novel, first-in-class proteasome inhibitor for the treatment of multiple myeloma and other cancers. *Cancer Control*, **10**, 361-369.
220. Demo, S.D., Kirk, C.J., Aujay, M.A., Buchholz, T.J., Dajee, M., Ho, M.N., Jiang, J., Laidig, G.J., Lewis, E.R., Parlati, F. *et al.* (2007) Antitumor activity of

PR-171, a novel irreversible inhibitor of the proteasome. *Cancer Res*, **67**, 6383-6391.
221. Warlick, E.D., Cao, Q. and Miller, J. (2013) Bortezomib and vorinostat in refractory acute myelogenous leukemia and high-risk myelodysplastic syndromes: produces stable disease but at the cost of high toxicity. *Leukemia*, **27**, 1789-1791.
222. Kubiczkova, L., Pour, L., Sedlarikova, L., Hajek, R. and Sevcikova, S. (2014) Proteasome inhibitors - molecular basis and current perspectives in multiple myeloma. *J Cell Mol Med*, **18**, 947-961.
223. Schauer, N.J., Magin, R.S., Liu, X., Doherty, L.M. and Buhrlage, S.J. (2020) Advances in Discovering Deubiquitinating Enzyme (DUB) Inhibitors. *J Med Chem*, **63**, 2731-2750.
224. Rowinsky, E.K., Paner, A., Berdeja, J.G., Paba-Prada, C., Venugopal, P., Porkka, K., Gullbo, J., Linder, S., Loskog, A., Richardson, P.G. *et al.* (2020) Phase 1 study of the protein deubiquitinase inhibitor VLX1570 in patients with relapsed and/or refractory multiple myeloma. *Invest New Drugs*, **38**, 1448-1453.
225. Ruiz, E.J., Pinto-Fernandez, A., Turnbull, A.P., Lan, L., Charlton, T.M., Scott, H.C., Damianou, A., Vere, G., Riising, E.M., Da Costa, C. *et al.* (2021) USP28 deletion and small-molecule inhibition destabilizes c-MYC and elicits regression of squamous cell lung carcinoma. *Elife*, **10**.
226. Wang, H., Meng, Q., Ding, Y., Xiong, M., Zhu, M., Yang, Y., Su, H., Gu, L., Xu, Y., Shi, L. *et al.* (2021) USP28 and USP25 are downregulated by Vismodegib in vitro and in colorectal cancer cell lines. *FEBS J*, **288**, 1325-1342.
227. Cox, J. and Mann, M. (2008) MaxQuant enables high peptide identification rates, individualized p.p.b.-range mass accuracies and proteome-wide protein quantification. *Nat Biotechnol*, **26**, 1367-1372.
228. Nieminuszczy, J., Schwab, R.A. and Niedzwiedz, W. (2016) The DNA fibre technique - tracking helicases at work. *Methods*, **108**, 92-98.
229. Meers, M.P., Bryson, T.D., Henikoff, J.G. and Henikoff, S. (2019) Improved CUT&RUN chromatin profiling tools. *Elife*, **8**.
230. Dobin, A., Davis, C.A., Schlesinger, F., Drenkow, J., Zaleski, C., Jha, S., Batut, P., Chaisson, M. and Gingeras, T.R. (2013) STAR: ultrafast universal RNA-seq aligner. *Bioinformatics*, **29**, 15-21.
231. Robinson, M.D., McCarthy, D.J. and Smyth, G.K. (2010) edgeR: a Bioconductor package for differential expression analysis of digital gene expression data. *Bioinformatics*, **26**, 139-140.
232. Xie, Z., Bailey, A., Kuleshov, M.V., Clarke, D.J.B., Evangelista, J.E., Jenkins, S.L., Lachmann, A., Wojciechowicz, M.L., Kropiwnicki, E., Jagodnik, K.M. *et al.* (2021) Gene Set Knowledge Discovery with Enrichr. *Curr Protoc*, **1**, e90.
233. Galardy, P., Ploegh, H.L. and Ovaa, H. (2005) Mechanism-based proteomics tools based on ubiquitin and ubiquitin-like proteins: crystallography, activity profiling, and protease identification. *Methods Enzymol*, **399**, 120-131.
234. Zhen, Y., Knobel, P.A., Stracker, T.H. and Reverter, D. (2014) Regulation of USP28 deubiquitinating activity by SUMO conjugation. *J Biol Chem*, **289**, 34838-34850.
235. McGouran, J.F., Gaertner, S.R., Altun, M., Kramer, H.B. and Kessler, B.M. (2013) Deubiquitinating enzyme specificity for ubiquitin chain topology profiled by di-ubiquitin activity probes. *Chem Biol*, **20**, 1447-1455.

236. Hamperl, S., Bocek, M.J., Saldivar, J.C., Swigut, T. and Cimprich, K.A. (2017) Transcription-Replication Conflict Orientation Modulates R-Loop Levels and Activates Distinct DNA Damage Responses. *Cell*, **170**, 774-786 e719.
237. Alabert, C., Bukowski-Wills, J.C., Lee, S.B., Kustatscher, G., Nakamura, K., de Lima Alves, F., Menard, P., Mejlvang, J., Rappsilber, J. and Groth, A. (2014) Nascent chromatin capture proteomics determines chromatin dynamics during DNA replication and identifies unknown fork components. *Nat Cell Biol*, **16**, 281-293.
238. Hughes, B.T., Sidorova, J., Swanger, J., Monnat, R.J., Jr. and Clurman, B.E. (2013) Essential role for Cdk2 inhibitory phosphorylation during replication stress revealed by a human Cdk2 knockin mutation. *Proc Natl Acad Sci U S A*, **110**, 8954-8959.
239. Maya-Mendoza, A., Moudry, P., Merchut-Maya, J.M., Lee, M., Strauss, R. and Bartek, J. (2018) High speed of fork progression induces DNA replication stress and genomic instability. *Nature*, **559**, 279-284.
240. Fairbairn, D.W., Olive, P.L. and O'Neill, K.L. (1995) The comet assay: a comprehensive review. *Mutat Res*, **339**, 37-59.
241. Kurashige, T., Shimamura, M. and Nagayama, Y. (2016) Differences in quantification of DNA double-strand breaks assessed by 53BP1/gammaH2AX focus formation assays and the comet assay in mammalian cells treated with irradiation and N-acetyl-L-cysteine. *J Radiat Res*, **57**, 312-317.
242. Chen, G. and Deng, X. (2018) Cell Synchronization by Double Thymidine Block. *Bio Protoc*, **8**.
243. Cuella-Martin, R., Oliveira, C., Lockstone, H.E., Snellenberg, S., Grolmusova, N. and Chapman, J.R. (2016) 53BP1 Integrates DNA Repair and p53-Dependent Cell Fate Decisions via Distinct Mechanisms. *Mol Cell*, **64**, 51-64.
244. Liu, S.Q., Yu, J.P., Yu, H.G., Lv, P. and Chen, H.L. (2006) Activation of Akt and ERK signalling pathways induced by etoposide confer chemoresistance in gastric cancer cells. *Dig Liver Dis*, **38**, 310-318.
245. Zhang, A., Peng, B., Huang, P., Chen, J. and Gong, Z. (2017) The p53-binding protein 1-Tudor-interacting repair regulator complex participates in the DNA damage response. *J Biol Chem*, **292**, 6461-6467.
246. Clausen, D.M., Guo, J., Parise, R.A., Beumer, J.H., Egorin, M.J., Lazo, J.S., Prochownik, E.V. and Eiseman, J.L. (2010) In vitro cytotoxicity and in vivo efficacy, pharmacokinetics, and metabolism of 10074-G5, a novel small-molecule inhibitor of c-Myc/Max dimerization. *J Pharmacol Exp Ther*, **335**, 715-727.
247. Jones, S. and Thornton, J.M. (1996) Principles of protein-protein interactions. *Proc Natl Acad Sci U S A*, **93**, 13-20.
248. Goodsell, D.S. and Olson, A.J. (2000) Structural symmetry and protein function. *Annu Rev Biophys Biomol Struct*, **29**, 105-153.
249. Gabizon, R. and Friedler, A. (2014) Allosteric modulation of protein oligomerization: an emerging approach to drug design. *Front Chem*, **2**, 9.
250. Marianayagam, N.J., Sunde, M. and Matthews, J.M. (2004) The power of two: protein dimerization in biology. *Trends Biochem Sci*, **29**, 618-625.
251. Davis, R.J., Welcker, M. and Clurman, B.E. (2014) Tumor suppression by the Fbw7 ubiquitin ligase: mechanisms and opportunities. *Cancer Cell*, **26**, 455-464.

252. Paul, A. and Wang, B. (2017) RNF8- and Ube2S-Dependent Ubiquitin Lysine 11-Linkage Modification in Response to DNA Damage. *Mol Cell*, **66**, 458-472 e455.
253. French, M.E., Koehler, C.F. and Hunter, T. (2021) Emerging functions of branched ubiquitin chains. *Cell Discov*, **7**, 6.
254. Adhikary, S., Marinoni, F., Hock, A., Hulleman, E., Popov, N., Beier, R., Bernard, S., Quarto, M., Capra, M., Goettig, S. *et al.* (2005) The ubiquitin ligase HectH9 regulates transcriptional activation by Myc and is essential for tumor cell proliferation. *Cell*, **123**, 409-421.
255. Chan, C.H., Li, C.F., Yang, W.L., Gao, Y., Lee, S.W., Feng, Z., Huang, H.Y., Tsai, K.K., Flores, L.G., Shao, Y. *et al.* (2012) The Skp2-SCF E3 ligase regulates Akt ubiquitination, glycolysis, herceptin sensitivity, and tumorigenesis. *Cell*, **149**, 1098-1111.
256. Kim, S.Y., Herbst, A., Tworkowski, K.A., Salghetti, S.E. and Tansey, W.P. (2003) Skp2 regulates Myc protein stability and activity. *Mol Cell*, **11**, 1177-1188.
257. Popov, N., Schulein, C., Jaenicke, L.A. and Eilers, M. (2010) Ubiquitylation of the amino terminus of Myc by SCF(beta-TrCP) antagonizes SCF(Fbw7)-mediated turnover. *Nat Cell Biol*, **12**, 973-981.
258. Thomas, J.J., Abed, M., Heuberger, J., Novak, R., Zohar, Y., Beltran Lopez, A.P., Trausch-Azar, J.S., Ilagan, M.X.G., Benhamou, D., Dittmar, G. *et al.* (2016) RNF4-Dependent Oncogene Activation by Protein Stabilization. *Cell Rep*, **16**, 3388-3400.
259. Ye, Y. and Rape, M. (2009) Building ubiquitin chains: E2 enzymes at work. *Nat Rev Mol Cell Biol*, **10**, 755-764.
260. Chern, Y.J., Lee, H.J. and Chan, C.H. (2021) RNF8 stabilizes MYC via K63-linked ubiquitination to promote metabolic reprogramming in triple-negative breast cancer. *Faseb J*, **35**.
261. Yamano, H. (2019) APC/C: current understanding and future perspectives. *F1000Res*, **8**.
262. Zhang, Z., Lv, X., Yin, W.C., Zhang, X., Feng, J., Wu, W., Hui, C.C., Zhang, L. and Zhao, Y. (2013) Ter94 ATPase complex targets k11-linked ubiquitinated ci to proteasomes for partial degradation. *Dev Cell*, **25**, 636-644.
263. Bassermann, F., Eichner, R. and Pagano, M. (2014) The ubiquitin proteasome system - implications for cell cycle control and the targeted treatment of cancer. *Biochim Biophys Acta*, **1843**, 150-162.
264. von der Lehr, N., Johansson, S., Wu, S., Bahram, F., Castell, A., Cetinkaya, C., Hydbring, P., Weidung, I., Nakayama, K., Nakayama, K.I. *et al.* (2003) The F-box protein Skp2 participates in c-Myc proteosomal degradation and acts as a cofactor for c-Myc-regulated transcription. *Mol Cell*, **11**, 1189-1200.
265. Zhang, Q., Spears, E., Boone, D.N., Li, Z., Gregory, M.A. and Hann, S.R. (2013) Domain-specific c-Myc ubiquitylation controls c-Myc transcriptional and apoptotic activity. *Proc Natl Acad Sci U S A*, **110**, 978-983.
266. Chen, F.X., Woodfin, A.R., Gardini, A., Rickels, R.A., Marshall, S.A., Smith, E.R., Shiekhattar, R. and Shilatifard, A. (2015) PAF1, a Molecular Regulator of Promoter-Proximal Pausing by RNA Polymerase II. *Cell*, **162**, 1003-1015.
267. Van Oss, S.B., Cucinotta, C.E. and Arndt, K.M. (2017) Emerging Insights into the Roles of the Paf1 Complex in Gene Regulation. *Trends Biochem Sci*, **42**, 788-798.

268. Michel, M.A., Swatek, K.N., Hospenthal, M.K. and Komander, D. (2017) Ubiquitin Linkage-Specific Affimers Reveal Insights into K6-Linked Ubiquitin Signaling. *Mol Cell*, **68**, 233-246 e235.
269. Yuan, Y., Wang, L.H., Zhao, X.X., Wang, J., Zhang, M.S., Ma, Q.H., Wei, S., Yan, Z.X., Cheng, Y., Chen, X.Q. *et al.* (2022) The E3 ubiquitin ligase HUWE1 acts through the N-Myc-DLL1-NOTCH1 signaling axis to suppress glioblastoma progression. *Cancer Commun (Lond)*, **42**, 868-886.
270. Trujillo, K.M. and Osley, M.A. (2012) A role for H2B ubiquitylation in DNA replication. *Mol Cell*, **48**, 734-746.
271. Zheng, S., Li, D., Lu, Z., Liu, G., Wang, M., Xing, P., Wang, M., Dong, Y., Wang, X., Li, J. *et al.* (2018) Bre1-dependent H2B ubiquitination promotes homologous recombination by stimulating histone eviction at DNA breaks. *Nucleic Acids Res*, **46**, 11326-11339.
272. Somyajit, K., Gupta, R., Sedlackova, H., Neelsen, K.J., Ochs, F., Rask, M.B., Choudhary, C. and Lukas, J. (2017) Redox-sensitive alteration of replisome architecture safeguards genome integrity. *Science*, **358**, 797-802.
273. Dellino, G.I., Cittaro, D., Piccioni, R., Luzi, L., Banfi, S., Segalla, S., Cesaroni, M., Mendoza-Maldonado, R., Giacca, M. and Pelicci, P.G. (2013) Genome-wide mapping of human DNA-replication origins: levels of transcription at ORC1 sites regulate origin selection and replication timing. *Genome Res*, **23**, 1-11.
274. Miotto, B., Ji, Z. and Struhl, K. (2016) Selectivity of ORC binding sites and the relation to replication timing, fragile sites, and deletions in cancers. *Proc Natl Acad Sci U S A*, **113**, E4810-4819.
275. Chen, Y.H., Keegan, S., Kahli, M., Tonzi, P., Fenyo, D., Huang, T.T. and Smith, D.J. (2019) Transcription shapes DNA replication initiation and termination in human cells. *Nat Struct Mol Biol*, **26**, 67-77.
276. Ge, X.Q. and Blow, J.J. (2010) Chk1 inhibits replication factory activation but allows dormant origin firing in existing factories. *J Cell Biol*, **191**, 1285-1297.
277. Yekezare, M., Gomez-Gonzalez, B. and Diffley, J.F. (2013) Controlling DNA replication origins in response to DNA damage - inhibit globally, activate locally. *J Cell Sci*, **126**, 1297-1306.
278. Macheret, M. and Halazonetis, T.D. (2019) Monitoring early S-phase origin firing and replication fork movement by sequencing nascent DNA from synchronized cells. *Nat Protoc*, **14**, 51-67.
279. Guerra, L., Albihn, A., Tronnersjo, S., Yan, Q., Guidi, R., Stenerlow, B., Sterzenbach, T., Josenhans, C., Fox, J.G., Schauer, D.B. *et al.* (2010) Myc is required for activation of the ATM-dependent checkpoints in response to DNA damage. *PLoS One*, **5**, e8924.
280. Phesse, T.J., Myant, K.B., Cole, A.M., Ridgway, R.A., Pearson, H., Muncan, V., van den Brink, G.R., Vousden, K.H., Sears, R., Vassilev, L.T. *et al.* (2014) Endogenous c-Myc is essential for p53-induced apoptosis in response to DNA damage in vivo. *Cell Death Differ*, **21**, 956-966.
281. Vafa, O., Wade, M., Kern, S., Beeche, M., Pandita, T.K., Hampton, G.M. and Wahl, G.M. (2002) c-Myc can induce DNA damage, increase reactive oxygen species, and mitigate p53 function: a mechanism for oncogene-induced genetic instability. *Mol Cell*, **9**, 1031-1044.
282. Iwabuchi, K., Bartel, P.L., Li, B., Marraccino, R. and Fields, S. (1994) Two cellular proteins that bind to wild-type but not mutant p53. *Proc Natl Acad Sci U S A*, **91**, 6098-6102.

283. Harrigan, J.A., Belotserkovskaya, R., Coates, J., Dimitrova, D.S., Polo, S.E., Bradshaw, C.R., Fraser, P. and Jackson, S.P. (2011) Replication stress induces 53BP1-containing OPT domains in G1 cells. *J Cell Biol*, **193**, 97-108.
284. Lukas, C., Savic, V., Bekker-Jensen, S., Doil, C., Neumann, B., Pedersen, R.S., Grofte, M., Chan, K.L., Hickson, I.D., Bartek, J. *et al.* (2011) 53BP1 nuclear bodies form around DNA lesions generated by mitotic transmission of chromosomes under replication stress. *Nat Cell Biol*, **13**, 243-253.
285. Mirman, Z. and de Lange, T. (2020) 53BP1: a DSB escort. *Genes Dev*, **34**, 7-23.
286. Spies, J., Lukas, C., Somyajit, K., Rask, M.B., Lukas, J. and Neelsen, K.J. (2019) 53BP1 nuclear bodies enforce replication timing at under-replicated DNA to limit heritable DNA damage. *Nat Cell Biol*, **21**, 487-497.
287. Chapman, J.R., Taylor, M.R. and Boulton, S.J. (2012) Playing the end game: DNA double-strand break repair pathway choice. *Mol Cell*, **47**, 497-510.
288. Zimmermann, M. and de Lange, T. (2014) 53BP1: pro choice in DNA repair. *Trends Cell Biol*, **24**, 108-117.
289. Lukas, J., Lukas, C. and Bartek, J. (2011) More than just a focus: The chromatin response to DNA damage and its role in genome integrity maintenance. *Nat Cell Biol*, **13**, 1161-1169.
290. Lottersberger, F., Bothmer, A., Robbiani, D.F., Nussenzweig, M.C. and de Lange, T. (2013) Role of 53BP1 oligomerization in regulating double-strand break repair. *Proc Natl Acad Sci U S A*, **110**, 2146-2151.
291. Lou, J., Priest, D.G., Solano, A., Kerjouan, A. and Hinde, E. (2020) Spatiotemporal dynamics of 53BP1 dimer recruitment to a DNA double strand break. *Nat Commun*, **11**, 5776.
292. Schultz, L.B., Chehab, N.H., Malikzay, A. and Halazonetis, T.D. (2000) p53 binding protein 1 (53BP1) is an early participant in the cellular response to DNA double-strand breaks. *J Cell Biol*, **151**, 1381-1390.
293. Anderson, L., Henderson, C. and Adachi, Y. (2001) Phosphorylation and rapid relocalization of 53BP1 to nuclear foci upon DNA damage. *Mol Cell Biol*, **21**, 1719-1729.
294. Hu, Y., Wang, C., Huang, K., Xia, F., Parvin, J.D. and Mondal, N. (2014) Regulation of 53BP1 protein stability by RNF8 and RNF168 is important for efficient DNA double-strand break repair. *PLoS One*, **9**, e110522.

Appendix

Abbreviations:

Prefixes

k	kilo
c	centi
m	milli
µ	micro
n	nano
p	pico

Units

°C	degree Celsius
G	gravity
g	gram
h	hour
l	liter
M	mol/l
m	meter
min	minute
rpm	revolutions per minute
sec	second
V	voltage
v/v	volume per volume

Others

CIdU	5-Chloro-2'-deoxyuridine
EdU	5-Ethynyl-2′-deoxyuridine
IdU	5-Iodo-2'-deoxyuridine
APS	Ammonium persulfate
Apc/c	Anaphase-promoting complex or cyclosome
ATM	Ataxia telangiectasia-mutated
ATR	ATM and RAD3-related protein
BER	Base excision repair
bHLHLZ	basic helix-loop-helix leucine zipper
BCA	Bicinchoninic acid colorimetric assay
BET	Bromodomain and extra terminal domain
BRD4	Bromodomain-containing 4
ChIP	Chromatin immunoprecipitation
CRISPR	Clustered Regularly Interspaced Short Palindromic Repeats
Cas9	CRISPR-associated protein 9
CTD	C-terminal domain
CDKN	Cyclin dependent kinase inhibitor

CDK2	Cyclin-dependent kinase 2
CDK9	Cyclin-dependent kinase 9
CDKs	Cyclin-dependent kinases
CHX	Cycloheximide
Cys, C	Cysteine
dNTP	Deoxyribonucleotide triphosphate
DUB	Deubiquitinase
DTT	Dithiothreitol
DDR	DNA damage response
DNA-PKcs	DNA-dependent protein kinase catalytic subunit
DSB	Double strand break
DMEM	Dulbecco's Modified Eagle Medium-high glycose
4EBP1	eIF4E binding protein 1
E-box	Enhancer box
EGFR	Epidermal growth factor receptor
EMT	Epithelial-mesenchymal transition
Eto	Etoposide
eIF4E	Eukaryotic initiation factor 4E
FBXW7	F-Box and WD Repeat Domain Containing 7
FBS	Fetal Bovine Serum
Gcn5	General control nonderepressible 5
Glu, E	Glutamic acid
Gsk3	Glycogen synthase kinase 3
GFI-1	Growth factor independence 1
HCC	Hepatocelluar carcinoma
HTS	High-throughput screening
H3K27	Histone 3 lysine 27
H3K9	Histone 3 lysine 9
HDAC3	Histone Deacetylase 3
HAT	Histone-acetylation
HR	Homologous recombination
HECT	Homologous to the E6-AP Carboxyl Terminus
HU	Hydroxyurea
HIF1-α	Hypoxia-inducible factor 1-alpha
IF	Immunofluorescence
IP	Immunoprecipitation
IBR	In-between-RINGs
IR	Ionizing radiation
iPOND	Isolation of proteins on nascent DNA
JAMMs	JAB1/MPN/MOV34 metalloprotease
Leu, L	Leucine
LMP	Low Melting Point
LSCC	Lung squamous cell carcinoma
Lys, K	Lysine
MJD	Machado-Josephin domain protease
MINDY	MIU- containing novel DUB family
Usp28-M	Monomeric Usp28
MIU	Motif interacting with ubiquitin
MRN	MRE11–RAD50–NBS1

MM	Multiple myeloma
MB	Myc box
Max	Myc-associated protein X
MIZ1	MYC-interacting zinc finger protein 1
NHEJ	Non-homologous end-joining
NER	Nucleotide excision repair
ORF	Open reading frame
OTU	Ovarian tumour protease
53bp1	p53 binding protein
PFA	Paraformaldehyde
PIKK	Phosphatidylinositol 3-kinase-like kinase
PEI	Polyethylenimine
PCR	Polymerase chain reaction
P-TEFb	Positive Transcription Elongation Factor b
PTM	Posttranslational modifications
pre-RC	Pre-replicative complex
PCNA	Proliferating cell nuclear antigen
PPI	Protein-protein interaction
PROTAC	Proteolysis Targeting Chimera
PLA	Proximity Ligation Assays
qPCR	Quantitative real-time PCR
RING	Really Interesting New Gene
Rb	Retinoblastoma-associated protein
rRNA	Ribosomal RNA
RBR	RING-IBR-RING
RNMT	RNA methyltransferase
RNAPI	RNA polymerase I
RNAPII	RNA polymerase II
RNAPIII	RNA polymerase III
ROS	Reactive oxygen species
SSB	Single strand break
SDS-PAGE	SDS polyacrylamide gel electrophoresis
shRNA	Short hairpin RNA
SCF	Skp1-cullin 1-F-box
SIM	Sumo interacting motif
SE	Super-enhancer
Tip60	Tat-interactive protein 60
TEMED	Tetramethylethylenediamine
Thy	Thymidine
TAD	Transactivation domain
TF	Transcription factor
TFIIF	Transcription factor IIF
TRC	Transcription-replication conflict
tRNA	Transfer RNA
TRRAP	Transformation/transcription domain-associated protein
UBA	Ubiquitin associated domain
UBR	Ubiquitin binding region
UCH	Ubiquitin C-terminal hydrolase
UIM	Ubiquitin interacting motif

UPS	Ubiquitin-proteasome system
USP	Ubiquitin-specific protease
UV	Ultraviolet
WDR5	WD repeat-containing protein 5
Usp28-WT	Wildtype Usp28
ZF	Zinc-finger
ZUFSP	Zn-finger and UFSP domain protein

Acknowledgments

First of all, I would like to express my sincere gratitude to Prof. Dr. Nikita Popov for providing me with the wonderful opportunity to come to Germany and doing my doctoral project in the field of Usp28 which I am interested in under his supervision. I really want to say thank you to Nikita, not only for all the skills you taught me, all the instructive discussions you had with me, all the fruitful suggestions you gave me, but also for all other benefits you offered so that I can calm down and focus on my project.

I would also like to say thank you to Prof. Dr. Jennifer Ewald for being my primary supervisor and providing me the opportunity to discuss about my study to make it a better one.

I also thank Prof. Dr. Matthias Gehringer for being my dissertation committee member and thereby allowing me have the possibility to present and defend for my project.

I am also grateful to the postgraduate school of the science faculty, Eberhard Karls Universität Tübingen for all the help they offered so that I can proceed every step during my PhD career, especially for the defense, more smoothly.

Many thanks to all the previous and present members in our group: Dr. Liudmyla Taranets, Valentina Andrioletti, Kseniya Popova, Ravi Babu Kollampaly, Dr. Vanessa Rousseau. Thank you all for the perfect years we spent together and all the kindness help you gave me.

In particular, I want to show my big thank to Elias Einig, for all the enthusiastic help from you and all those wonderful and inspirational discussions (absolutely not only limited in the scientific fields) between us.

Besides, I also very grateful to all the colleagues from Prof. Dr. Lars Zender group and Dr. Daniel Dauch group. Thank you very much for those technical assistances and the good research environment. Particularly, I would like to show my gratitude to Dr. Hu Zexi and Dr. Cui Wei, for those endless supports both in the lab and in my daily life.

Thank you to the Schütte family, thank you Peter and Karin, for your hospitality and I will keep in mind all those interesting emails and useful advices you gave.

Especially, I want to say thank you to my parents, Jin Baohong and Hu Zhenping, for your care and unconditional love for me over the years. 谁言寸草心， 报得三春晖！

Last, but not the least, I have to express my great gratitude to my wife, Chen Wenwen, who gave up her splendid career and cozy life in China and to come alone to Germany to take care of my life. It is because of you that I can carry out my own research without any worry. Of course, how could I forget my two beloved daughters, Jin Zhiting and Jin Qingchu,

it is because of you that I have had so much more fun in my monotonous research life. I love you all.

I would never have been able to complete my PhD project without the help of all of you!